Special Report

Toward a Consistent Design of Structural Concrete

Jörg Schlaich,
Dr.-Ing.
Professor at the Institute of Reinforced Concrete
University of Stuttgart
West Germany

Kurt Schäfer,
Dr.-Ing.
Professor at the Institute of Reinforced Concrete
University of Stuttgart
West Germany

Mattias Jennewein,
Dipl.-Ing.
Research Associate
University of Stuttgart
West Germany

This report (which is being considered by Comité Euro-International du Béton in connection with the revision of the Model Code) represents the latest and most authoritative information in formulating a consistent design approach for reinforced and prestressed concrete structures.

CONTENTS

1. INTRODUCTION — THE STRUT-AND-TIE-MODEL

The truss model is today considered by researchers and practitioners to be the rational and appropriate basis for the design of cracked reinforced concrete beams loaded in bending, shear and torsion. However, a design based on the standard truss model can cover only certain parts of a structure.

At statical or geometrical discontinuities such as point loads or frame corners, corbels, recesses, holes and other openings, the theory is not applicable. Therefore, in practice, procedures which are based on test results, rules of thumb and past experience are usually applied to cover such cases.

Since all parts of a structure including those mentioned above are of similar importance, an acceptable design concept must be valid and consistent for every part of any structure. Furthermore, since the function of the experiment in design should be restricted to verify or dispute a theory but not to derive it, such a concept must be based on physical models which can be easily understood and therefore are unlikely to be misinterpreted.

For the design of structural concrete* it is, therefore, proposed to generalize the truss analogy in order to apply it in the form of strut-and-tie-models to every part of any structure.

This proposal is justified by the fact that reinforced concrete structures carry loads through a set of compressive stress fields which are distributed and interconnected by tensile ties. The ties may be reinforcing bars, prestressing tendons, or concrete tensile stress fields. For analytical purposes, the strut-and-tie-models condense all stresses in compression and tension members and join them by nodes.

This paper describes how strut-and-tie-models can be developed by following the path of the forces throughout a structure. A consistent design approach for a structure is attained when its tension and compression members (including their nodes) are designed with regard to safety and serviceability using uniform design criteria.

The concept also incorporates the major elements of what is today called "detailing," and replaces empirical procedures, rules of thumb and guess work by a rational design method. Strut-and-tie-models could lead to a clearer understanding of the behavior of structural concrete, and codes based on such an approach would lead to improved structures.

The authors are aware of the encouraging fact that, although they published papers on this topic earlier,[1,2,3] they are neither the first nor the only ones thinking and working along these lines. It was actually at the turn of the last century, when Ritter[4] and Mörsch[5] introduced the truss analogy. This method was later refined and expanded by Leonhardt,[6] Rüsch, [7] Kupfer,[8] and others until Thürlimann's Zürich school,[9] with Marti[10] and Mueller,[27] created its scientific basis for a rational application in tracing the concept back to the theory of plasticity.

Collins and Mitchell further considered the deformations of the truss model and derived a rational design method for shear and torsion.[11]

In various applications, Bay, Franz, Leonhardt and Thürlimann had shown that strut-and-tie-models could be usefully applied to deep beams and corbels. From that point, the present authors began their efforts to systematically expand such models to entire structures

*Following a proposal by Dr. J. E. Breen and Dr. A. S. G. Bruggeling, the term "structural concrete" covers all loadbearing concrete, including reinforced, prestressed and also plain (unreinforced) concrete, if the latter is part of a reinforced concrete structure.

Synopsis

Certain parts of structures are designed with almost exaggerated accuracy while other parts are designed using rules of thumb or judgment based on past experience. However, all parts of a structure are of similar importance.

A unified design concept, which is consistent for all types of structures and all their parts, is required. To be satisfactory, this concept must be based on realistic physical models. Strut-and-tie-models, a generalization of the well known truss analogy method for beams, are proposed as the appropriate approach for designing structural concrete, which includes both reinforced and prestressed concrete structures.

This report shows how suitable models are developed and proposes criteria according to which the model's elements can be dimensioned uniformly for all possible cases. The concept is explained using numerous design examples, many of which treat the effect of prestress.

This report was initially prepared for discussion within CEB (Comité Euro-International du Béton) in connection with the revision of the Model Code.

and all structures.

The approaches of the various authors cited above differ in the treatment of the prediction of ultimate load and the satisfaction of serviceability requirements. From a practical viewpoint, true simplicity can only be achieved if solutions are accepted with sufficient (but not perfect) accuracy. Therefore, it is proposed here to treat in general the ultimate limit state and serviceability in the cracked state by using one and the same model for both. As will be shown later, this is done by orienting the geometry of the strut-and-tie-model at the elastic stress fields and designing the model structure following the theory of plasticity.

The proposed procedure also permits the demonstration that reinforced and prestressed concrete follow the same principles although their behavior under working loads is quite distinct.

It should be mentioned that only the essential steps of the proposed method are given here. Further support of the theory and other information may be found in Ref. 3.

2. THE STRUCTURE'S B- AND D-REGIONS

Those regions of a structure, in which the Bernoulli hypothesis of plane strain distribution is assumed valid, are usually designed with almost exaggerated care and accuracy. These regions are referred to as B-regions (where B stands for beam or Bernoulli). Their internal state of stress is easily derived from the sectional forces (bending and torsional moments, shear and axial forces).

As long as the section is uncracked, these stresses are calculated with the help of section properties like cross-sectional areas and moments of inertia. If the tensile stresses exceed the tensile strength of the concrete, the truss model or its variations apply.

The B-regions are designed on the basis of truss models as discussed later on in Section 5.1.

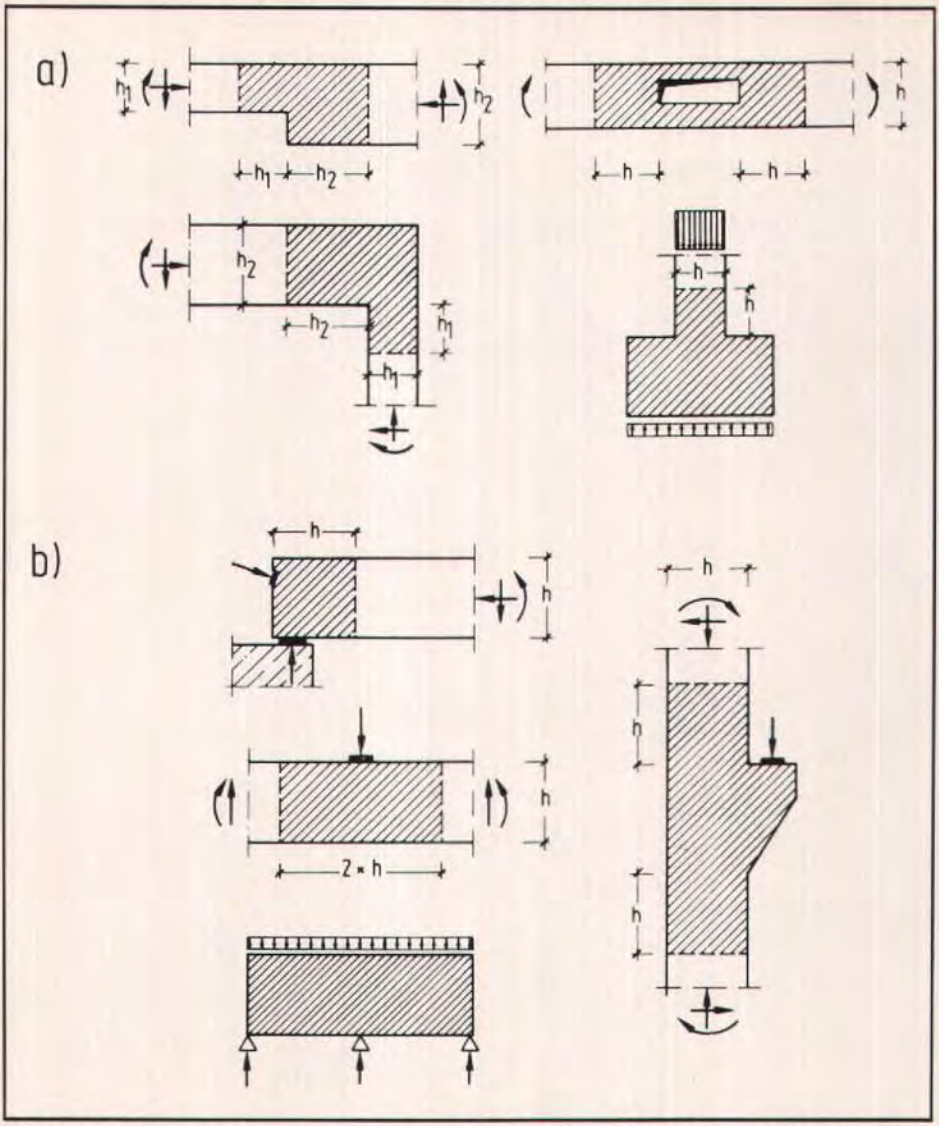

Fig. 1. D-regions (shaded areas) with nonlinear strain distribution due to (a) geometrical discontinuities; (b) statical and/or geometrical discontinuities.

The above standard methods are not applicable to all the other regions and details of a structure where the strain distribution is significantly nonlinear, e.g., near concentrated loads, corners, bends, openings and other discontinuities (see Fig. 1). Such regions are called D-regions (where D stands for discontinuity, disturbance or detail).

As long as these regions are uncracked, they can be readily analyzed by the linear elastic stress method, i.e., applying Hooke's Law. However, if the sections are cracked, accepted design approaches exist for only a few cases such as beam supports, frame corners,

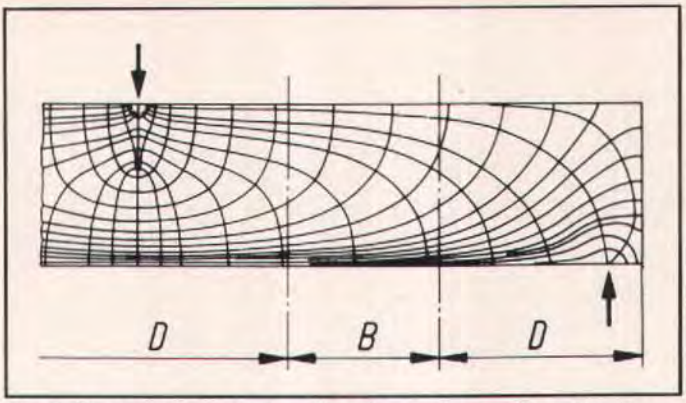

Fig. 2. Stress trajectories in a B-region and near discontinuities (D-regions).

corbels and splitting tension at prestressed concrete anchorages. And even these approaches usually only lead to the design of the required amount of reinforcement; they do not involve a clear check of the concrete stresses.

The inadequate (and inconsistent) treatment of D-regions using so-called "detailing," "past experience" or "good practice" has been one of the main reasons for the poor performance and even failures of structures. It is apparent, then, that a consistent design philosophy must comprise both B- and D-regions without contradiction.

Considering the fact that several decades after Mörsch, the B-region design is still being disputed, it is only reasonable to expect that the more complex D-region design will need to be simplified with some loss of accuracy. However, even a simplified methodical concept of D-region design will be preferable to today's practice. The preferred concept is to use the strut-and-tie-model approach. This method includes the B-regions with the truss model as a special case of a strut-and-tie model.

In using the strut-and-tie-model approach, it is helpful and informative to first subdivide the structure into its B- and D-regions. The truss model and the design procedure for the B-regions are then readily available and only the strut-and-tie-models for the D-regions remain to be developed and added.

Stresses and stress trajectories are quite smooth in B-regions as compared to their turbulent pattern near discontinuities (see Fig. 2). Stress intensities decrease rapidly with the distance from the origin of the stress concentration. This behavior allows the identification of B- and D-regions in a structure.

In order to find roughly the division lines between B- and D-regions, the following procedure is proposed, which is graphically explained by four examples as shown in Fig. 3:

1. Replace the real structure (a) by the fictitious structure (b) which is loaded in such a way that it complies with the Bernoulli hypothesis and satisfies equilibrium with the sectional forces. Thus, (b) consists entirely of one or several B-regions. It usually violates the actual boundary conditions.

2. Select a self-equilibrating state of stress (c) which, if superimposed on (b), satisfies the real boundary conditions of (a).

3. Apply the principle of Saint-Vénant (Fig. 4) to (c) and find that the stresses are negligible at a distance a from the equilibrating forces, which is approxi-

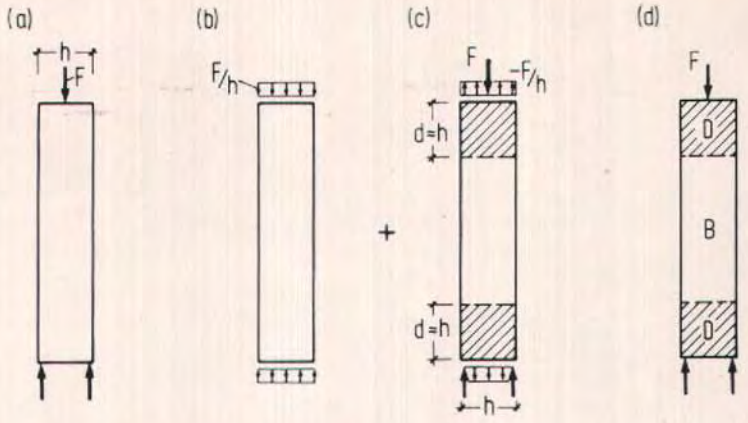

Fig. 3.1. Column with point loads.

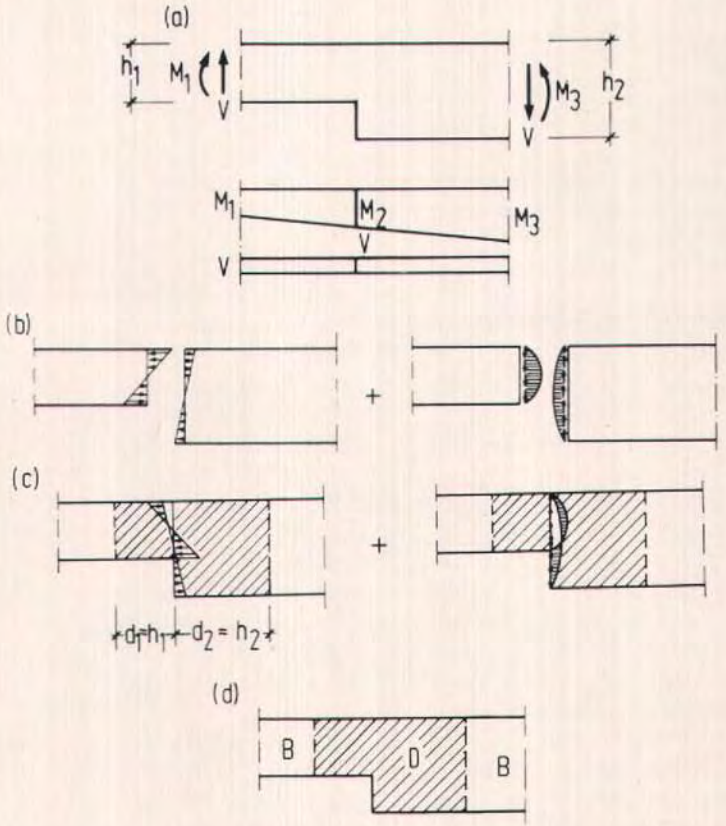

Fig. 3.3. Beam with a recess.

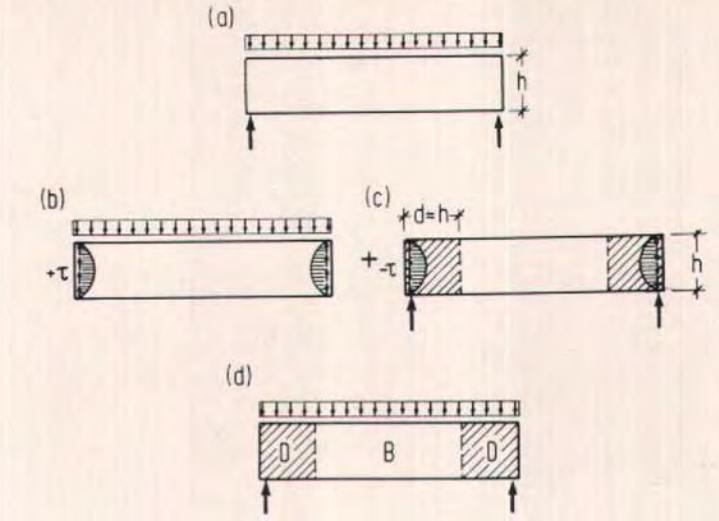

Fig. 3.2. Beam with direct supports.

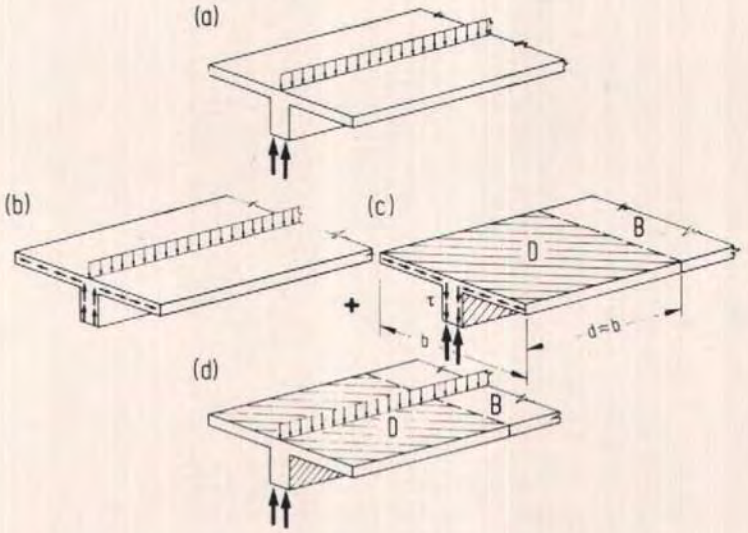

Fig. 3.4. T-beam.

(a) real structure
(b) loads and reactions applied in accordance with Bernoulli hypothesis
(c) self-equilibrating state of stress
(d) real structure with B- and D-regions

Fig. 3. Subdivision of four structures into their B- and D-regions, using Saint Vénant's principle (Fig. 4).

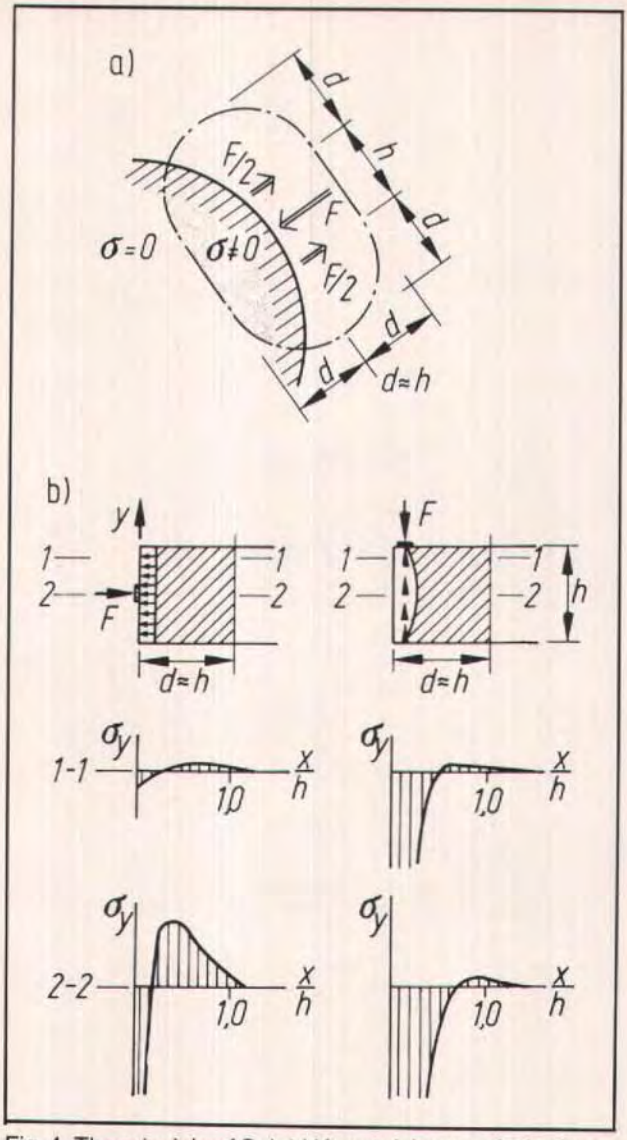

Fig. 4. The principle of Saint-Vénant: (a) zone of a body affected by self-equilibrating forces at the surface; (b) application to a prismatic bar (beam) loaded at one face.

mately equal to the maximum distance between the equilibrating forces themselves. This distance defines the range of the D-regions (d).

It should be mentioned that cracked concrete members have different stiffnesses in different directions. This situation may influence the extent of the D-regions but needs no further discussion since the principle of Saint-Vénant itself is not precise and the dividing lines between the B- and D-regions proposed here only serve as a qualitative aid in developing the strut-and-

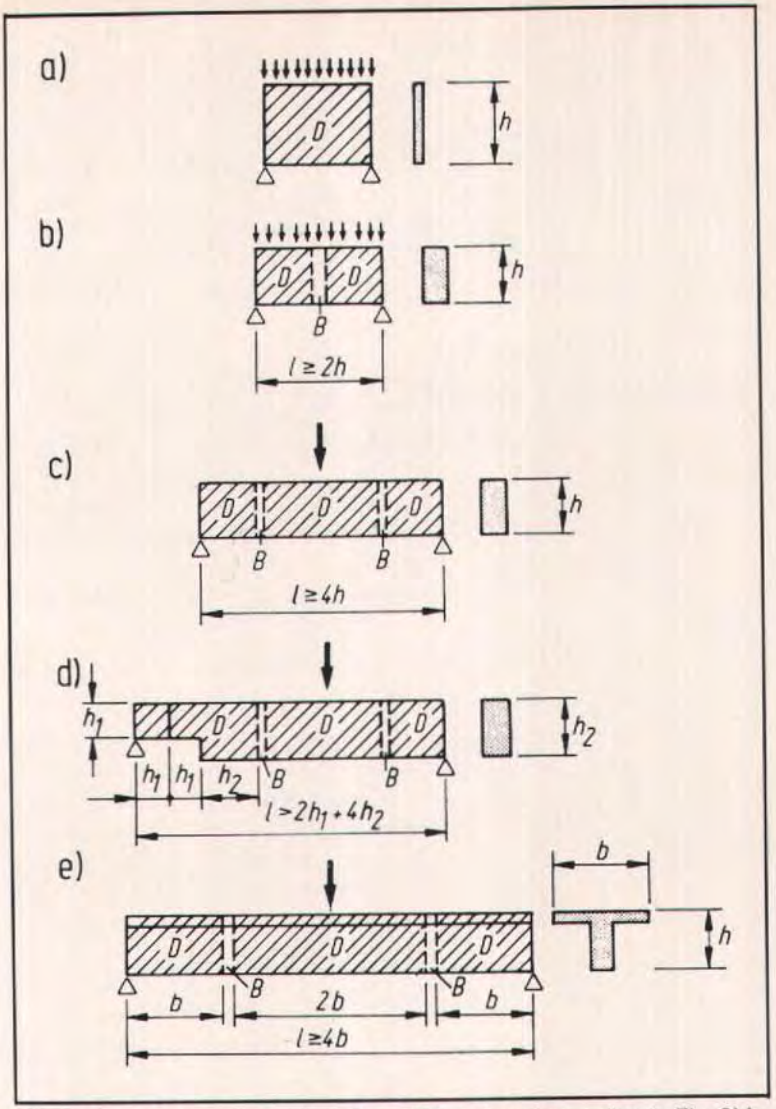

Fig. 5. The identification of their B- and D-regions (according to Fig. 3) is a rational method to classify structures or parts thereof with respect to their loadbearing behavior: (a) deep beam; (b) through (d) rectangular beams; (e) T-beam.

tie-models.

The subdivision of a structure into B- and D-regions is, however, already of considerable value for the understanding of the internal forces in the structure. It also demonstrates, that simple $1/h$ rules used today to classify beams, deep beams, short/long/high corbels and other special cases are misleading. For proper classification, both geometry and loads must be considered (see Figs. 3, 5 and 6).

If a structure is not plane or of constant width, it is for simplicity sub-

divided into its individual planes, which are treated separately. Similarly, three-dimensional stress patterns in plane or rectangular elements may be looked at in different orthogonal planes. Therefore, in general, only two-dimensional models need to be considered. However, the interaction of models in different planes must be taken into account by appropriate boundary conditions.

Slabs may also be divided into B-regions, where the internal forces are easily derived from the sectional forces, and D-regions which need further explanation. If the state of stress is not predominantly plane, as for example in the case with punching or concentrated loads, three-dimensional strut-and-tie-models should be developed.

3. GENERAL DESIGN PROCEDURE AND MODELLING

3.1 Scope

For the majority of structures it would be unreasonable and too cumbersome to begin immediately to model the entire structure with struts and ties. Rather, it is more convenient (and common practice) to first carry out a general structural analysis. However, prior to starting this analysis, it is advantageous to subdivide the given structure into its B- and D-regions. The overall analysis will, then, include not only the B-regions but also the D-regions.

If a structure contains to a substantial part B-regions, it is represented by its statical system (see Fig. 6). The general analysis of linear structures (e.g., beams, frames and arches) results in the support reactions and sectional effects, the bending moments *(M)*, normal forces *(N)*, shear forces *(V)* and torsional moments (M_T) (see Table 1).

The B-regions of these structures can then be easily dimensioned by applying standard B-region models (e.g., the truss model, Fig. 8) or standard methods using handbooks or advanced codes of practice. Note that the overall structural

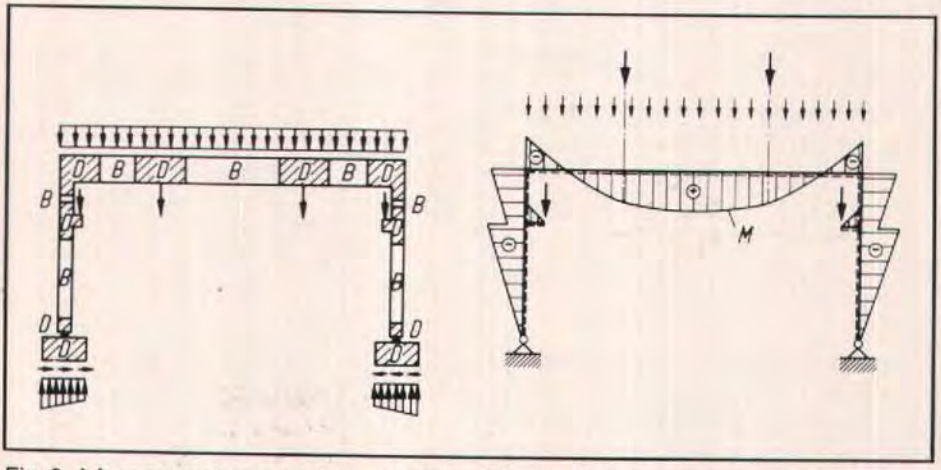

Fig. 6. A frame structure containing a substantial part of B-regions, its statical system and its bending moments.

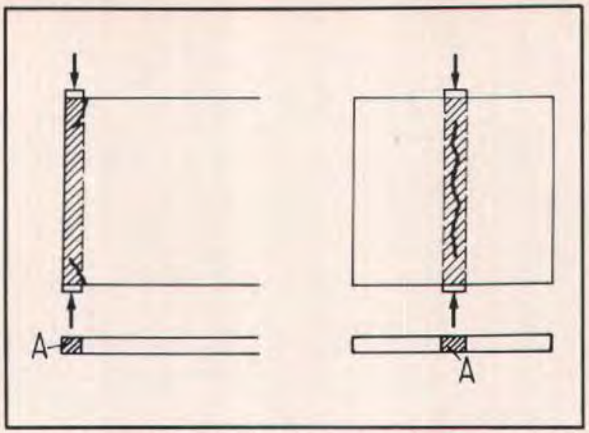

Fig. 7. Prismatic stress fields according to the theory of plasticity (neglecting the transverse tensile stresses due to the spreading of forces in the concrete) are unsafe for plain concrete.

analysis and B-region design provide also the boundary forces for the D-regions of the same structure.

Slabs and shells consist predominantly of B-regions (plane strain distribution). Starting from the sectional effects of the structural analysis, imaginary strips of the structure can be modelled like linear members.

If a structure consists of one D-region only (e.g., a deep beam), the analysis of sectional effects by a statical system may be omitted and the inner forces or stresses can be determined directly from the applied loads following the principles outlined for D-regions in Section 3.3. However, for structures with redundant supports, the support reactions have to be determined by an overall analysis before strut-and-tie-models can be properly developed.

In exceptional cases, a nonlinear fi-

Table 1. Analysis leading to stresses or strut-and-tie-forces.

<table>
<tr><td colspan="2" rowspan="2">Analysis \ Structure</td><td colspan="3">Structure consisting of:</td></tr>
<tr><td colspan="2">B- and D-regions
e.g., linear structures, slabs and shells</td><td>D-regions only
e.g., deep beams</td></tr>
<tr><td colspan="2"></td><td>B-regions</td><td colspan="2">D-regions</td><td>D-regions</td></tr>
<tr><td colspan="2" rowspan="2">Overall structural analysis (Table 2) gives:</td><td rowspan="2">Sectional effects
M, N, V, M_T</td><td colspan="2">Boundary forces:</td></tr>
<tr><td>Sectional effects</td><td>Support reactions</td></tr>
<tr><td rowspan="3">Analysis of inner forces or stresses in individual regions</td><td>State I (uncracked)</td><td>Via sectional values
A, J_B, J_T</td><td colspan="2">Linear elastic analysis*
(with redistributed stress peaks)</td></tr>
<tr><td>State II (cracked)</td><td colspan="3">Strut-and-tie-models
and/or nonlinear stress analysis*</td></tr>
<tr><td></td><td>Usually truss</td><td colspan="2"></td></tr>
</table>

* May be combined with overall analysis.

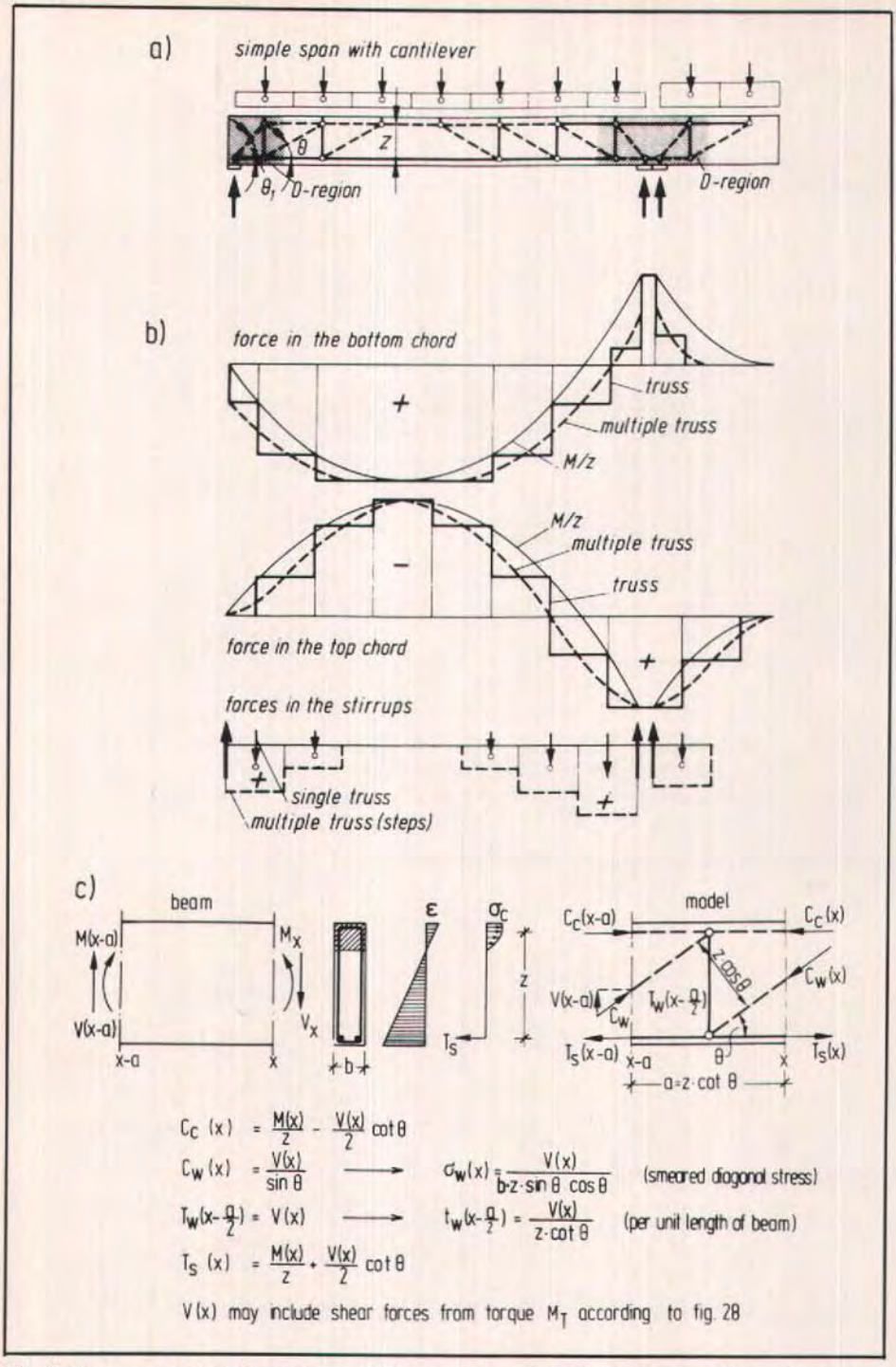

Fig. 8. Truss model of a beam with cantilever: (a) model; (b) distribution of inner forces; (c) magnitude of inner forces derived from equilibrium of a beam element.

Table 2. Overall structural behavior and method of overall structural analysis of statically indeterminate structures.

Limit state	Overall structural behavior	Corresponding method of analysis of sectional effects and support reactions	
		Most adequate	Acceptable
Serviceability	Essentially uncracked	Linear elastic	—
	Considerably cracked, with steel stresses below yield	Nonlinear	Linear elastic (or plastic if design is oriented at elastic behavior)
Ultimate capacity	Widely cracked, forming plastic hinges	Plastic with limited rotation capacity or elastic with redistribution	Linear elastic or nonlinear or perfectly plastic with structural restrictions

nite element method analysis may be applied. A follow-up check with a strut-and-tie-model is recommended, especially if the major reinforcement is not modelled realistically in the FEM analysis.

3.2 Comments on the Overall Analysis

In order to be consistent, the overall analysis of statically indeterminate structures should reflect the realistic overall behavior of the structure. The intent of the following paragraph (summarized in Table 2) is to give some guidance for the design of statically indeterminate structures. Some of this discussion can also be applied to statically determinate structures especially with regard to determining deformations.

Plastic methods of analysis (usually the static method) are suitable primarily for a realistic determination of ultimate load capacity, while elastic methods are more appropriate under serviceability conditions. According to the theory of plasticity, a safe solution for the ultimate load is also obtained, if a plastic analysis is replaced by a linear or nonlinear analysis. Experience further shows that the design of cracked concrete structures for the sectional effects using a linear elastic analysis is conservative. Vice versa, the distribution of sectional effects derived from plastic methods may for simplification purposes also be used for serviceability checks, if the structural design (layout of reinforcement) is oriented at the theory of elasticity.

3.3 Modelling of Individual B- and D-Regions

3.3.1 Principles and General Design Procedure

After the sectional effects of the B-regions and the boundary forces of the D-regions have been determined by the overall structural analysis, dimensioning follows, for which the internal flow of forces has to be searched and quantified:

For uncracked B- and D-regions, standard methods are available for the analysis of the concrete and steel stresses (see Table 1). In the case of high compressive stresses, the linear stress distribution may have to be modified by replacing Hooke's Law with a nonlinear materials law (e.g., parabolic stress-strain relation or stress block).

If the tensile stresses in individual B- or D-regions exceed the tensile strength of the concrete, the inner forces of those

regions are determined and are designed according to the following procedure:

1. Develop the strut-and-tie-model as explained in Section 3.3. The struts and ties condense the real stress fields by resultant straight lines and concentrate their curvature in nodes.

2. Calculate the strut and tie forces, which satisfy equilibrium. These are the inner forces.

3. Dimension the struts, ties and nodes for the inner forces with due consideration of crack width limitations (see Section 5).

This method implies that the structure is designed according to the lower bound theorem of plasticity. Since concrete permits only limited plastic deformations, the internal structural system (the strut-and-tie-model) has to be chosen in a way that the deformation limit (capacity of rotation) is not exceeded at any point before the assumed state of stress is reached in the rest of the structure.

In highly stressed regions this ductility requirement is fulfilled by adapting the struts and ties of the model to the direction and size of the internal forces as they would appear from the theory of elasticity.

In normally or lightly stressed regions the direction of the struts and ties in the model may deviate considerably from the elastic pattern without exceeding the structure's ductility. The ties and hence the reinforcement may be arranged according to practical considerations. The structure adapts itself to the assumed internal structural system. Of course, in every case an analysis and safety check must be made using the finally chosen model.

This method of orienting the strut-and-tie-model along the force paths indicated by the theory of elasticity obviously neglects some ultimate load capacity which could be utilized by a pure application of the theory of plasticity. On the other hand, it has the major advantage that the same model can be used for both the ultimate load and the serviceability check. If for some reason the purpose of the analysis is to find the actual ultimate load, the model can easily be adapted to this stage of loading by shifting its struts and ties in order to increase the resistance of the structure. In this case, however, the inelastic rotation capacity of the model has to be considered. (Note that the optimization of models is discussed in Section 3.3.3.)

Orienting the geometry of the model to the elastic stress distribution is also a safety requirement because the tensile strength of concrete is only a small fraction of the compressive strength. Cases like those given in Fig. 7 would be unsafe even if both requirements of the lower bound theorem of the theory of plasticity are fulfilled, namely, equilibrium and $F/A \leq f_c$. Compatibility evokes tensile forces, usually transverse to the direction of the loads which may cause premature cracking and failure. The "bottle-shaped compressive stress field," which is introduced in Section 4.1, further eliminates such "hidden" dangers when occasionally the model chosen is too simple.

For cracked B-regions, the proposed procedure obviously leads to a truss model as shown in Fig. 8, with the inclination of the diagonal struts oriented at the inclination of the diagonal cracks from elastic tensile stresses at the neutral axis. A reduction of the strut angle by 10 to 15 degrees and the choice of vertical stirrups, i.e., a deviation from the principal tensile stresses by 45 degrees, usually (i.e., for normal strength concrete and normal percentage of stirrup reinforcement) causes no distress. Since prestress decreases the inclination of the cracks and hence of the diagonal struts, prestress permits savings of stirrup reinforcement, whereas additional tensile forces increase the inclination.

The distance z between the chords should usually be determined from the plane strain distribution at the points of

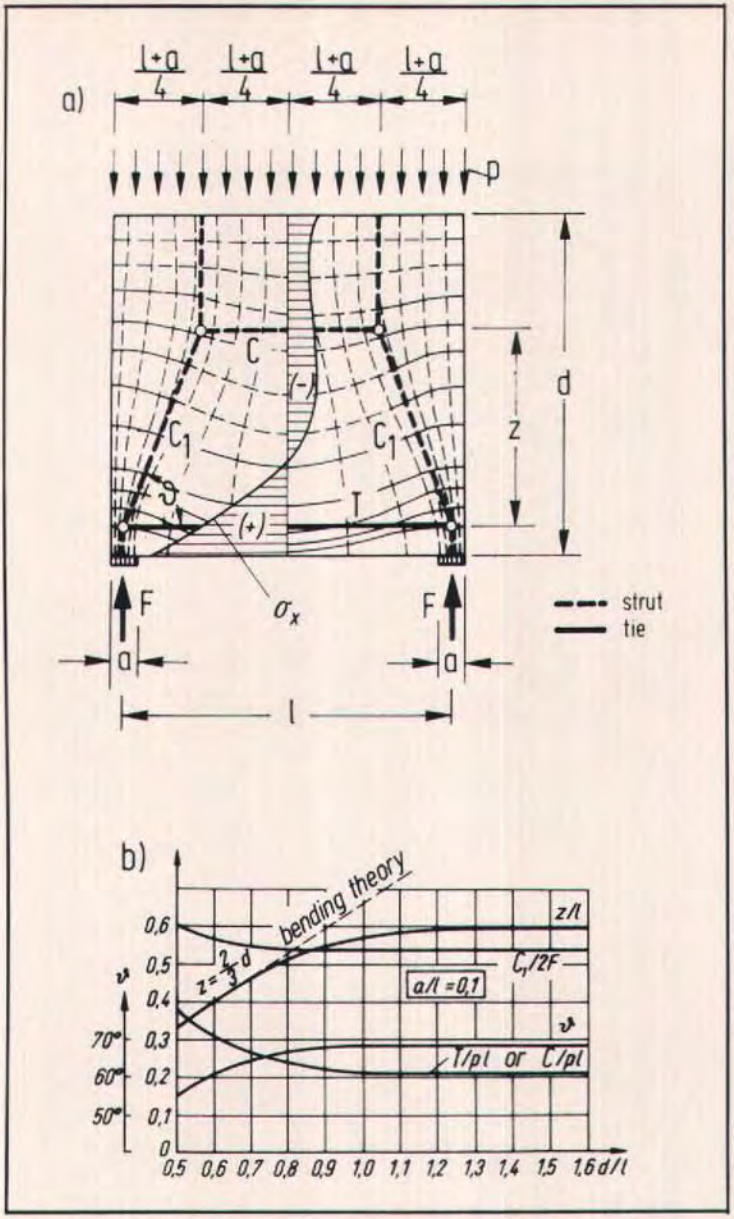

Fig. 9. A typical D-region: (a) elastic stress trajectories, elastic stresses and strut-and-tie-model; (b) diagram of internal forces, internal lever arm z and strut angle ϑ.

maximum moments and zero shear and for simplicity be kept constant between two adjacent points of zero moments. Refinements of B-region design will be discussed later in Section 5.1.

For the D-regions it is necessary to develop a strut-and-tie-model for each case individually. After some training,

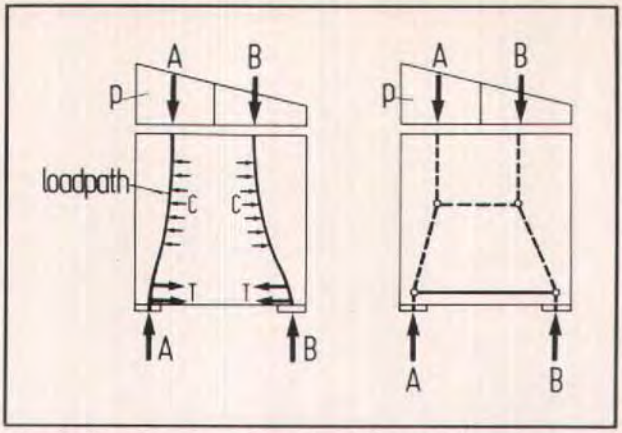

Fig. 10. Load paths and strut-and-tie-model.

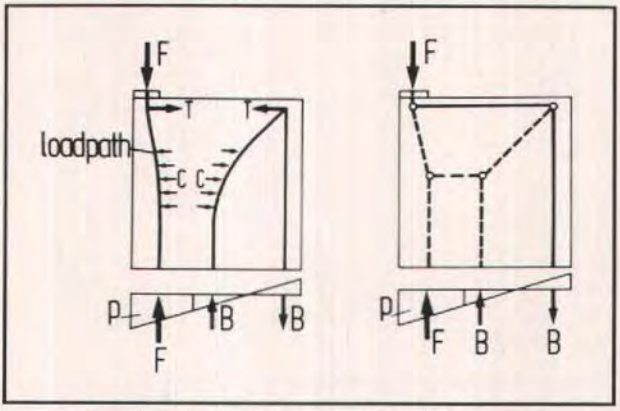

Fig. 11. Load paths (including a "U-turn") and strut-and-tie-model.

this can be done quite simply. Developing a strut-and-tie-model is comparable to choosing an overall statical system. Both procedures require some design experience and are of similar relevance for the structure.

Developing the model of a D-region is much simplified if the elastic stresses and principal stress directions are available as in the case of the example shown in Fig. 9. Such an elastic analysis is readily facilitated by the wide variety of computer programs available today. The direction of struts can then be taken in accordance with the mean direction of principal compressive stresses or the more important struts and ties can be located at the center of gravity of the corresponding stress diagrams, C and T in Fig. 9a, using the σ_x diagram given there.

However, even if no elastic analysis is available and there is no time to prepare one, it is easy to learn to develop strut-and-tie-models using so-called "load paths." This is demonstrated in more detail by some examples in the next section.

3.3.2 The Load Path Method

First, it must be ensured that the outer

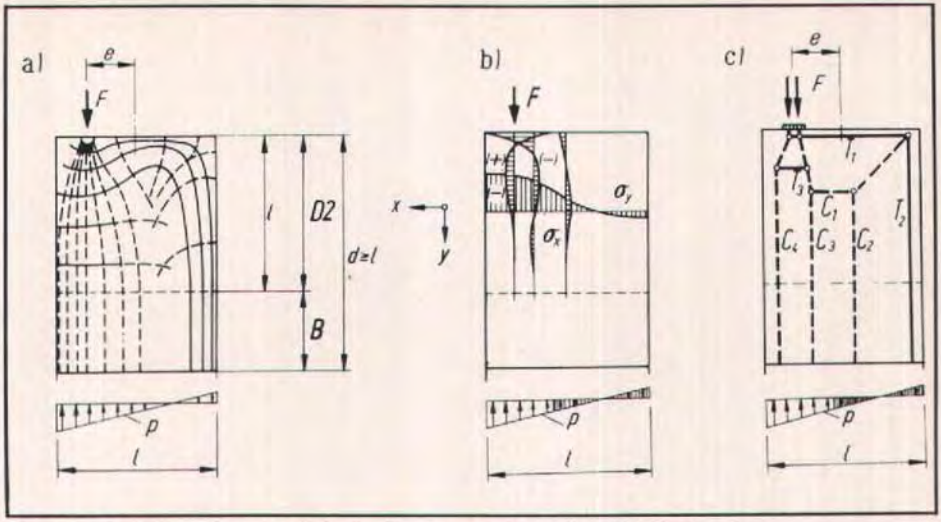

Fig. 12.1. A typical D-region: (a) elastic stress trajectories; (b) elastic stresses; (c) strut-and-tie-models.

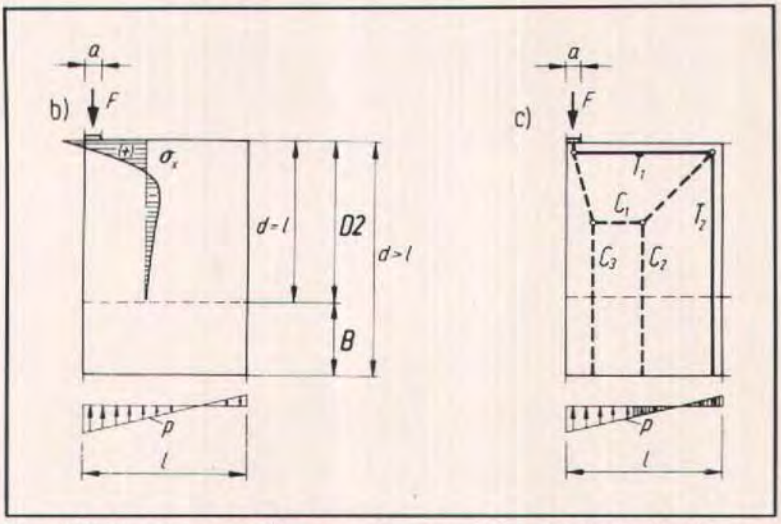

Fig. 12.2. Special case of the D-region in Fig. 12.1 with the load at the corner; (b) elastic stresses; (c) strut-and-tie-models.

equilibrium of the D-region is satisfied by determining all the loads and reactions (support forces) acting on it. In a boundary adjacent to a B-region the loads on the D-region are taken from the B-region design, assuming for example that a linear distribution of stresses (p) exists as in Figs. 10 and 11.

The stress diagram is subdivided in such a way, that the loads on one side of the structure find their counterpart on the other, considering that the load paths connecting the opposite sides will not cross each other. The load paths

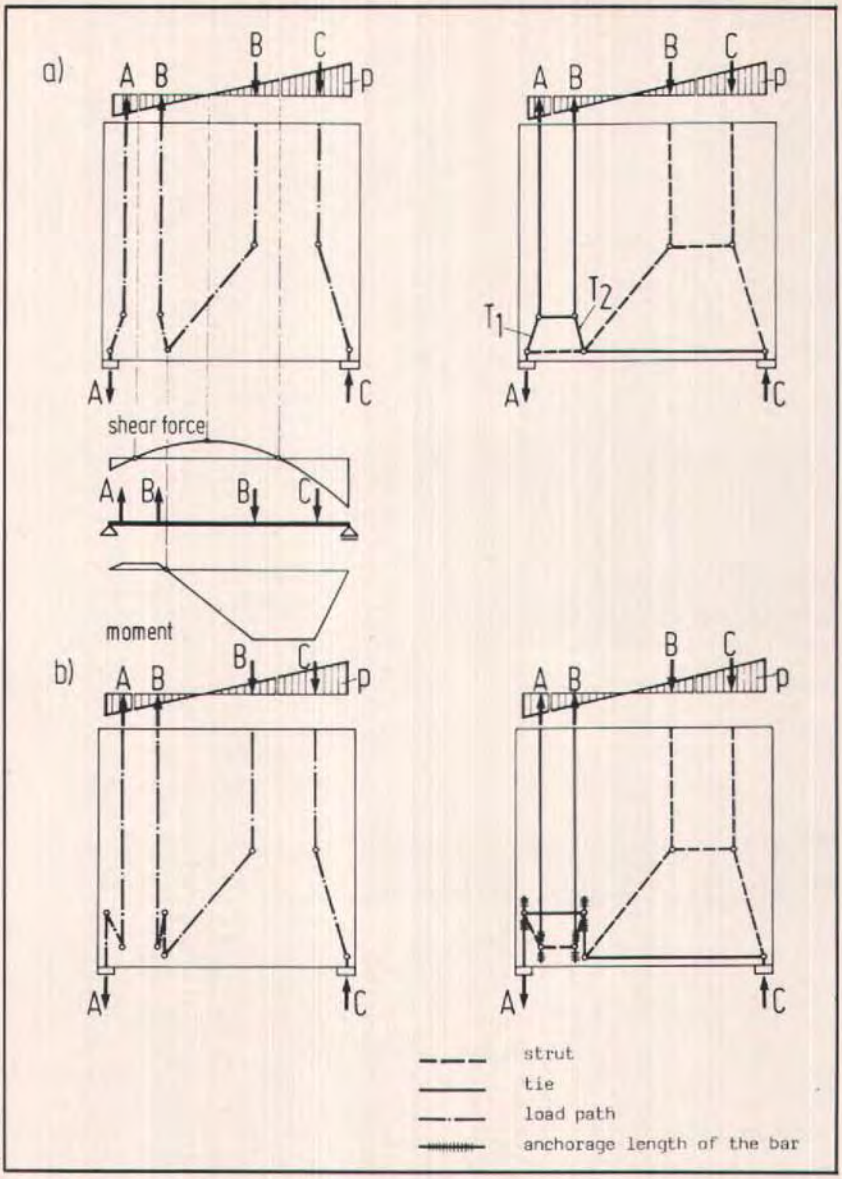

Fig. 13. Two models for the same case: (a) requiring oblique reinforcement; (b) for orthogonal reinforcement.

begin and end at the center of gravity of the corresponding stress diagrams and have there the direction of the applied loads or reactions. They tend to take the shortest possible streamlined way in between. Curvatures concentrate near stress concentrations (support reactions or singular loads).

Obviously, there will be some cases where the stress diagram is not completely used up with the load paths described; there remain resultants (equal

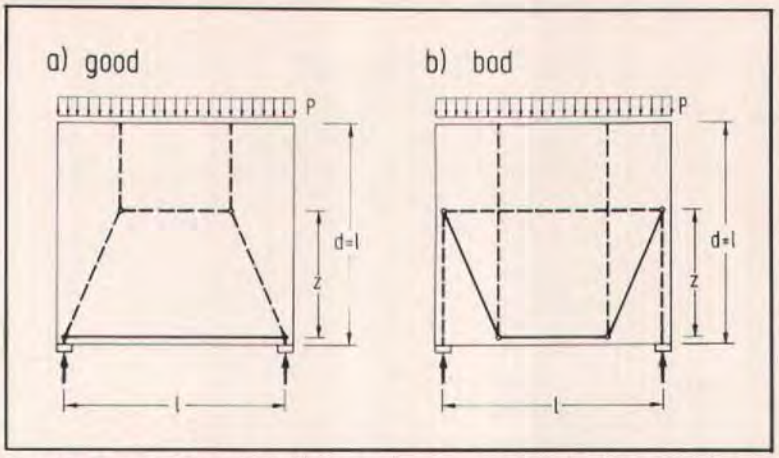

Fig. 14. The good model (a) has shorter ties than the bad model (b).

in magnitude but with opposite sign) which enter the structure and leave it again on U-turn or form a whirl as illustrated by forces B or Figs. 11 and 13a.

Until now, equilibrium only in the direction of the applied loads has been considered. After plotting all load paths with smooth curves and replacing them by polygons, further struts and ties must be added for transverse equilibrium acting between the nodes, including those of the U-turn.

While doing so, the ties must be arranged with proper consideration of practicality of the reinforcement layout (generally parallel to the concrete surface) and of crack distribution requirements.

The resulting models are quite often kinematic which means that equilibrium in a given model is possible only for the specific load case. Therefore, the geometry of the appropriate model has to be adapted to the load case and is in most cases determined by equilibrium conditions after only a few struts or ties have been chosen.

A very powerful means of developing new strut-and-tie-models for complicated cases is the combination of an elastic finite element method analysis with the load path method. This combined approach is applied in Fig. 12 and the numerical example in Section 5.2.1.

In Fig. 12.1 the vertical struts and ties are found by the load path method as explained in the previous examples: The structure is divided into a B-region and a D-region. The bottom of the D-region is acted on by the stresses (p) as derived for the adjacent B-region.

These stresses are then resolved into four components: The two compressive forces $C_3 + C_4 = F$, which leaves two equal forces T_2 and C_2. The forces C_3 and C_4 are the components, respectively, on the left hand and right hand side of the vertical plane which is determined by the load F. By laterally shifting the load components into the given positions, transverse stresses are generated.

The corresponding horizontal struts and ties are located at the center of gravity of stress diagrams in typical sections which are derived from an elastic analysis (Fig. 12.1b). Their nodes with the vertical struts also determine the position of the diagonal struts (see Fig. 12.1c).

The example in Fig. 12.2 shows that the tie T_3 of Fig. 12.1c disappears, if the load F moves toward the corner of the D-region.

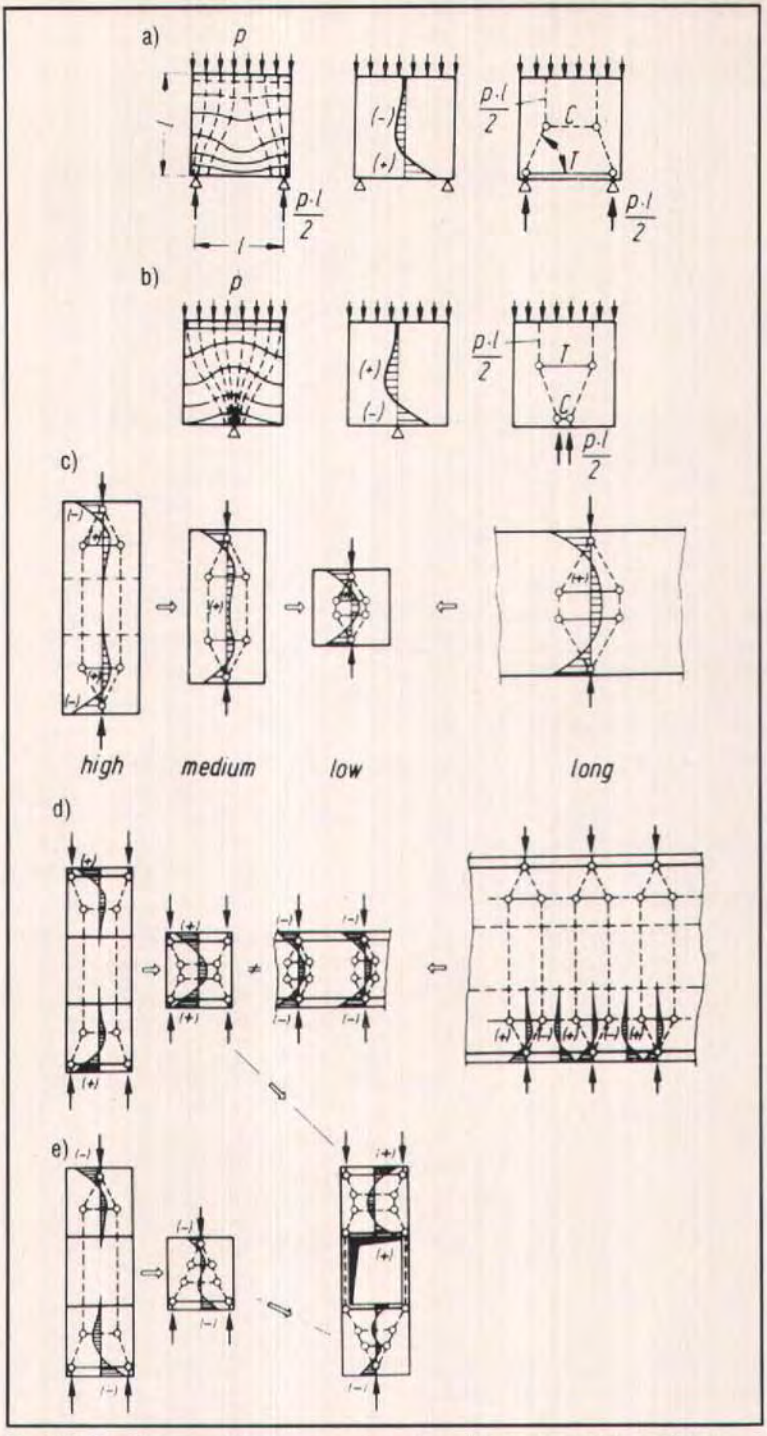

Fig. 15. The two most frequent and most useful strut-and-tie models: (a) through (b), and some of their variations (c) through (e).

3.3.3 Model Optimization

In Fig. 13 one load case has been solved with two different models. The left part of Figs. 13a and 13b shows how they were developed by the load path method and how they are connected to the overall sectional effects of the D-regions. The ties T_1 and T_2 in Fig. 13a would require inclined reinforcement, which is undesirable from a practical viewpoint.

Therefore, a tie arrangement has been chosen in Fig. 13b which can be satisfied by an orthogonal reinforcing net with the bars parallel to the edges. Thereby, special methods such as those given in Ref. 17, which consider deviations of reinforcement directions from the principal stress directions, are not needed.

Doubts could arise as to whether the correct model has been chosen out of several possible ones. In selecting the model, it is helpful to realize that loads try to use the path with the least forces and deformations. Since reinforced ties are much more deformable than concrete struts, the model with the least and shortest ties is the best. This simple criterion for optimizing a model may be

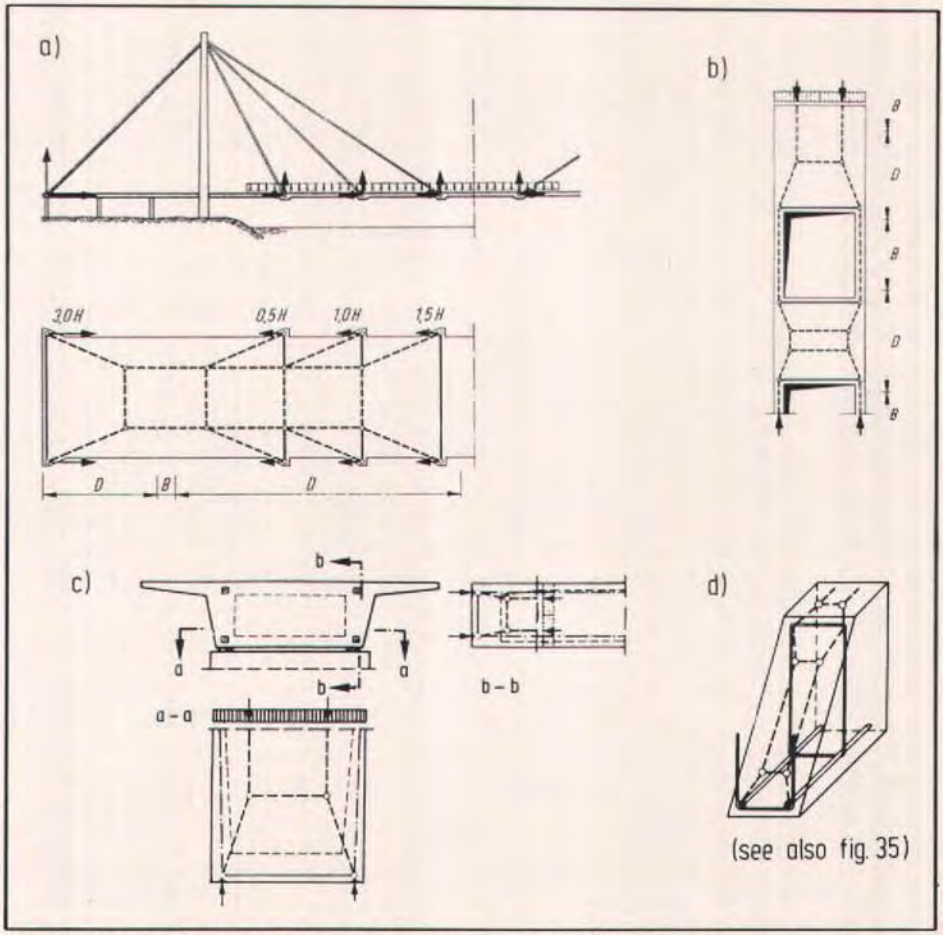

Fig. 16. One single type of a D-model appears in many different structures; here four examples are given.

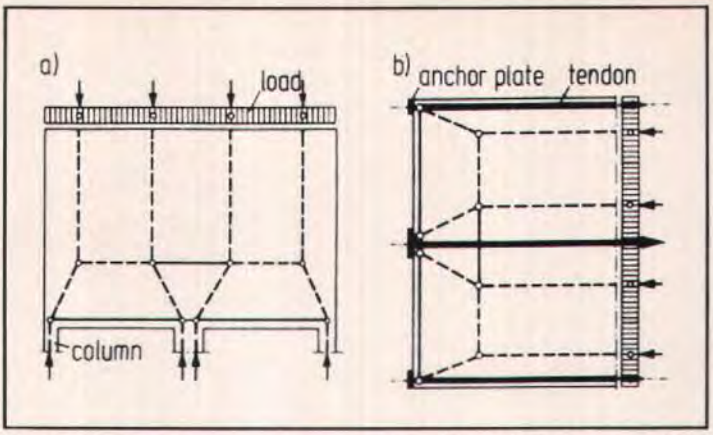

Fig. 17. (a) Deep beam on three supports; (b) end of a beam or slab with anchorages of three prestressing tendons. Both cases are identical if the reactions in (a) and the prestressing forces in (b) are equal.

formulated as follows:

$$\Sigma F_i l_i \epsilon_{mi} = \text{Minimum}$$

where

F_i = force in strut or tie i
l_i = length of member i
ϵ_{mi} = mean strain of member i

This equation is derived from the principle of minimum strain energy for linear elastic behavior of the struts and ties after cracking. The contribution of the concrete struts can generally be omitted because the strains of the struts are usually much smaller than those of the steel ties. This criterion is also helpful in eliminating less desirable models (see Fig. 14).

Of course, it should be understood that there are no unique or absolute optimum solutions. Replacing a continuous set of smooth curves by individual polygonal lines is an approximation in itself and leaves ample room for subjective decisions. Furthermore, individual input such as the size of the region or reinforcement layout are always different. But an engineer with some experience in strut-and-tie-modelling will always find a satisfactory solution.

3.3.4 The Pedagogical Value of Modelling

Anyone who spends time developing strut-and-tie-models will observe that some types of D-regions appear over and over again even in apparently very different structures. The two most frequent D-regions, which are even related to one another because they have the same characteristic stress distribution along their centerline, are given in Fig. 15 with some of their variations.

Fig. 16 shows applications of the first type of model (Fig. 15a) to four different structures: The distribution of cable forces in a bridge deck (Fig. 16a); a wall with big openings (Fig. 16b); a box girder with anchor loads from prestressing tendons (Fig. 16c); and a detail of internal forces in a rectangular beam which shows that stirrups need to be closed (Fig. 16d). In all of these cases the pattern of internal forces is basically identical.

To recognize such common features of structures is of considerable pedagogical value and very helpful to the design engineer. On the other hand, it is confusing if the same facts are given dif-

ferent designations only because they appear under different circumstances. For example, the deep beam in Fig. 17 "does not care" whether its identical loads result from supports or from prestressing tendons. It, therefore, does not react with "bending" in the one case and with "splitting tension" in the other case, but simply with tension and compression.

Numerous other strut-and-tie-models are found in Ref. 3.

4. DIMENSIONING THE STRUTS, TIES AND NODES

4.1 Definitions and General Rule

Fig. 18 shows some typical examples of strut-and-tie models, the corresponding stress trajectories and reinforcement layout. Node regions are indicated by shading. Looking closely at these examples as well as those in the previous and following sections, the following conclusions may be drawn:

Dimensioning not only means sizing and reinforcing the individual struts and ties for the forces they carry, but also ensuring the load transfer between them by checking the node regions. There is a close relation between the detailing of the nodes and the strength of the struts bearing on them and of the ties anchored in them because the detail of the node chosen by the design engineer affects the flow of forces. Therefore, it is necessary to check whether the strut-and-tie-model initially chosen is still valid after detailing or needs correction. Thus, modelling and dimensioning is in principle an iterative process.

There are basically three types of struts and ties to be dimensioned:

C_c: Concrete struts in compression

T_c: Concrete ties in tension without reinforcement

T_s: Ties in tension with reinforcement (mild steel reinforcement or prestressing steel)

There are essentially four types of nodes depending on the combination of struts C and ties T (see Fig. 19):

CCC-node

CCT-node

CTT-node

TTT-node

The principle remains the same if more than three struts and ties meet.

Struts and Ties

Whereas the T_s are essentially linear or one-dimensional elements between two nodes, the C_c and T_c are two- (or three-) dimensional stress fields, tending to spread in between two adjacent nodes. This spreading, indicated by the bulging of the struts in Figs. 18 and 19a, can result in transverse tensile and compressive stresses which then must be considered either by introducing these stresses into the failure criterion of the C_c-struts and the T_c-ties or by again applying a strut-and-tie-model to them (see Figs. 18c and 18d). Both approaches lead to the same result.

The struts in the model are resultants of the stress fields. Since by definition the curvatures or deviations of the forces are concentrated in the nodes, the struts are straight. This is, of course, an idealization of reality. If doubts arise whether by doing so in a highly stressed structure some tensile forces are not sufficiently accounted for, the straight lengths of the struts can be reduced either by refining the model itself or by smearing (or spreading) the node over a substantial length of the strut (see for example Figs. 18a2 and 18b2).

To cover all cases of compression fields including those of the B-regions, three typical configurations are sufficient:

(a) The "fan" (see Fig. 20a).[9]

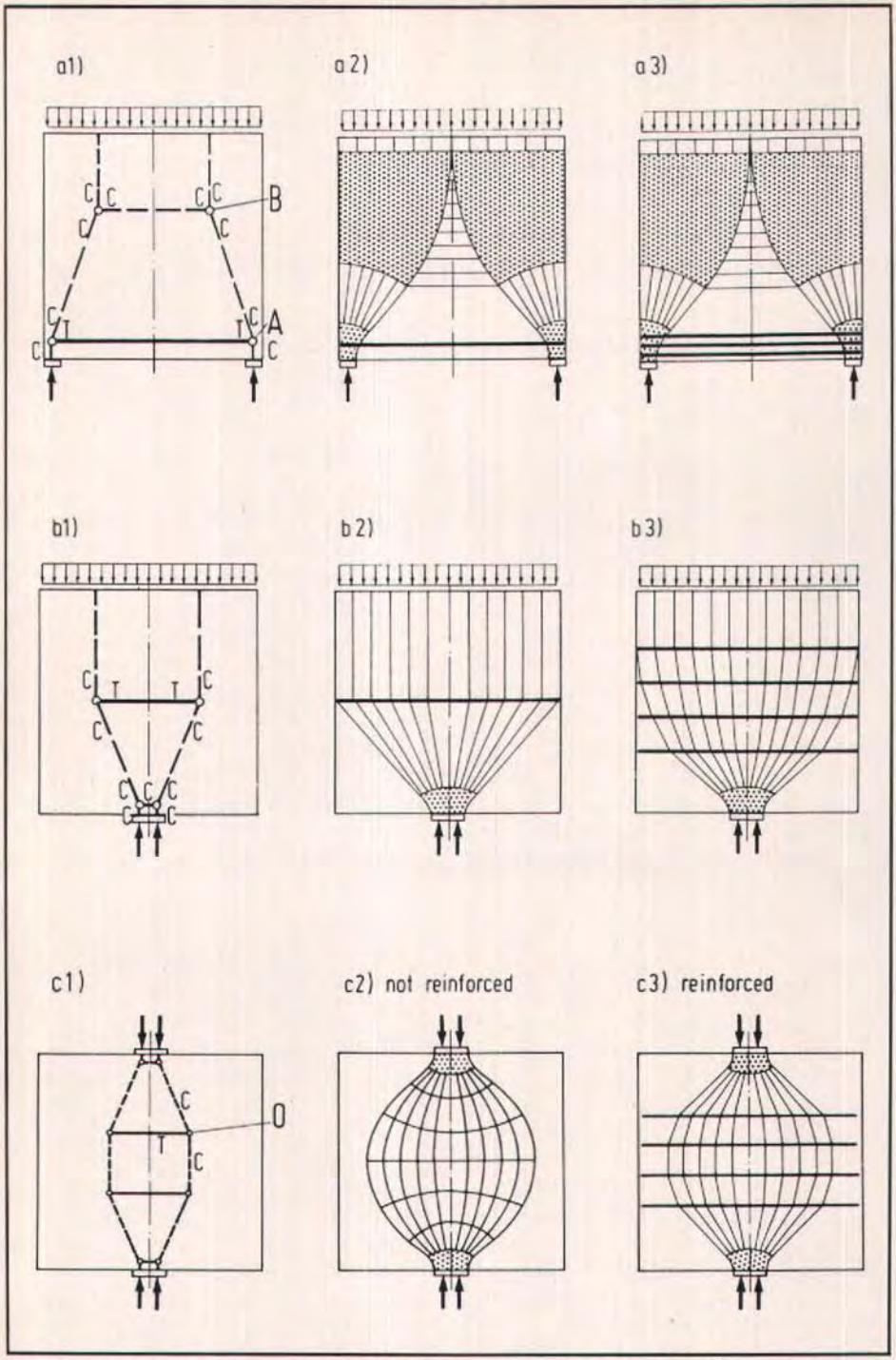

Fig. 18. Some typical examples of strut-and-tie-models, their stress fields, nodes and corresponding reinforcement (if any is provided).

(b) The "bottle" (see Fig. 20b).
(c) The "prism" or parallel stress field (see Fig. 20c), being the limit case of both $\alpha = 0$ and $b/a = 1$.

Nodes

The nodes of the model are a simplified idealization of reality. They are formally derived as the intersection points of three or more straight struts or ties, which themselves represent either straight or curved stress fields or reinforcing bars or tendons. A node as introduced into the model implies an abrupt change of direction of forces. In the actual reinforced concrete structure this deviation usually occurs over a certain length and width.

If one of the struts or ties represents a concentrated stress field, the deviation of forces tends to be locally concentrated also. On the other hand, for wide concrete stress fields joining each other or with tensile ties, which consist of many closely distributed reinforcing bars, the deviation of forces may be smeared (or spread) over some length. Therefore, in the former case the nodes are called *singular* (or concentrated) nodes, whereas in the latter case they are called *smeared* (or continuous) nodes. Nodes A and B in Fig. 18a1 serve as typical examples of both types of nodes.

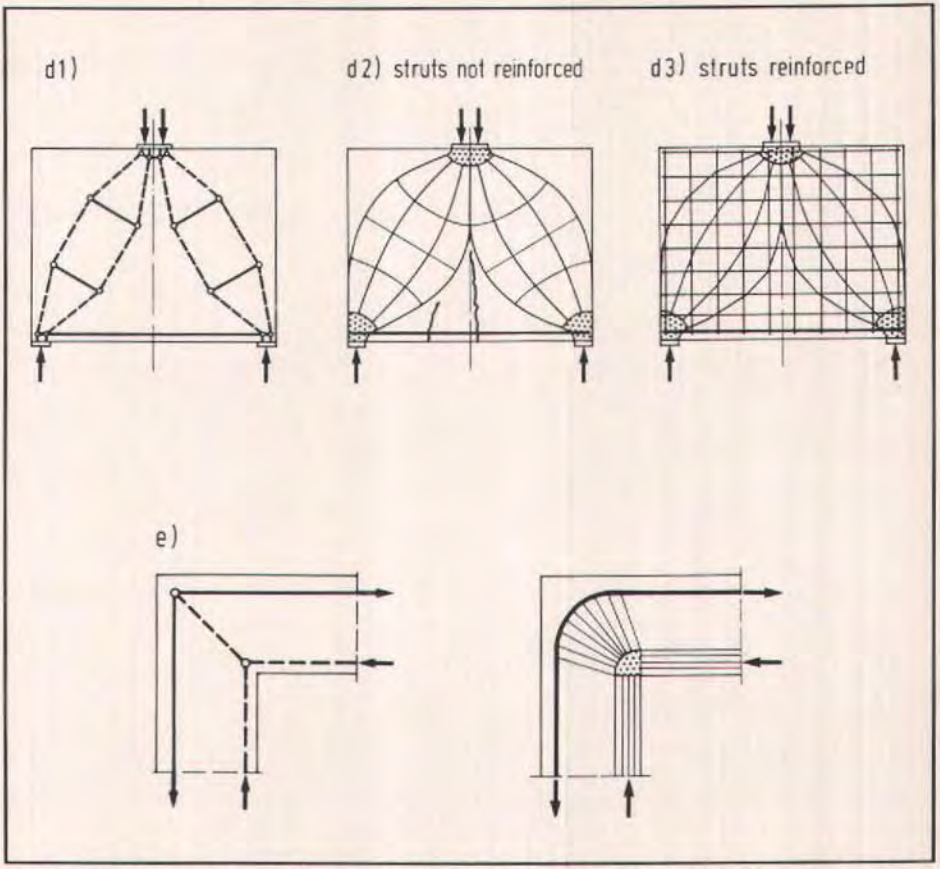

Fig. 18 (cont.). Some typical examples of strut-and-tie-models, their stress fields, nodes and corresponding reinforcement (if any is provided).

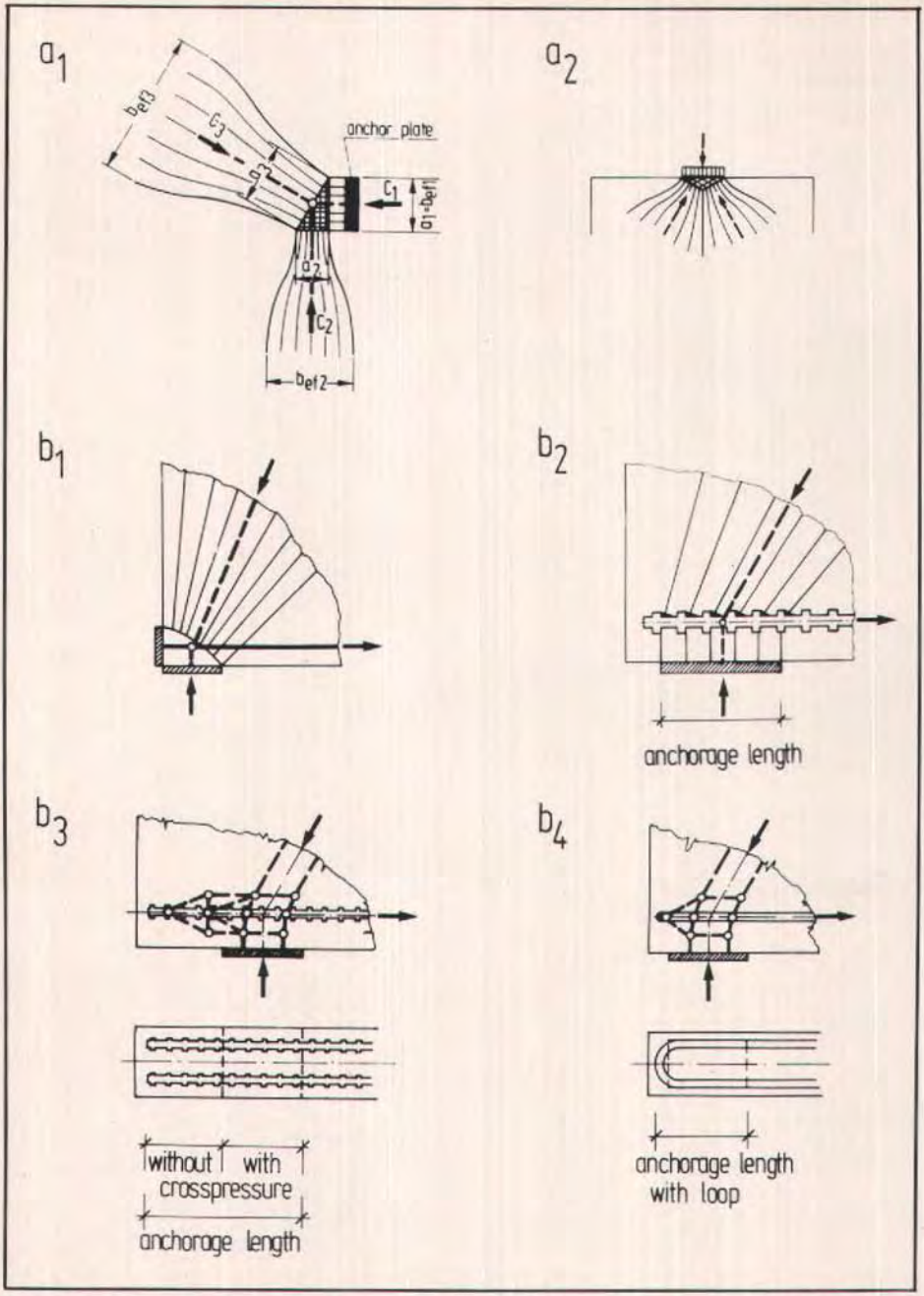

Fig. 19. Examples of the basic types of nodes: (a) CCC-nodes. Idealized "hydrostatic" singular nodes transfer the concentrated loads from an anchor plate (a_1) or bearing plate (a_2) into (bottle shaped) compression fields; (b) CCT-nodes. A diagonal compression strut and the vertical support reaction are balanced by reinforcement which is anchored by an anchor plate behind the node (b_1), bond within the node (b_2), bond within and behind the node (b_3), bond and radial pressure (b_4).

Failure Criteria for Concrete

The strength of the concrete in compression fields or within nodes depends to a large extent on its multiaxial state of stress and on disturbances from cracks and reinforcement.

(a) Transverse compression is favorable especially if it acts in both transverse directions, as for example in confined regions. Confinement may be provided by transverse reinforcement or by bulk concrete surrounding a relatively small compression field (see Fig. 21).

(b) Transverse tensile stresses and the cracks caused by them are detrimental.[23] The concrete may fail considerably below its cylinder strength if the transverse tension causes closely spaced cracks approximately parallel to the principal compression stresses such that the prisms between those cracks are ragged and narrow. The reduction of compressive strength is small or nominal if the tensile forces are carried by the reinforcement and the cracks are wide enough apart.

(c) In particular, cracks which are not parallel to the compressive stresses are detrimental.

In 1982, an empirical formula for calculating the strength of parallel concrete compression fields with transverse tension was published by Collins et al.,[23] and 2 years later a similar formula was introduced into the new Canadian CSA-Standard A 23.3-M 84.[24] These formulas summarize the influence of such significant parameters as crack width, crack distance and crack direction by the transverse tensile strain ϵ_t

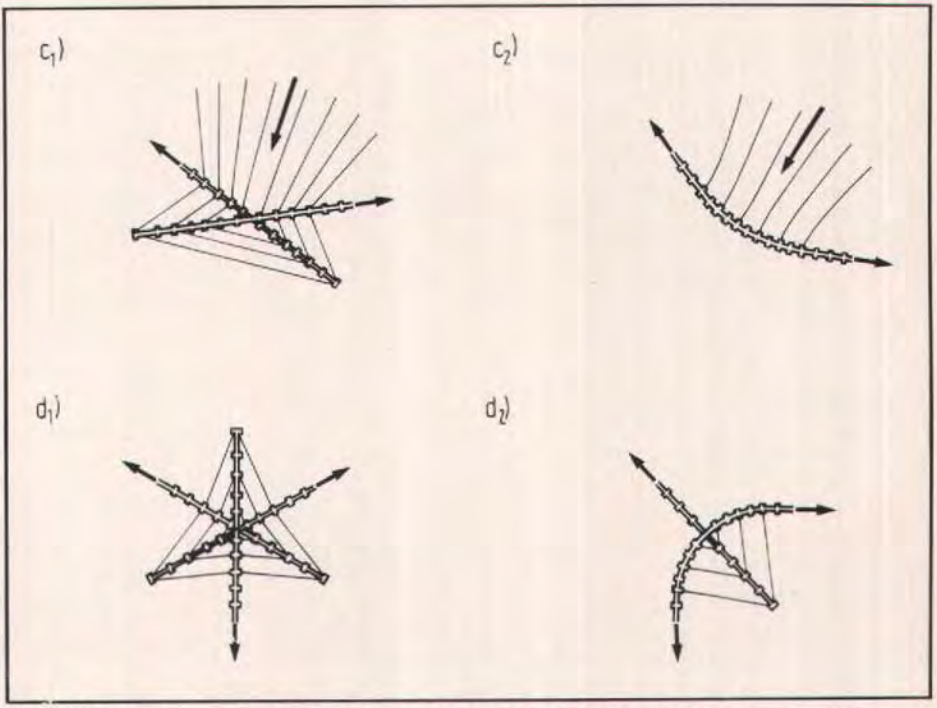

Fig. 19 (cont.). Examples of the basic types of nodes: (c) CTT-nodes. A compression strut is supported by two bonded reinforcing bars (c_1), respectively, by radial pressure from a bent-up bar (c_2); (d) TTT-nodes, as above with the compression strut replaced by a bonded tie.

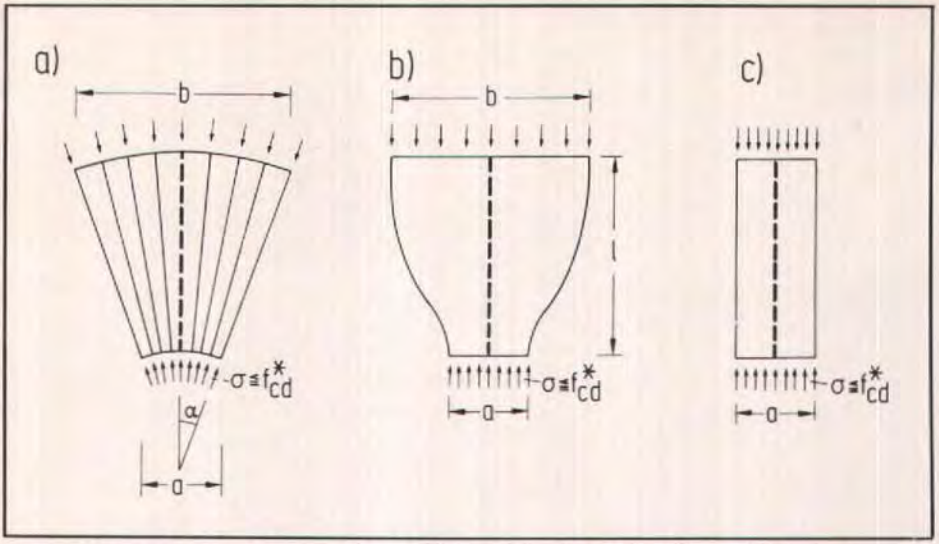

Fig. 20. The basic compression fields: (a) the "fan"; (b) the "bottle"; (c) the "prism".

which, however, is not readily available in the analysis.

For practical purposes, the following simplified strength values of f_{cd}^* are proposed for dimensioning all types of struts and nodes:

$f_{cd}^* = 1.0\ f_{cd}$: for an undisturbed and uniaxial state of compressive stress as shown in Fig. 20c;

$f_{cd}^* = 0.8\ f_{cd}$: if tensile strains in the cross direction or transverse tensile reinforcement may cause cracking parallel to the strut with normal crack width; this applies also to node regions where tension steel bars are anchored or crossing (see Fig. 19b);

$f_{cd}^* = 0.6\ f_{cd}$: as above for skew cracking or skew reinforcement;

$f_{cd}^* = 0.4\ f_{cd}$: for skew cracks with extraordinary crack width. Such cracks must be expected, if modelling of the struts departs significantly from the theory of elasticity's flow of internal forces (e.g., due to redistribution of internal forces in order to exploit a maximum ultimate capacity).

Note that f_{cd} denotes the concrete compressive design strength, which is related to the specified compressive strength f_c' and which in turn depends on the safety factor of the designated code of practice. According to the CEB Code, f_{cd} is determined by:

$$f_{cd} = \frac{0.85\ f_c'}{\gamma_c}$$

where $\gamma_c = 1.5$ is the partial safety factor for the concrete in compression and the coefficient 0.85 accounts for sustained loading. In the CEB Code,[26] $\phi = 1.0$ in all cases and the load factors for dead and live loads are 1.35 and 1.5, respectively.

The increase in strength due to two- or three-dimensional states of compressive stresses may be taken into account if the simultaneously acting transverse compressive stresses are considered reliable.

Skew cracks are not expected, if the theory of elasticity is followed sufficiently closely during modelling. This means that the angle between struts and ties entering a singular node should not

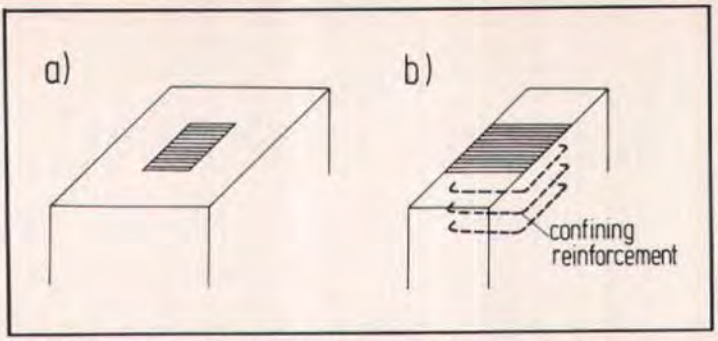

Fig. 21. Confinement (a) by the surrounding concrete; (b) by reinforcement increases the design compression strength f^*_{cd}.

be too small. However, skew cracks may also be left over from a previous loading case with a different stress situation.

Before deciding on one of the given strength values, both transverse directions must always be considered.

General rule

Since singular nodes are bottlenecks of the stresses, it can be assumed that an entire D-region is safe, if the pressure under the most heavily loaded bearing plate or anchor plate is less than 0.6 f_{cd} (or in unusual cases 0.4 f_{cd}) and if all significant tensile forces are resisted by reinforcement and further if sufficient development lengths are provided for the reinforcement. Only refinements will be discussed in the following Sections 4.2 through 4.5.

4.2 Singular Nodes

Singular nodes equilibrate the forces of the ties and struts acting on them relatively abruptly as compared to the smeared nodes. The deviation of the forces occurs over a short length or small area around the theoretical nodal point. Such nodes originate mainly from single loads or support reactions and from concentrated forces introduced by the reinforcement through anchor plates, bond, or radial pressure inside bent reinforcing bars such as loops. Furthermore, geometrical discontinuities (e.g., reentrant corners) can cause stress concentrations which are represented by a singular node.

Although numerous possibilities exist for detailing nodes (and despite the fact that they all behave somewhat differently), in most cases their forces balance each other in the interior of the node through direct concrete compressive stresses, which is a helpful observation. The ideal tie anchor (with a plate) transfers the load "from behind" and thus causes compression in the node (Fig. 19b$_1$). Also, bond is essentially a load transfer via concrete compressive stresses which are supported by the ribs of the steel bar (Fig. 19b$_2$ and b$_3$) and by radial pressure in bent bars (Fig. 19b$_4$).

Even in these cases the flow of forces can be visualized by strut-and-tie-models with singular nodes at the ribs of the bar. If these models require concrete tensile ties, this is valuable information for the design engineer. However, for practical purposes, the anchorage and lap lengths of the applicable codes of practice should be used.

In summary, then, dimensioning singular nodes means:

(a) Tuning the geometry of the node with the applied forces.

For CCC-nodes it is helpful, though not at all mandatory, to assume the bor-

derline to be perpendicular to the resultant of the stress field and the state of stress within the interior of the node to be plane hydrostatic. In this particular case the unequivocal geometrical relation $a_1 : a_2 : a_3 = C_1 : C_2 : C_3$ results (Fig. 19a$_1$), which may be used for dimensioning the length of the support or the width of an anchor plate. However, arrangements of forces which lead to stress ratios down to 0.5 on adjacent edges of a node are satisfactory. Departing even more from hydrostatic stress and still disregarding the nonuniform stress distribution in the node may lead to compatibility stresses, which are not covered by the strength values given above.

When designing a singular CCT-node, the design engineer must be aware that the curvature of the load path and the corresponding compression

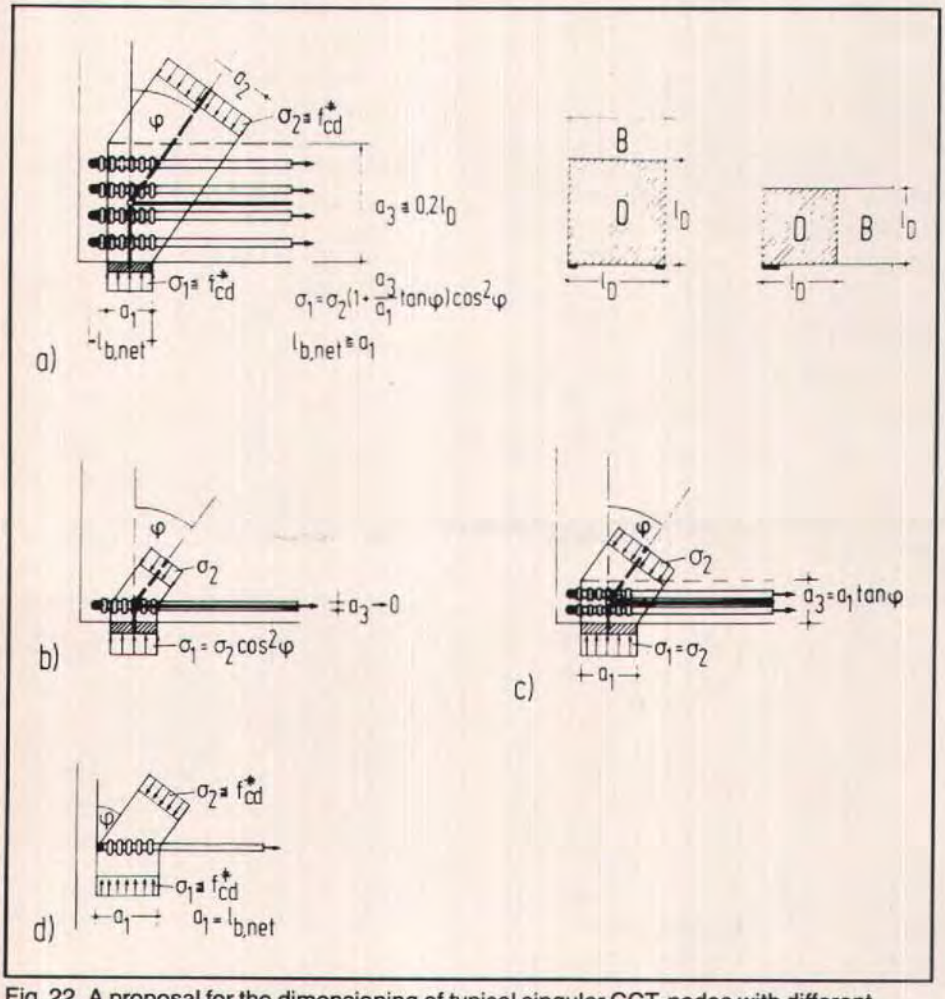

Fig. 22. A proposal for the dimensioning of typical singular CCT-nodes with different reinforcement layouts: (a) multilayered tie (a_3 relatively large, $\sigma_2 < \sigma_1$); (b) single layer tie (a_3 small $\sigma_2 > \sigma_1$); (c) special case in between ($\sigma_2 = \sigma_1$); (d) same type as (b) with pressure from a compression field.

field is largest at the origin of the concentrated load, i.e., next to the bearing plate or anchor plate (see Figs. 9 and 10). The ties and plates should be arranged accordingly.

(b) Checking whether the concrete pressures within the node are within the limits given in Section 4.1.

This condition is automatically satisfied for the entire node region, if the stresses along the borderlines of the node do not exceed those limits and if the anchorage of the reinforcement in the node is safe. If the reinforcement is anchored in the node region, cracks are possible and correspondingly the concrete strength for cracked concrete applies.

For CCT-nodes with bonded reinforcement arranged according to Fig. 22, a check of concrete stresses σ_1, respectively, σ_2 in the adjacent compression struts is sufficient. Since in most cases it is apparent from the geometry of the node which pressure out of the two struts controls, only one of them needs to be analyzed. An analysis on the basis of Fig. 22 rewards reasonably the arrangement of multilayered reinforcement distributed over the width a_3 (Fig. 22a) compared with a tie consisting of one layer only (Fig. 22b and d).

(c) Ensuring a safe anchorage of ties in the nodes (except for CCC-nodes).

In the case of anchor plates, this involves a check of the bending strength of the anchor plate and of the welded connection with the tie. In this case a smooth surface of the tie where it crosses the node is better than good bond quality because strain compatibility with the bonded bar will tend to crack the node's concrete.

In the case of directly anchored reinforcing bars, hook or loop anchorages (with cross-pressure in CCT-nodes) are preferred. Generally, the minimum radius allowed by the applicable code is selected.

For straight bar anchorages, the length of the anchorage is selected following the designated code. The design engineer must ensure that it is located within and "behind" the node (Fig. 19b_2 and b_3). Anchorage begins where the transverse compression stress trajectories of the struts meet the bar and are deviated; the bar must extend to the other end of the node region in order to catch the outermost fibers of the deviated compression stress field (Fig. 18b_3, c_3).

4.3 Smeared Nodes

Since D-regions usually contain both smeared and singular nodes, the latter will be critical and a check of concrete stresses in smeared nodes is unnecessary. However, if a smeared CCT-node is assumed to remain uncracked, the tensile stresses of the corresponding concrete stress field need to be checked (Section 4.5). An example of this case is Node 0 in Fig. 18c1 and the stress field in Fig. 18c2.

Safe anchorage of reinforcement bars in smeared nodes must be ensured following the rules for singular nodes (Section 4.2).

4.4 Concrete Compression Struts — Stress Fields C_c

The fan-shaped and prismatic stress fields do not develop transverse stresses and accordingly the uniaxial concrete strenth f_{cd} applies. If transverse stresses, cracks or tension bars cross the strut, the strength may be based on the values given in Section 4.1.

The bottle-shaped compression stress field (Fig. 20b) applies to the frequent case of compressive forces being introduced into concrete which is unreinforced in the transverse direction. Spreading of the forces causes biaxial or triaxial compression under the load and transverse tensions farther away. The transverse tension (combined with longitudinal compressive stresses) can re-

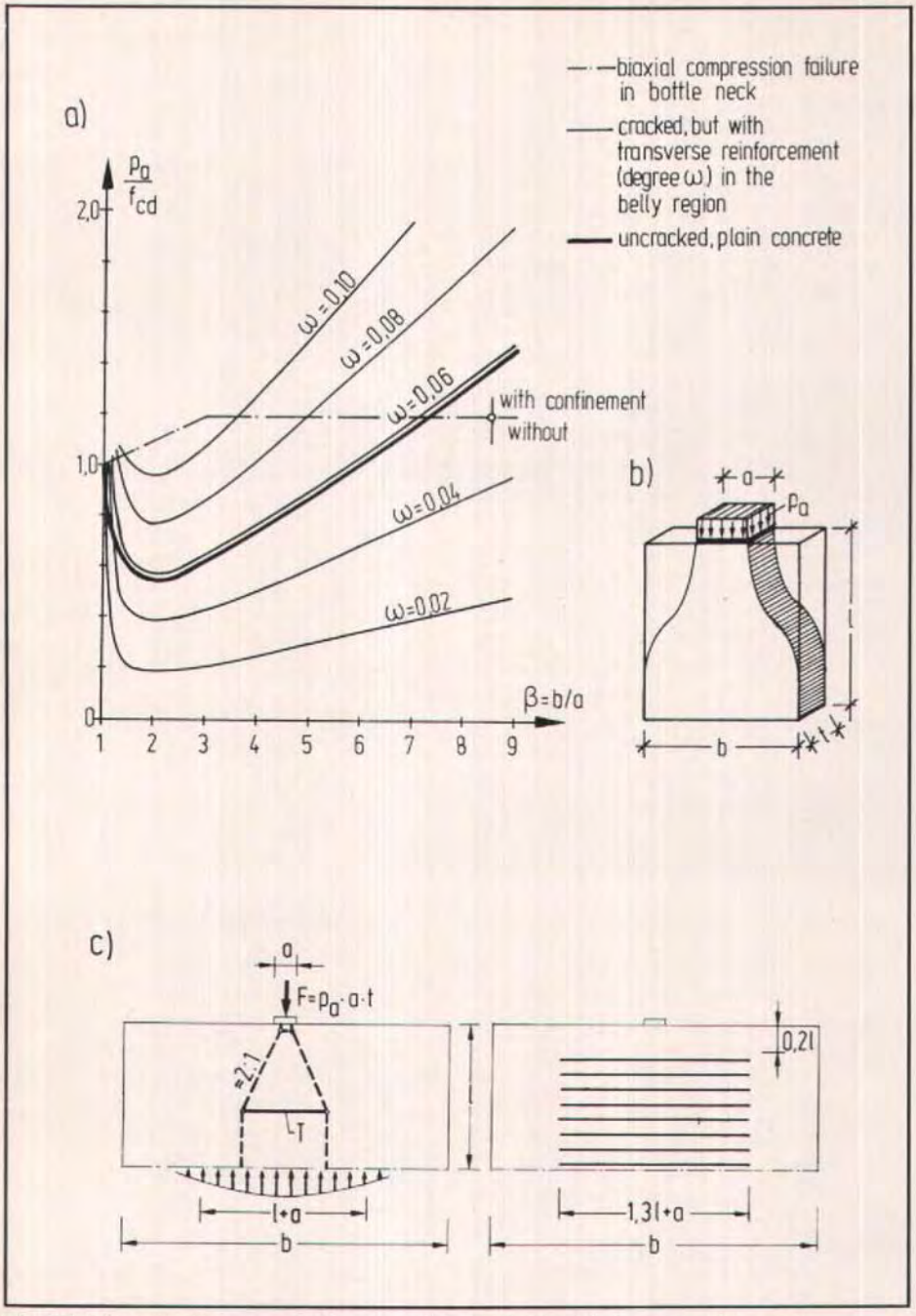

Fig. 23. Dimensioning plane bottle shaped stress fields: (a) diagrams giving safe pressure values P_a with regard to cracking and crushing of plain unreinforced concrete stress fields, yielding of transverse reinforcement and biaxial compression failure in the bottle neck region; (b) geometry of the stress field; (c) model and reinforcement layout of stress field with transverse reinforcement ω.

sult in early failure. Again, the failure criteria from Section 4.1 apply.

The general rule given at the end of Section 4.1 usually makes the calculation of stresses within the stress field unnecessary. However, for questionable cases, computational aids should be provided to facilitate the safety check.

As an example, Fig. 23a shows diagrams for checking plane bottle shaped stress fields in D-regions.[12,13,17] This stress field can be characterized by the width a of the anchor plate, the maximum width b available in the structure for the stress field and the distance l of the anchor plate from the section where the stress trajectories are again parallel (see Fig. 23b and also Fig. 20b). The diagram for compression fields without transverse reinforcement (bold line) is based on an elastic analysis, a concrete tensile strength of $f_{ct} = f'_c/15$ and a biaxial compressive tensile failure criterion as given in Fig. 26b.

It can be seen, that for certain geometrical relations a pressure at the anchor plate as low as $0.6f'_c$ could cause cracking. However, the failure load of the strut is usually higher than its cracking load. A comparison of test results shows that the diagram generally appears to be considerably on the safe side and further research in this area is required. Better knowledge is also needed on substantially nonsymmetrical stress fields which originate from singular nodes with tension ties crossing or anchored there. Comparisons with test results suggest that checking the singular node (Section 4.2) and applying the diagrams of Fig. 23 is also safe for those cases.

The bottle shaped stress field provides a safe lower bound for unreinforced compression struts, whereas an indiscriminate application of the theory of plasticity to cases such as those shown in Fig. 7 (mainly Fig. 7a) would permit prismatic stress fields between two opposite anchor plates with $1.0f_c$ as a failure stress and could lead to a premature failure.

For compression struts with transverse reinforcement the failure loads analyzed with the model in Fig. 23c are also given in Fig. 23a. It can be seen that a reinforcement ratio:

$$\omega = \frac{a_s f_{sy}}{t f_{cd}} = 0.06$$

(where a_s is the cross section of reinforcement per unit length) approximately compensates for the tensile strength of the concrete.

If it is desired not to rely so heavily on the concrete tensile strength, lower reinforcement ratios may be used with reduced values of p_d/f_{cd} as shown in Fig. 23a.

The compressive strength of compression reinforcement may be added to the concrete strength if the reinforcement is prevented from buckling.

4.5 Concrete Tensile Ties — Stress Fields T_c

In the case of uncracked tensile stress fields, the tensile strength of concrete is used. Although it is difficult to develop design criteria for this case, it would be even worse to maintain the formalistic view that the tensile strength of concrete cannot and therefore must not be utilized. Following the flow of forces gap free and consistently with strut-and-tie-models will inevitably show that equilibrium can frequently only be satisfied if ties or tensile forces can be accepted in places where, for practical reasons, reinforcement cannot be provided, i.e., if the tensile strength of concrete is utilized.[18] It should be apparent that no anchorage, no lap, no frame corner, no slab without stirrups and (as shown) no unreinforced strut or compression member can work without using the tensile strength of concrete. Unfortunately, most codes of practice do not recognize this fact and, therefore, surrogates such as bond, shear

and other misnomers have been introduced. As a result, codes have become unduly imprecise and complicated.

Until further research work is available in this field, the following simple guidelines are proposed, which appear to yield safe results when compared to tests:

The tensile strength of concrete should only be utilized for equilibrium forces where no progressive failure is expected. Thereby, restraint forces and microcracks have to be taken into account, even in "uncracked" and unloaded concrete. As shown in Fig. 24, redistribution of stresses which avoids progressive cracking may be assumed to be possible if at any part of the stress field a cracked failure zone with an area ΔA_c can be assumed, without the increased tensile stresses in the remaining section exceeding the tensile strength f_{ct}.

As a preliminary proposal, it is suggested that:

$$\Delta A_c \geq 4 d_g^2 \text{ and } \geq A_{ct}/10$$

where

A_{ct} = area of tensile zone and

d_g = diameter of largest aggregate

Progressive failure of a section or member generally starts from the periphery of structures in the case of steep stress gradients, as for example in the bending tensile zone of beams (Fig. 25).

The tensile stresses may be analyzed with a linear elastic materials law. Stress peaks in the outer fibers or at failure zones may be distributed over a width of 5 cm (2 in.) but not more than $3\,d_g$, a rule which finds its justification in fracture mechanics of concrete.[13]

The design engineer will have to decide case by case which fraction of the tensile strength can be used for carrying loads and which fraction has been used up by restraint stresses. The latter stresses are usually large in the longitudinal direction of a structural member and at its surface, but are smaller in the transverse direction and in greater depth.

If the tensile stress field is crossed by a compression field, the reduced biaxial strength must be considered. The graph (see Fig. 26c) provides a safe assumption.

4.6 Reinforced Ties T_s

Usually, reinforcing steel should be provided to resist tensile forces. The axis of the steel reinforcement must coincide with the axis of the tie in the model. The dimensioning of these ties is quite straightforward; it follows directly from the cross section A_s (reinforcing steel) or A_p (prestressing steel) and the yield strength f_{sy} and f_{py} of the respective steels:

$$T_s \leq A_s f_{sy} + A_p \Delta f_p$$

Since it is proposed here (see Section 5.3) to introduce prestress as an external load into the analysis and dimensioning, the acting tie force T_s is the result of all external loads (including prestress). Then, however, part of the strength of the prestressed steel is already utilized by prestressing and only the rest, Δf_p, is available to resist T_s.

4.7 Serviceability: Cracks and Deflections

If the forces in the reinforced ties under working loads are used and their effective concrete area $A_{c,ef}$ as defined in the CEB Model Code[26] or in Ref. 19 is attributed to them, the known relations for crack control can be applied directly.[19,20,26] In principle, it is proposed that the same model be used at the ultimate limit state and the serviceability limit state.

In very critical cases it may be advantageous to select a model very close to the theory of elasticity, i.e., to provide reinforcement that follows the path of the elastic stresses. However, proper

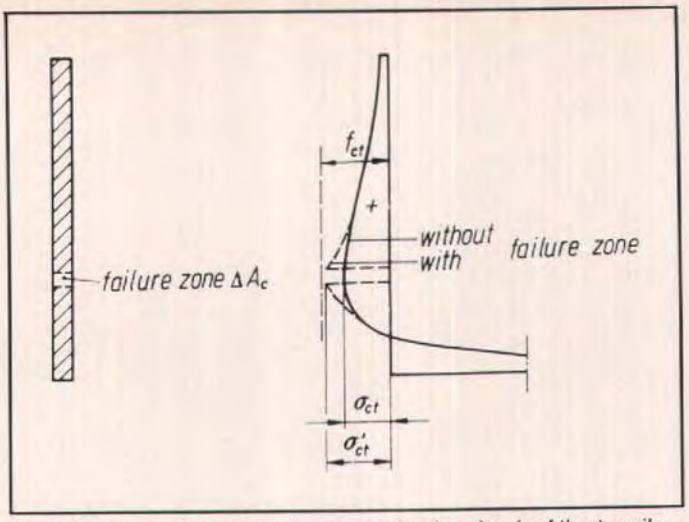

Fig. 24. Assumption of a failure zone for the check of the tensile strength of a concrete tension tie T_c.

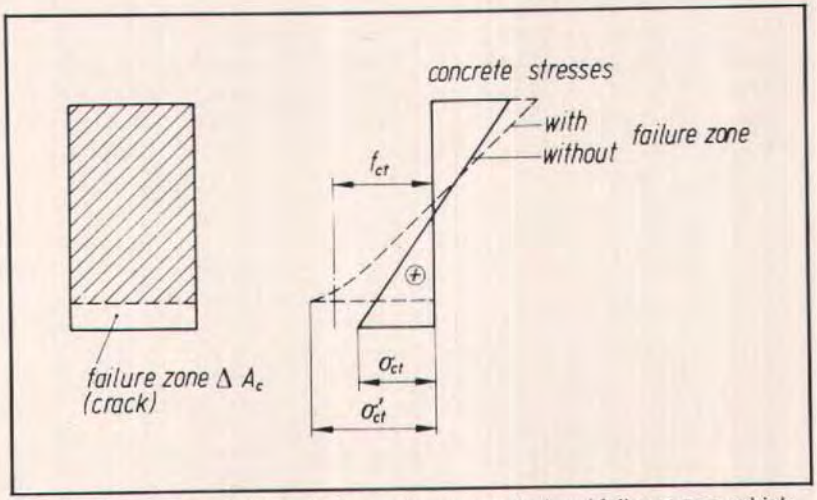

Fig. 25. Progressive failure of a beam because of a local failure zone, which increases maximum tensile stresses σ_{ct} to $\sigma_{ct} > f_{ct}$.

detailing (provision of minimum reinforcement, adequate selection of bar diameters and bar spacing) is usually better than sophisticated crack calculations.

Having determined the forces of the model, the analysis for the deformations is straightforward. Since the contribution of the concrete struts is usually small, it is sufficient to use a mean value of their cross section even though this varies over their length. For the ties, tension stiffening follows from the above crack analysis.

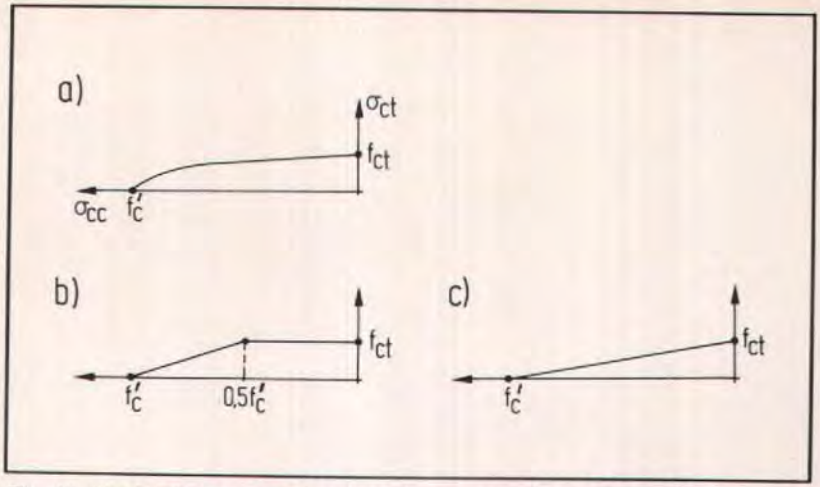

Fig. 26. The biaxial compressive-tensile strength of concrete and two simplified assumptions for analytical application.

4.8 Concluding Remarks

Despite the fact that the major principles have been set forth in this chapter, much research work remains to be done with respect to the more accurate dimensioning of the concrete ties and struts. This, however, should not preclude application of the proposed procedure as a whole. Current design methods of D-regions are, in fact, worse because they simply ignore such unsolved questions.

Following the flow of forces by strut-and-tie-models is of considerable value even if used only to find out if, and where, reinforcement is needed. In a structure with reasonable dimensions which is not over-reinforced, the concrete compressive stresses are usually not the main concern. Furthermore, it is much more important to determine where the tensile strength of the concrete is utilized, and then to react with reinforcement if possible, than to quantify the strength of the concrete ties.

In the next chapter the application of the foregoing principles is elaborated upon with many design examples.

5. EXAMPLES OF APPLICATION

With an unlimited number of examples it might be shown, that tracking down the internal forces by strut-and-tie-models results in safe structures and quite often provides simple solutions for problems which appear to be rather complicated. It should, however, also be admitted that it sometimes takes some effort to find the appropriate model. However, the strut-and-tie-model is always worthwhile because it can often reveal weak points in a structure which otherwise could remain hidden to the design engineer if he approaches them by standard procedures.

The major advantage of the method is to improve the design of the critical D-regions. However, the authors also believe that the concept will lead to more realistic and workable codes of practice also for the B-regions. Therefore, the B-regions are first discussed here by ap-

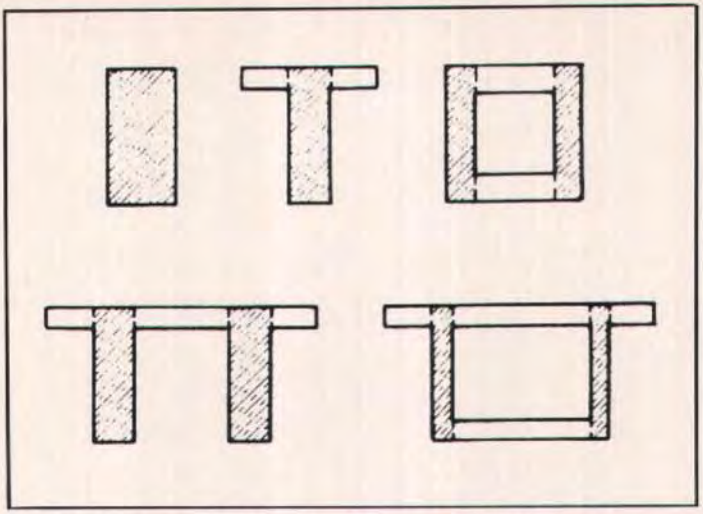

Fig. 27. Various cross sections of beams and their webs.

plying truss or strut-and-tie-models to them. Thereafter, some D-regions are treated (see Refs. 1 and 3 for additional design examples).

Finally, the basic approach to prestressed concrete is discussed and illustrated with several examples.

5.1 The B-Regions

The plane rectangular webs considered here apply not only to beams with rectangular cross section but may also be part of a T, I, double tee or box beam (see Fig. 27). The shear loading may result from shear forces or from torsion (see Fig. 28), the axial forces from external loads or prestress (see Section 5.3).

As discussed above, the web of a B-region modelled with the same criteria as proposed for the strut-and-tie models of the D-regions would in most cases lead to a standard truss (Fig. 8), with the inclination θ of the struts oriented at the inclination α of the principal compressive stresses according to the theory of elasticity.

The design of beams for bending, shear and torsion is then nothing more

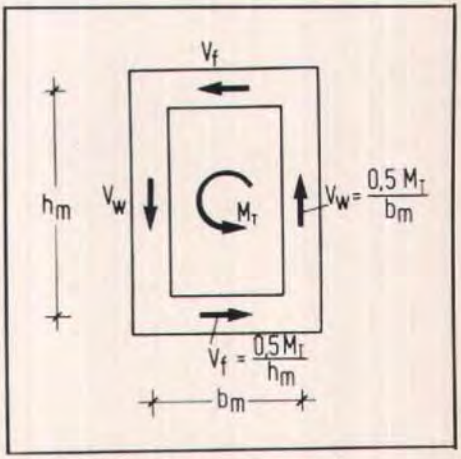

Fig. 28. Shear forces as a result of torsion.

than the well known analysis of the truss forces and the check of the compressive stresses of the concrete and the tensile stresses of the reinforcement. Since this analysis of the truss includes the chords, possible problems like the staggering effect or the question why both chords are simultaneously in tension at the points of inflection (moments = 0, shear forces $\neq$ 0) are solved automatically.

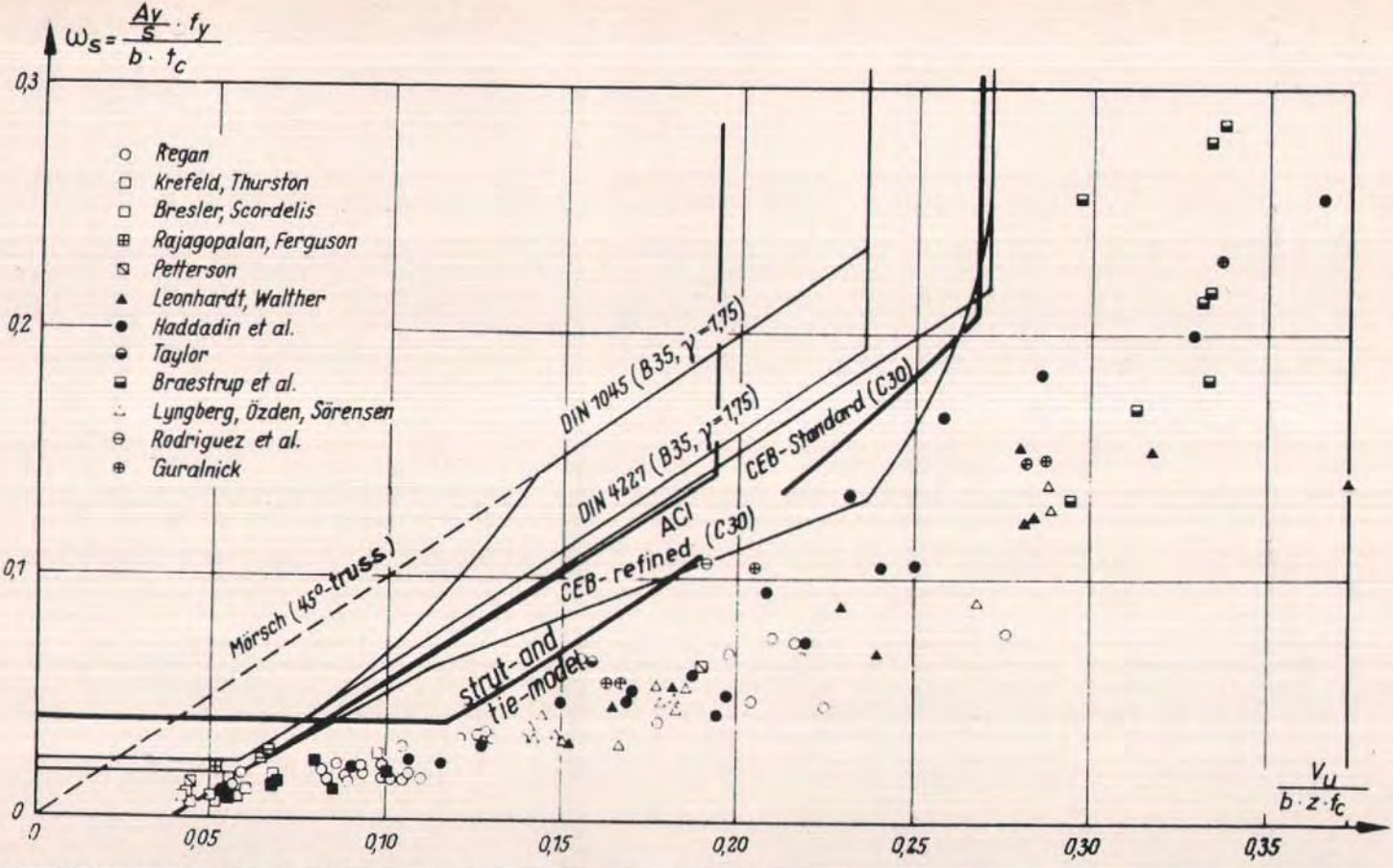

Fig. 29. Comparison of the required amount of vertical stirrups in a beam according to experiments, to different codes and to a strut-and-tie-model analysis, corresponding to Fig. 33, Ref. 15.

It should be mentioned also, that in contrast to the bending theory, truss models are capable of dealing with stresses perpendicular to the beam's axis and variable shear forces along the axis:

(Note that these shear forces are not compatible with Bernoulli's assumption of plane strains as defined for the B-regions.)

Why then, if everything appears to be so simple, is there a "shear riddle" and why has the "shear battle" been waged for so many decades. In fact, the endless discussions on shear could be "put to bed" if design engineers contented themselves with the same level of accuracy (and simplicity) in the B-regions as they do for the D-regions.

Since in principle it makes no sense to design B- and D-regions, which are parts of the *same* structure, at different levels of sophistication, there would be very good reasons for such a comparable accuracy in every aspect of the analysis. However, at present this seems not to be appropriate mainly because of historical reasons, i.e., since so many researchers have invested so much time investigating the B-regions, they have found that (under certain conditions) savings in stirrup reinforcement are possible compared to simple truss design.

Fig. 29 shows the well known plot (in dimensionless coordinates) of the ultimate shear forces V_u versus the amount of stirrups a_v (cm²/m) required to carry V_u for beams in pure bending and shear. If the straight line according to the truss model with 45 degree struts (Mörsch) is compared with the compiled test results, it is found that a large discrepancy results, mainly in the region of low to medium values of V_u.

The discrepancy is reduced if smaller angles of inclination of the struts than those taken from the elastic stresses at the neutral axis are assumed. In fact, from test results it is observed that the angle α of the initial crack from pure shear can be up to 10 degrees less than 45 degrees, depending on the amount of stirrup reinforcement and the width of the web expressed by b_w/b. If, in addition, axial compressive forces such as prestress act, α is a priori smaller than 45 degrees but deviates less, that is, the smaller α, the closer it is to the angle given by the theory of elasticity.[14]

However, the fact remains that the explanation of the real stirrup stresses only by the standard truss would imply the assumption of struts with less than realistic inclinations, in extreme cases down to $\theta = 15$ degrees. Other known explanations are also not satisfactory: An inclined compression chord would simultaneously reduce the inner lever arm z, which is not compatible with the B-region assumption of plane strains and can, therefore, develop only in the D-regions which extend from the supports; the pure arch or direct struts with tie action can only be applied if the tie is not bonded with the surrounding concrete or to "short" beams, i.e., beams without B-regions; the dowel action of the reinforcement, though leading in the right direction, can only to a small degree be responsible for the effect under discussion.

What does really happen in the web? On the following pages it will be shown, that it is the concrete's tensile strength and aggregate interlock in the web which really causes the reduction of the stirrup stresses. Readers who are satisfied with this explanation or with the pure truss design of B-regions may now jump ahead to Section 5.2. The authors wrote what follows not with the intention of adding one more paper to the shear dispute, but only to show the effectiveness of the strut-and-tie-model approach even for such cases.

After the principal tensile stresses have reached the tensile strength of the concrete, the web cracks at angles as discussed above. Consequently, following the direction of the load, individual pieces of the web, only controlled in their movement by the

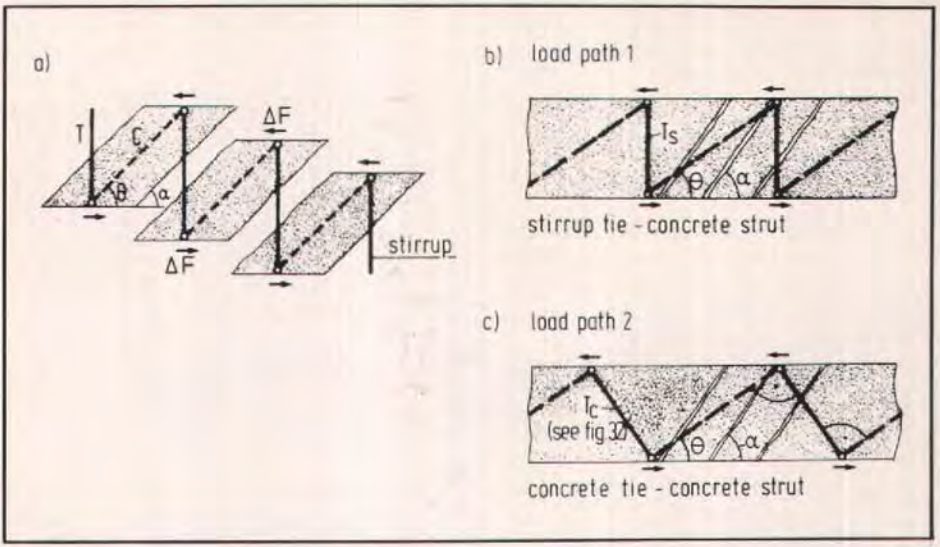

Fig. 30. Internal forces in the web due to shear: (a) kinematics of load path 1 if acting alone ($\theta = \alpha$); (b) through (c) load paths 1 and 2 in the web if acting combined ($\theta < \alpha$).

flanges, try to fall down. There, they are caught by the stirrups which hang up the load via T into the adjacent piece evoking C in the struts for vertical equilibrium (Fig. 30a). The chords (or flanges) provide horizontal equilibrium with additional tensile forces ΔF. This is the principal load path 1, if the concrete's tensile strength is disregarded (Fig. 30b).

Looking closer, it is recognized that the kinematics as described evoke an additional load path 2 (Fig. 30c) which combines with the load path 1 (Fig. 30b) but which is usually neglected: The vertical movement v has two components, the crack opening w perpendicular to the crack and a sliding Δ parallel to the crack (Fig. 31). The sliding Δ is obviously resisted by aggregate interlock in the crack and it appears reasonable to assume, that the resisting force R acts in the direction of Δ, i.e., parallel to the crack. The force R has two components, a compressive force C_c with an inclination $\theta < \alpha$ and a concrete tensile force T_c perpendicular to it (Fig. 32). Again, the chords are activated for equilibrium.

Both load paths jointly carry the load and therefore their combined compressive struts together assume the inclination $\theta \leq \alpha$. As long as it can be sustained by the concrete, the concrete tensile force perpendicular to the struts is responsible for the fact that the stirrups need to carry only part of the shear loads. However, it also causes the concrete of the struts to be biaxially loaded, thus either reducing their compressive strength or resulting in a second array of cracks with inclinations less than α, depending on the load case. Only if $\theta = \alpha$ does load path 2 disappear (Fig. 30a). When this occurs the compressive struts are uniaxially loaded and can therefore develop their maximum strength. Therefore, the maximum capacity of a beam for shear forces is achieved if the struts are parallel to the cracks and if the corresponding large amount of stirrups is provided.

What can so simply be described in words must also be accessible to a relatively transparent analysis. This is possible, if the compatibility between load

paths 1 and 2 is solved by plastic superposition of both the stirrup and the interlock forces, making use of the fact that aggregate interlock is sufficiently ductile. However, since a biaxial failure criterion for the concrete has to be applied, a reproduction of the analytical description (Ref. 15) would go beyond the scope of this paper. The result is plotted in Fig. 33 and compared there with results from experiments.

It is important to note that the beam "remembers" the initial inclination α of the diagonal cracks. This permits the logical introduction of the effect of prestress into web design, resulting in savings of stirrup reinforcement but also in an earlier compressive strut failure.

The analytical curve in Fig. 33, which gives also the actual inclinations $\theta \leq \alpha$ as a function of V_u, must be cut off before it intersects the abscissa (where $\theta = \alpha/2$), because a minimum of stirrup reinforcement is necessary in order to guarantee that a truss model can develop at all. As shown in Fig. 34, it is necessary to avoid that the flanges separate from the web after a diagonal crack has formed.

Of course, the longitudinal and transverse spacing of the stirrups must further be limited to ensure a parallel diagonal compression field. If the spacing is too large, the smeared diagonal compressive strength may be less than that taken for Fig. 33, because the stresses concentrate in the nodes with the stirrups (Fig. 35).

To use load path 2 in the practical design of the webs of B-regions — if it is considered desirable to be more sophisticated there than in the D-regions, where aggregate interlock or the concrete tensile strength is neglected — simple diagrams may be derived from Fig. 33. Even easier (and corresponding to the present CEB Model Code), it may be sufficient to reduce in the "low shear range" the acting shear force for stirrup design by an amount which is attributed to load path 2.

For that purpose, it may be sufficient

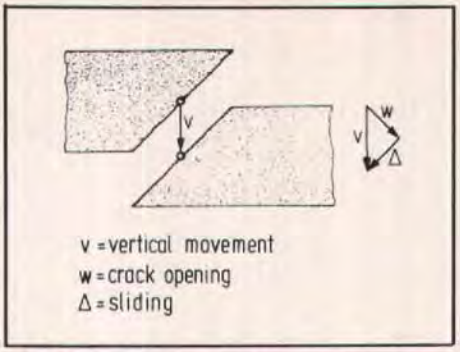

Fig. 31. Displacements in the web because of the crack.

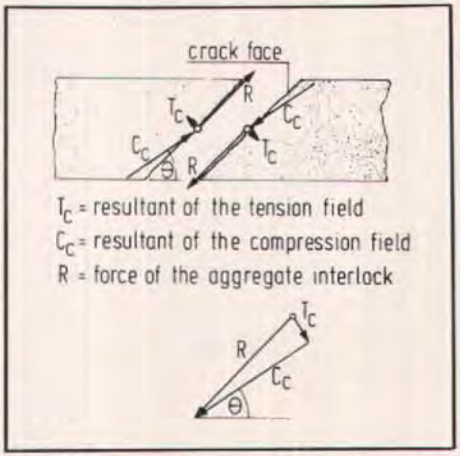

Fig. 32. Aggregate interlock force R and corresponding compression C_c and tension T_c in the concrete.

to replace the curved branch of the diagram in Fig. 33 by a straight line. It is only important that the design engineer is aware that reliance is placed on the concrete tensile strength in the web if this method is used to reduce the required amount of stirrups. Fig. 29 compares the amount of stirrup reinforcement derived in this way from the strut-and-tie-model with that from different codes and tests.

One might also ask whether the full design strength f_{cd} can be exploited in the compression chord of a beam, be-

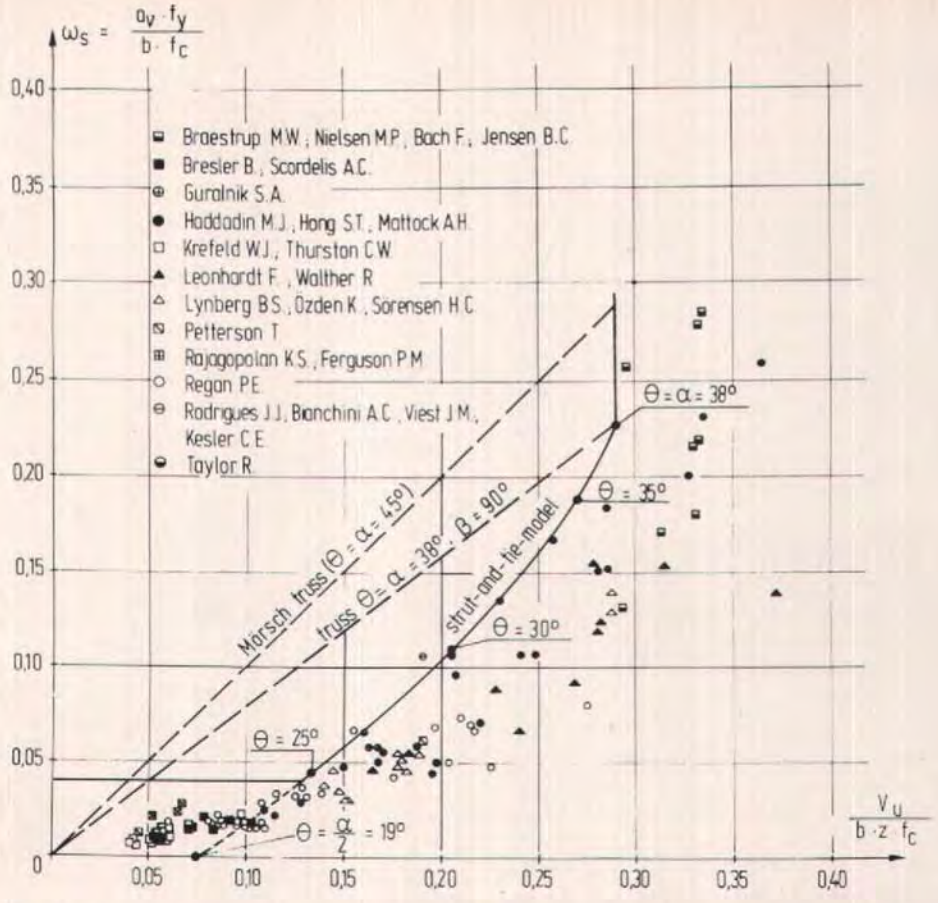

Fig. 33. Required amount of vertical stirrups in a web according to the strut-and-tie-model (for crack inclination $\alpha = 38$ degrees), compared with simple truss analogy and tests.

cause the chord is subject also to tensile strains in both transverse directions. In the horizontal direction such stresses are quite obvious in the flange of T-beams with transverse bending and transverse tension from the flange connection. In addition, there is vertical tension from compatibility with stirrup tensile strains. Some cross tension also exists in both directions in rectangular beams (Fig. 35).

The neglect of this fact in practical design is to some extent balanced by the usual neglect of the staggering effect in the compression chord, which reduces the forces in the compression chord as much as it increases the tension chord forces. However, if the chord forces are correctly derived from the truss model, the compression strength should be assumed to be only 0.8 f_{cd} according to Section 4.1.

Consider, in addition, a special but very frequent B-region, namely, beam or column with rectangular cross section loaded by an axial force in addition to shear forces and bending moments. This case is typical also for prestressed beams. If the axial force is large enough to keep the resultant of the normal force

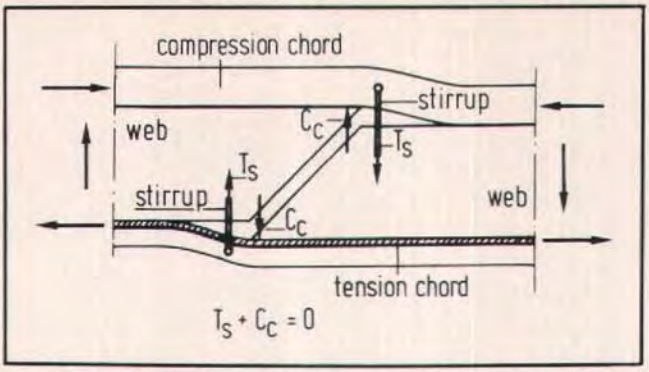

Fig. 34. A minimum amount of stirrups is necessary to tie together the web and the flanges.

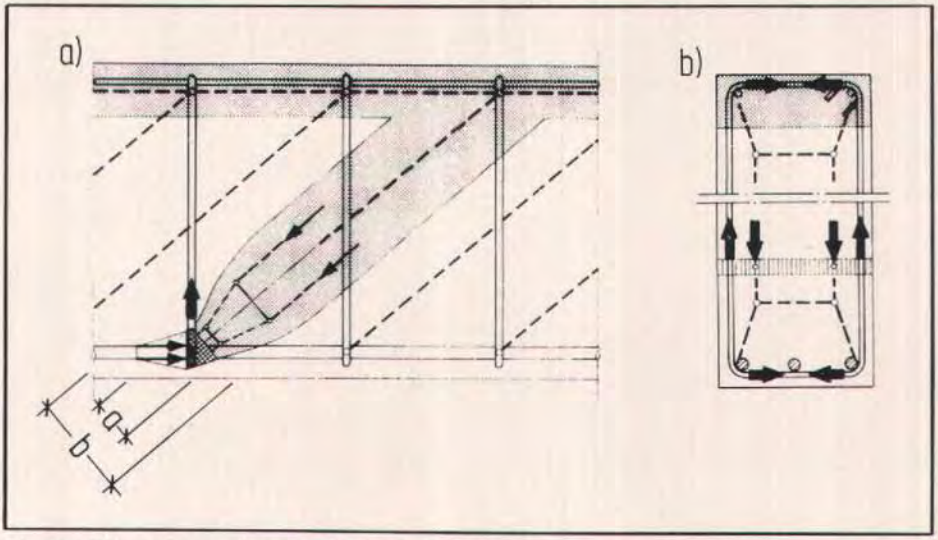

Fig. 35. The compression strut in the web with stirrups.

and of the moment within the kern of the cross section, the standard truss model no longer applies. Instead, all internal forces, including the shear force V, may be represented by a single inclined compression strut as in Fig. 36b.

Looking closer at the transition between such special B-regions and those represented by the truss model, it is found that the compression stresses distributed over the whole section have to converge into the narrow compression chord of the adjacent B-region, thereby creating transverse tensile stresses. These stresses can be assessed by the more refined model in Fig. 36c. Stirrups may be used to cover them; however, the model shows that tensile forces are inherently quite different from the shear forces in other B-regions but similar to those in the bottle shaped compression strut.

Speaking of B-region design, there remains the issue of "beams without

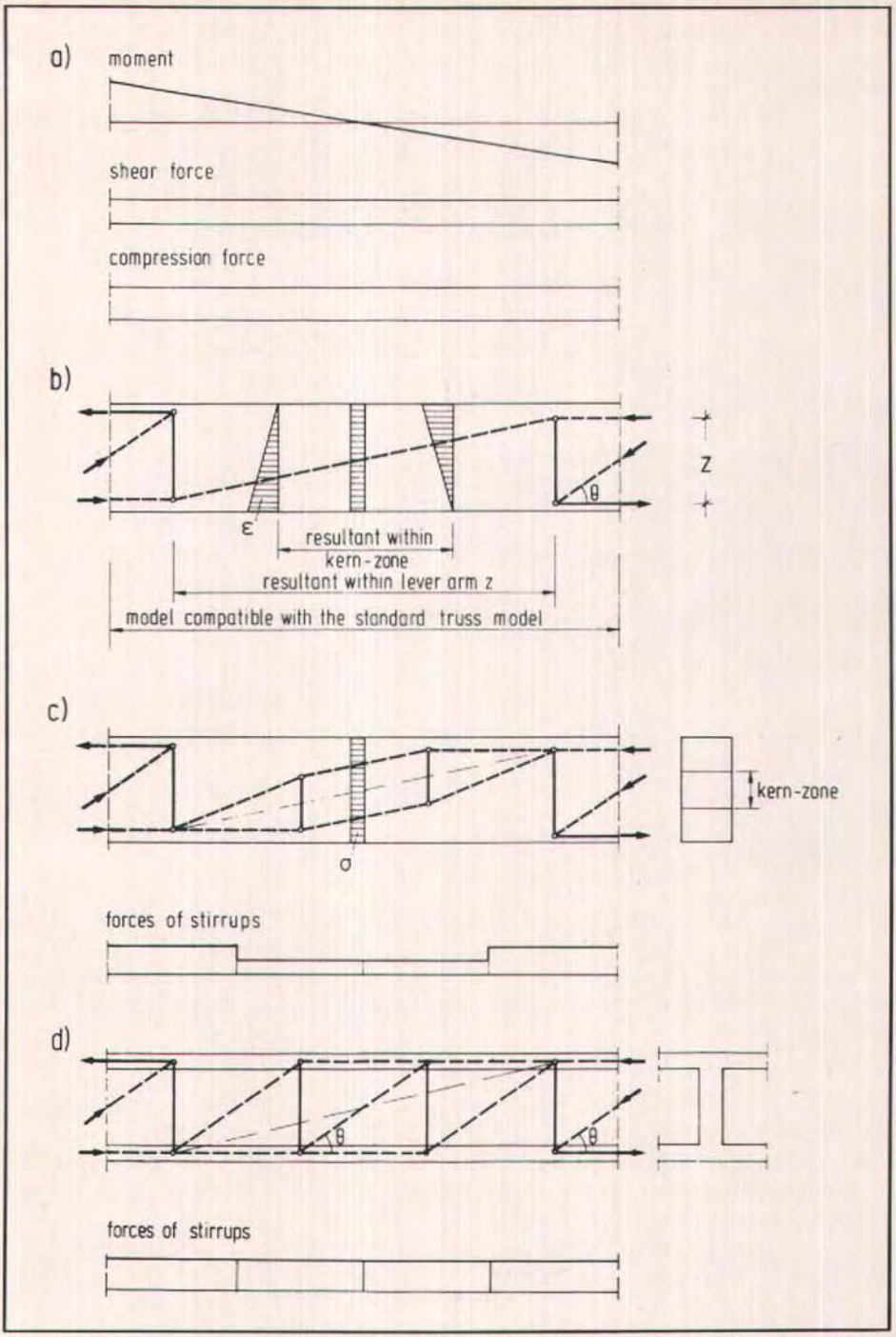

Fig. 36. Beam with compressive axial load: (a) sectional forces; (b) simplified model with a compression strut between the trusses; (c) refined model for a rectangular cross section with vertical tensile forces; (d) refined model for a I-beam.

shear reinforcement." Subdividing such beams into B- and D-regions first of all reveals that an arch-and-tie explanation only applies if the two D-regions of the opposite supports touch, leaving no significant B-region in between (see also Fig. 38a). Unbonded tensile chord reinforcement also stimulates arch-and-tie action, in other words it increases the length of the D-regions. The web of a real B-region, however, can carry shear loads only with the help of the concrete's tensile strength. There are several approaches based on rational models to exploit this finding.[12,16]

Again, as above, aggregate interlock is involved and, therefore, an analytical solution is rather complicated. On the other hand, the design engineer must know and understand what actually happens. Thus, it would realistically reflect the present situation to replace the permissible shear stresses of the current codes by the equivalent permissible concrete tensile stresses. Unfortunately, the stresses in the web are not uniformly distributed. Therefore, calibrated average admissible tensile stresses must be given in codes.

For completeness, it should be mentioned that a B-region contains several micro-D-regions, which again can be understood and designed with strut-and-tie-models. Fig. 35b shows why a stirrup must be closed on the top and bottom in a rectangular beam in order to take the cross tension from the strut support.

5.2 Some D-Regions

5.2.1 Deep Beam With a Large Hole (Numerical Example)

Given:
Dimensions (see Fig. 37a)
Factored load $F_u \equiv F = 3$ MN
Concrete compression design strength $f_{cd} = 17$ MPa
Reinforcement design yield strength $f_{yd} = 434$ MPa
Required:
Strut-and-tie-model
Forces in the struts and ties
Dimensioning of ties: reinforcement
Check of stresses of critical struts and nodes
Reinforcement layout
Solution:

(1) External equilibrium: reactions

$$A = 3 \times \frac{2.5}{7.0} = 1.07 \text{ MN}$$

$$B = 3 \times \frac{4.5}{7.0} = 1.93 \text{ MN}$$

$$F_u = A + B = 3.00 \text{ MN}$$

(2) Elastic stress analysis

This is a rather complicated structure. If the design engineer is not yet sufficiently experienced with modelling, he will first employ an elastic finite element program and plot the elastic stresses (see Fig. 37b) for orientation of the strut-and-tie-model.

(3) Modelling

The whole structure is essentially one D-region. Two short B-regions are discovered in the linear parts to the left and below the hole (see Fig. 37c).

The load path connecting the reaction B and its counterpart within F is readily plotted (see Fig. 37c). The positions of Nodes 1 and 2 are typical (see Fig. 15) and the forces C and T balancing these nodes in the horizontal direction are thus also given.

Before continuing modelling on the left side, the right side may be finished: The strut between Nodes 1 and 2 will spread and cause transverse tensile forces as sketched in Fig. 37d; optionally, it can be treated as a bottle shaped stress field as sketched in Fig. 37h and described later on.

Now the left side's boundary forces are clearly defined (Fig. 37e) and it can, therefore, be modelled independently from the right side. (In passing, it may be mentioned that the fictitious separation line between the two sides is where the overall shear force of the deep beam is zero and the bending moment is

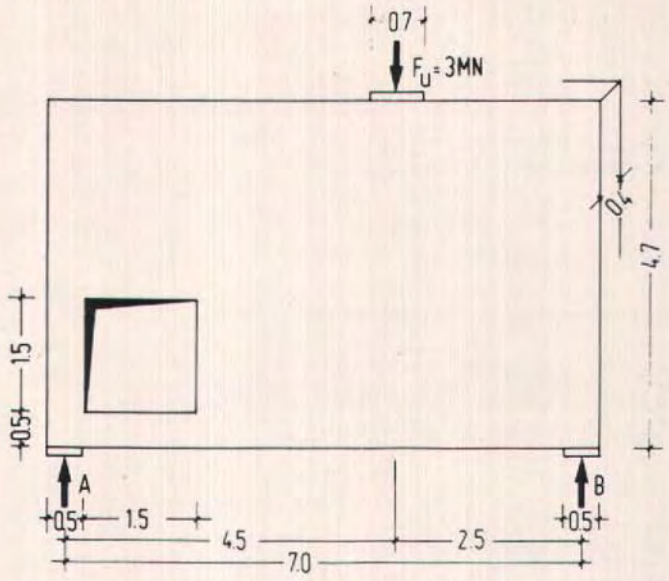

a) dimensions [m] and load

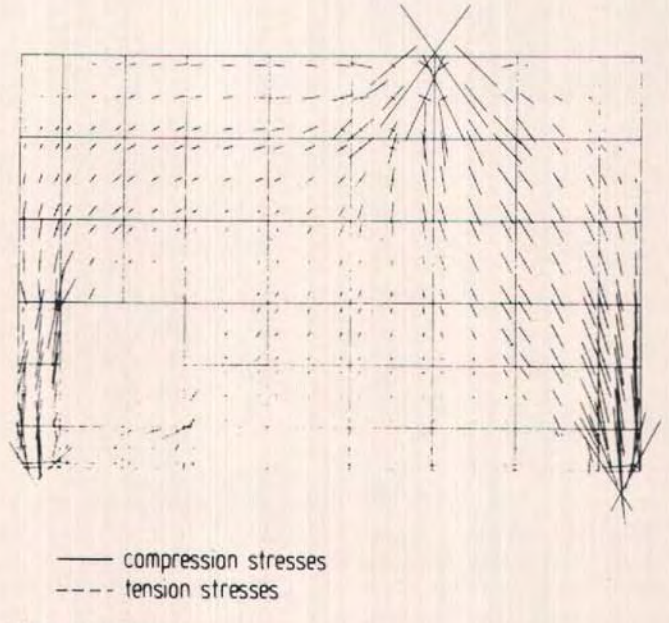

b) elastic stresses

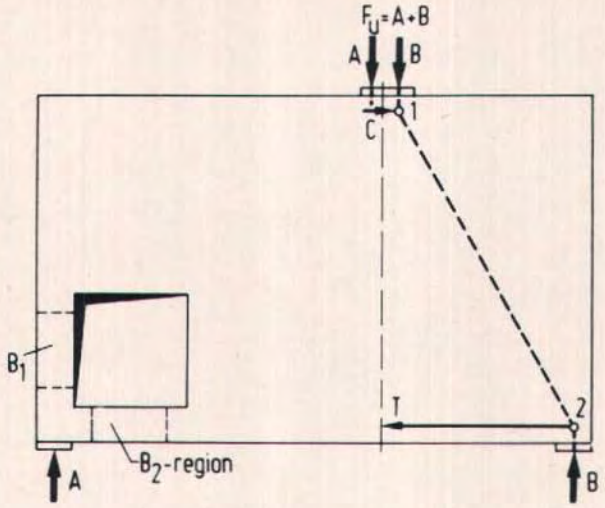

c) load path, right side

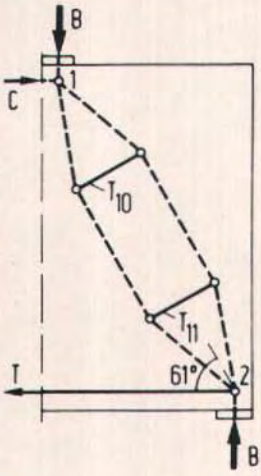

d) complete model, right side

Fig. 37. Deep beam with a large hole.

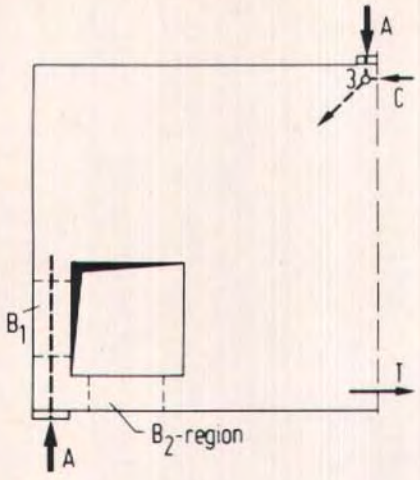

e) boundary forces, left side

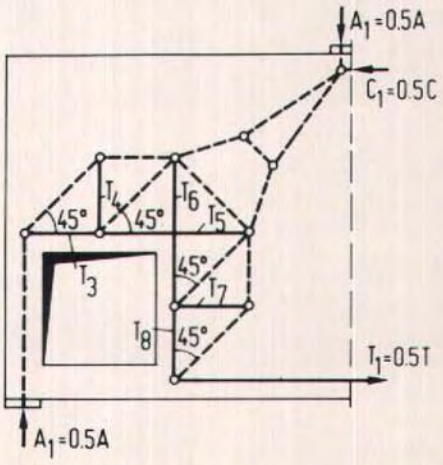

f) model 1, left side

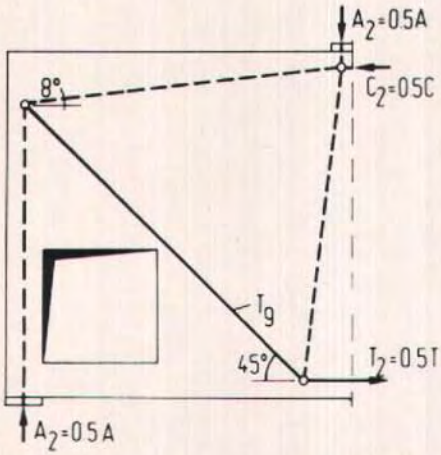

g) model 2, left side

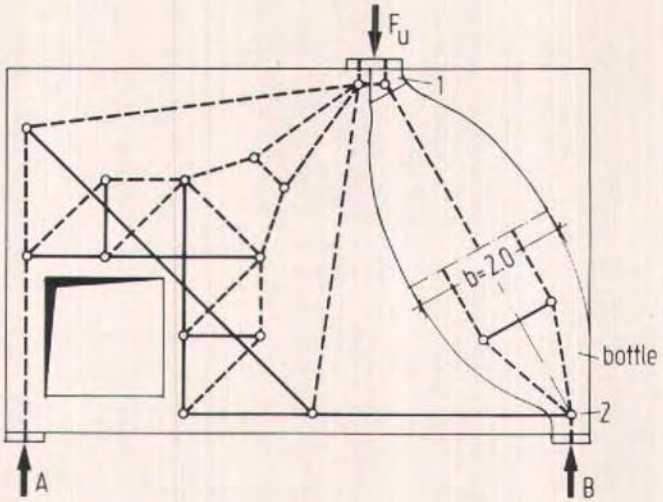

h) complete strut-and-tie-model

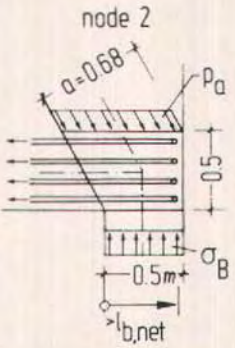

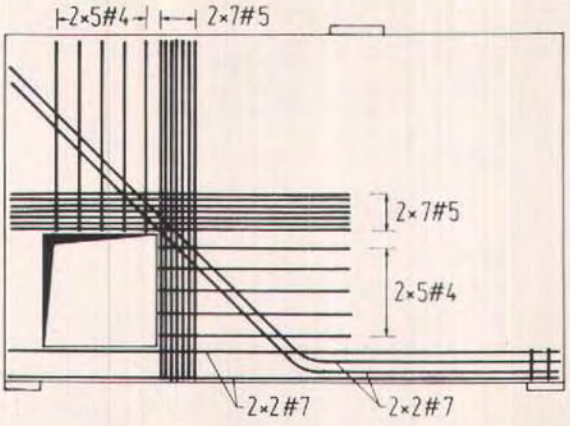

i) reinforcement

Fig. 37 (cont.). Deep beam with a large hole.

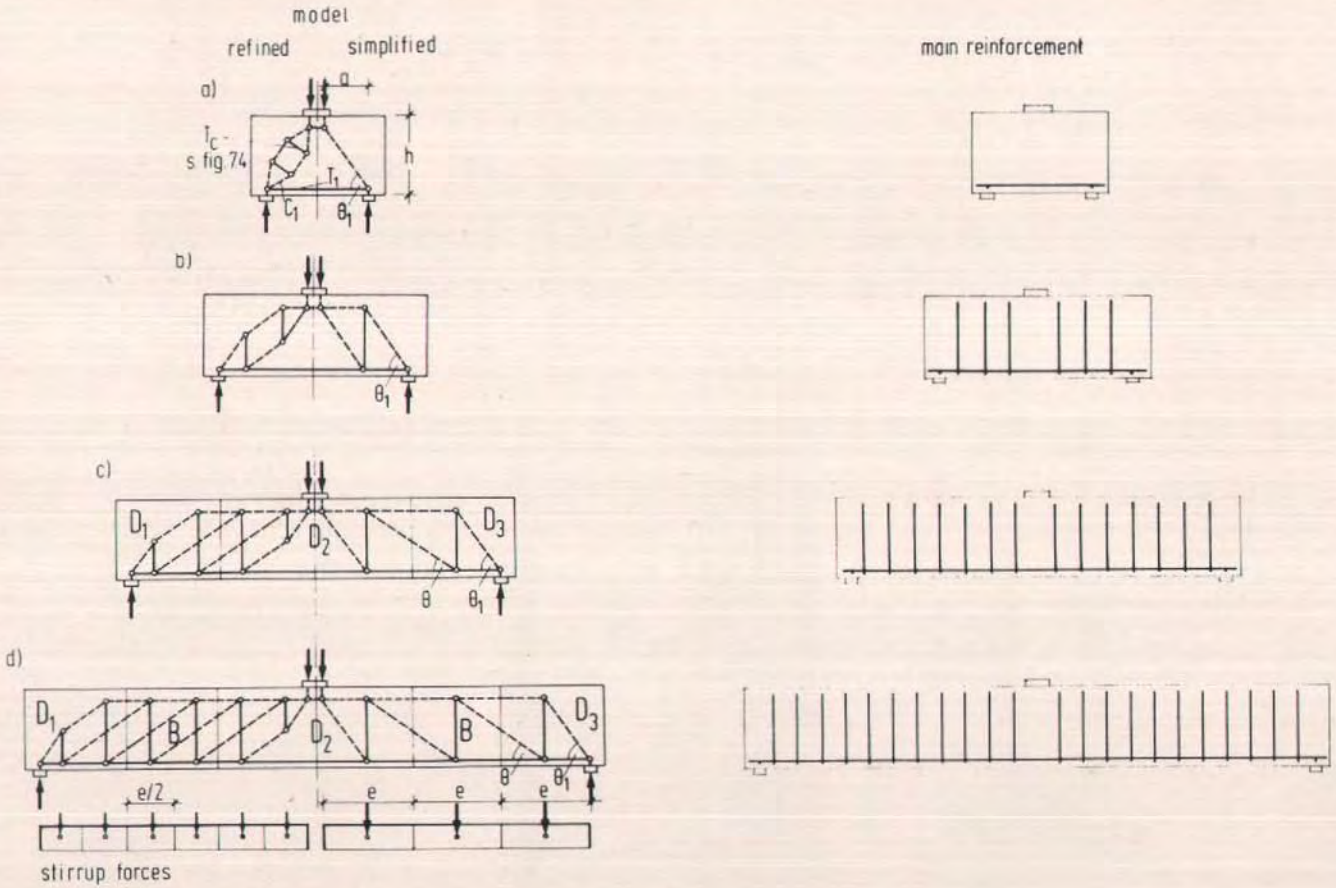

Fig. 38. Load near the support; transition from deep beam to beam.

maximum. Therefore, only the horizontal forces $|T| = |C|$ connect the two sides.)

Forces C and A meet at Node 3 and their resultant is given. From the bottom the reaction A enters the structure vertically and it is assumed that it remains in this direction until it has passed the hole. The B_1-region is thus a centrically loaded column.

In fact, part of the reaction A could also be transferred via the B_2-region by bending moments and shear forces. Comparing the axial stiffness of B_1 with the bending stiffness of B_2, this part is obviously negligible. This fact is also confirmed by the elastic stresses, which are very small there (Fig. 37b). Of course, some nominal reinforcement will be provided in the member below the hole for distribution of cracks due to imposed deformations.

Figs. 37f and 37g give two different strut-and-tie-models for the left side of the deep beam. It is seen that there is some similarity with a beam having a dapped end. The model in Fig. 37f is based on 45 degree struts and on ties also at 45 degrees from the struts. This gives a reinforcement layout, which for practical reasons is orthogonal.

The model in Fig. 37g assumes a 45 degree tie at the corner of the hole which is known to be effective in similar cases like opening frame corners or dapped beams. Each model in itself would be sufficient but — looking at the elastic stresses of Fig. 37b — a combination of both appears to be better than either of them. Therefore, it is assumed, that each model carries half the load.

Finally, Fig. 37h shows the superposition of both models of the left side including the right side as described before. When comparing model and elastic stresses one finds a satisfactory coincidence. The geometry of the model is indeed oriented at the elastic stress fields.

(4) Design of the ties

The reinforcement requirement for the respective tie forces is given in the table below.

Tie	Force [MN]	Req'd. A_s [cm²]	Use	@ [m]
T	1.07	24.6	8#7	
T_1	0.535	12.3	4#7	
T_2	0.535	12.3	4#7	
T_3	0.535	12.3	2x7#5	0.08
T_4	0.535	12.3	2x5#4	0.3
T_5	1.07	24.6	2x7#5	0.08
T_6	1.07	24.6	2x7#5	0.08
T_7	0.535	12.3	2x5#4	0.3
T_8	0.535	12.3	2x7#5	0.08
T_9	0.663	15.2	4#7	
T_{10}	0.402	9.2	or bottle check	
T_{11}	0.402	9.2	(see below)	

Note: 1 cm² = 0.155 in.²

(5) Check of the concrete stresses

Stresses under the bearing plates:

$$\sigma_F = \frac{3.0}{0.7 \times 0.4} = 10.7 \text{ MPa} < 1.2 f_{cd}$$

(biaxial compression)

$$\sigma_A = \frac{1.07}{0.5 \times 0.4} = 5.4 \text{ MPa} < 0.8 f_{cd}$$

$$\sigma_B = \frac{1.93}{0.5 \times 0.4} = 9.7 \text{ MPa} < 0.8 f_{cd}$$

(compression with transverse tension from tie)

The most heavily loaded node is the support B. Following Fig. 22a and the detail of Node 2 in Fig. 37h:

$$p_a = \sigma_2 = \frac{9.7}{\left(1 + \frac{0.5}{0.5} \tan 29°\right) \cos^2 29°} = 8.1 \text{ MPa} < 0.8 f_{cd}$$

Bottle shaped stress field at right side:

$p_a = 8.1$ MPa

$$\frac{p_a}{f_{cd}} = \frac{8.1}{17} = 0.48$$

From Fig. 23a for $a = 0.68$ m and $b = 2.0$ m and $b/a = 3.4$, the permissible

p_a/f_{cd} for uncracked plain concrete is $0.62 > 0.48$.

The stress field is safe without transverse reinforcement. If no dependence is placed on the concrete's tensile strength, the reinforcement as given by Fig. 23a or, equivalent, as calculated from T_{10} and T_{11} may be provided.

Chord C under the loaded plate:

$C = |T| = 1.07$ MN

Required depth of compression zone:

$$d \geq \frac{1.07}{0.4 \times 1.2 f_{cd}} = \frac{1.07}{0.4 \times 1.2 \times 17} = 0.13 \text{ m} < 0.4 \text{ m}$$

Nodes 1 and 3 were taken 0.2 m below the upper surface and are the centroids of the rectangular compression zone which has therefore an available depth of 0.4 m.

(6) Check of the anchorage lengths of the reinforcing bars

The anchorage length $l_{b,net}$ of the tie T in Node 2 must comply with the anchorage length given in the code, considering the favorable transverse compression from Reaction B. Anchorage begins at the left end of the bearing and extends over the whole length of the bearing. Accordingly, T_3 is anchored with cross pressure over the column type B_1-region to the left of the hole. Less favorable stress conditions with transverse tension exist in the node where T_1 and T_8 meet. Therefore, the T_8 bars should be loop anchored whereas the T_1 bars pass through those loops and find sufficient anchor length in the B_2-region below the hole. Anchorage in the other nodes is less critical.

(7) Reinforcement layout

In Fig. 37i only the main reinforcement resulting from the above design is shown. The design engineer should provide further reinforcement, such as a mesh on either surface of the wall, nominal column reinforcement at the left of the hole and stirrups below the hole.

5.2.2 Transition from Beam to Deep Beam — Variation of Span-to-Depth Ratio

If a single load is applied at a distance $a < h$ near the support (Fig. 38a), the load is carried directly to the support by a compression stress field; therefore, no "shear" reinforcement is required between the load and the support. However, the transverse tensile stresses in the compression strut may call for diagonal reinforcement or vertical reinforcement instead.

With increasing a, this single strut model gradually blends into the truss model as shown in Fig. 38b, c. Following the principle of minimum strain energy, the compression member C_1 and the tensile member T_1 (Fig. 38a) of the chord combine (Fig. 38b) and thereby cancel the compression force C_1 and an equivalent part of the tension force T_1. Simultaneously, the transverse tensile forces of the strut (Fig. 38a) blend into the vertical ties of the truss model (Fig. 38b), which are now also needed for hanging up the shear forces.

In the typical truss models on the right sides of Fig. 38c and d and of Fig. 8 the inclination θ_1 of the support strut is shown to be much steeper than θ of the interior struts. This can be proven by the principle of minimum potential energy if models with different strut inclinations are compared. Only the geometrical relation:

$$\cot \theta_1 = \frac{a}{2z} + \frac{\cot \theta}{2}$$

provides constant vertical web tension t_w or equal distances e between all vertical ties and thereby distributed stirrup forces which are proportional to the shear forces (Fig. 39). The force in the tensile chord would have to increase near the support, if θ were constant throughout, or in other words, the supplementary chord force from a constant shear force is constant along the

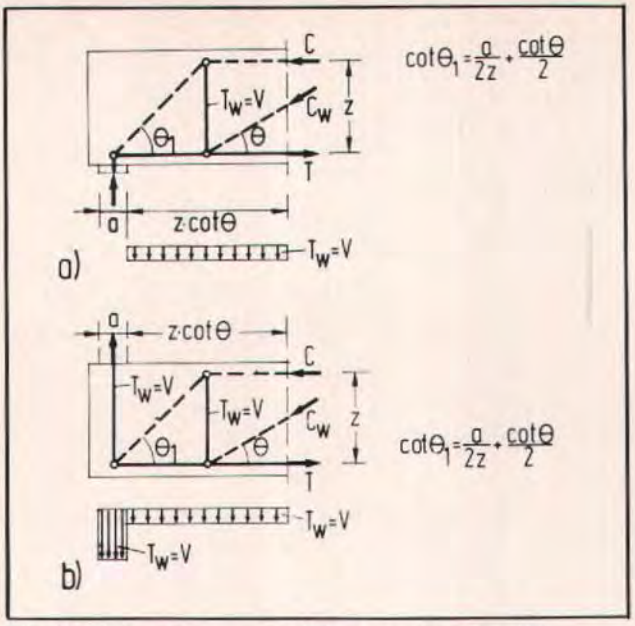

Fig. 39. Detailed geometry of D_2-region from Fig. 38: (a) direct support; (b) indirect support.

chord only if θ_1 satisfies the above given relation.

5.2.3 Corbels

Some of the so-called problems of corbel design result simply from the fact that the individually different boundary conditions are not consequently considered. Each case leads to a different strut-and-tie-model (Figs. 40 and 41). Furthermore, from Fig. 40d it becomes evident that the compression strengths of the struts, which according to Fig. 23 are a function of *a/b*, depend via a_{1A} on the detailing and via a_{1B} and a_{2B} on the depth x of the bending compression zone of the column.

The modelling of a deep corbel is shown in detail in Fig. 41: The stresses in the column of Fig. 41a may be evaluated according to standard methods or the theory of plasticity and are then applied to the D-regions together with the corbel load F_2. The fact that the vertical struts at both sides of the B_2-region in Fig. 41b do not coincide (the stress diagrams, of course, do) is due to the different grouping of stresses for the struts with respect to modelling of the D-regions D_2 and D_3.

Balancing the applied forces between the two boundaries of each D-region (Fig. 41b) shows that *two* tension chords develop, the first one as usual, right below the upper edge of the corbel, and a second one in the lower part of the corbel. Their forces are in this case $T_1 = 0.23\,F_2$ and $T_2 = 0.32\,F_2$, respectively.

The compression struts of the same corbel are not critical because the singular nodes in the D_1 and D_4 regions with maximum compressive failure strengths of $1.2\,f_{cd}$ according to Fig. 23 keep the compressive stresses in the rest of the structure relatively low.

5.2.4 Details of a Box Girder Bridge

The critical D-regions of a box girder bridge are described by strut-and-tie-

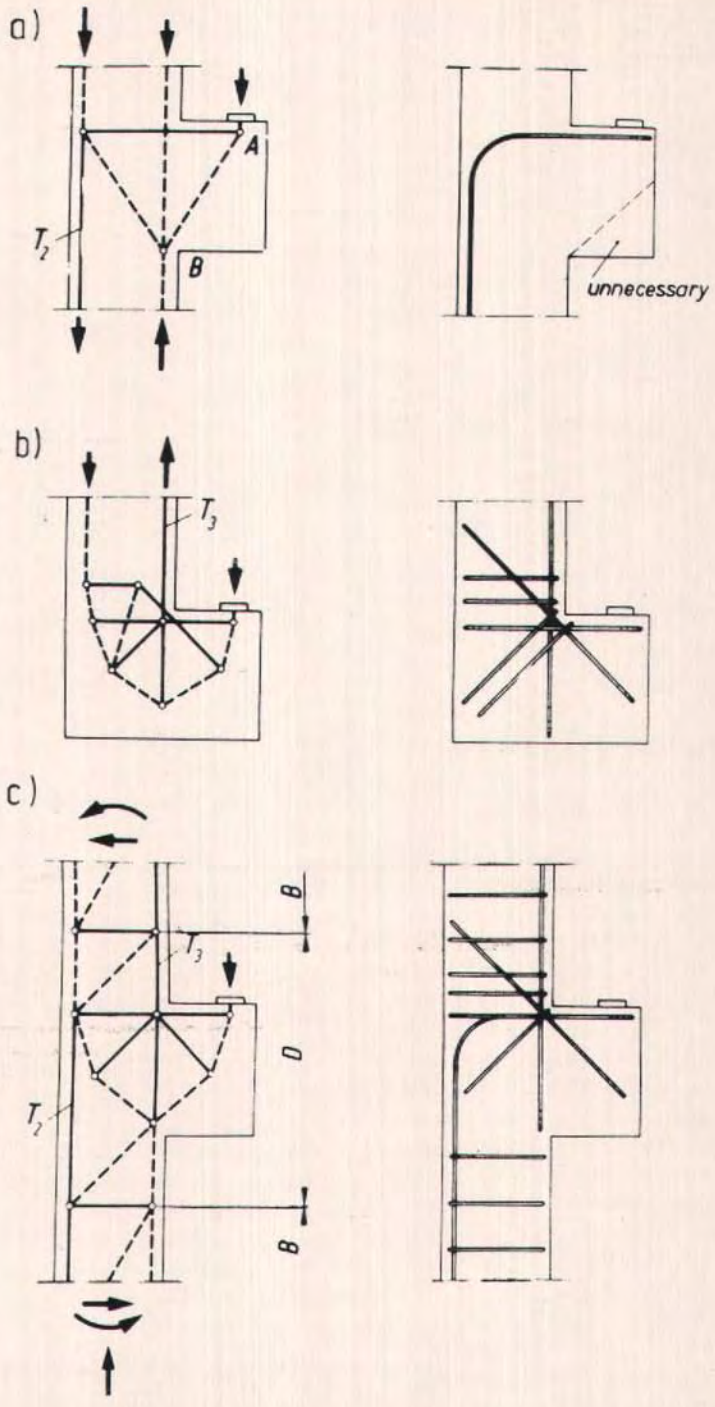
a)
A
B
T_2
unnecessary
b)
T_3
c)
B
T_3
D
T_2
B

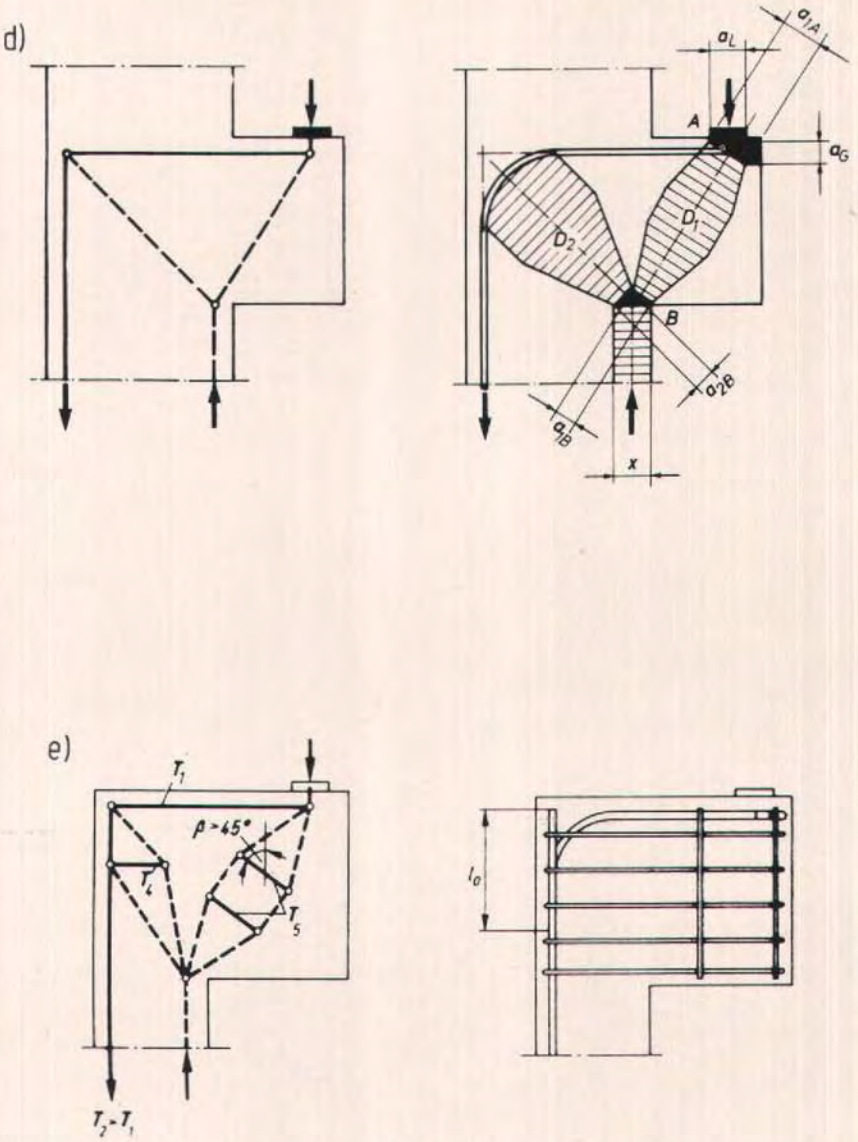

Fig. 40. Different support conditions lead to different strut-and-tie-models and different reinforcement arrangements of corbels.

models as shown in Fig. 42.

In Fig. 43 the diaphragm is prestressed: The shear forces V_1 carried by the diagonal struts C_1 in the webs of the box girder (Fig. 43a) are in this case transferred to the central support via a prestressed web reinforcement designed for $T_1 = V_1/\sin\beta = 1.01\,V_1$ and curved tendons designed for:

$T_2 = 0.82\,(2\,V_1)$ in the diaphragm.

5.2.5 Beam With Opening

Fig. 44a shows the sectional forces and the subdivision of the beam into B- and D-regions. Following the proposed procedure, the boundary forces of the B-regions have to be applied as loads to the D-regions.

The B_1-region will be represented by the standard truss, which yields for $\theta = 31$ degrees:

$$C_1 = \frac{M_1}{z} - \frac{V_1}{2}\cot\theta$$

$$C_2 = \frac{V_1}{\sin\theta}$$

$$T_1 = \frac{M_1}{z} + \frac{V_1}{2}\cot\theta$$

$$= \frac{3.55\,F_d}{1.15} + \frac{F_d}{2}1.66$$

$$= 3.92\,F_d$$

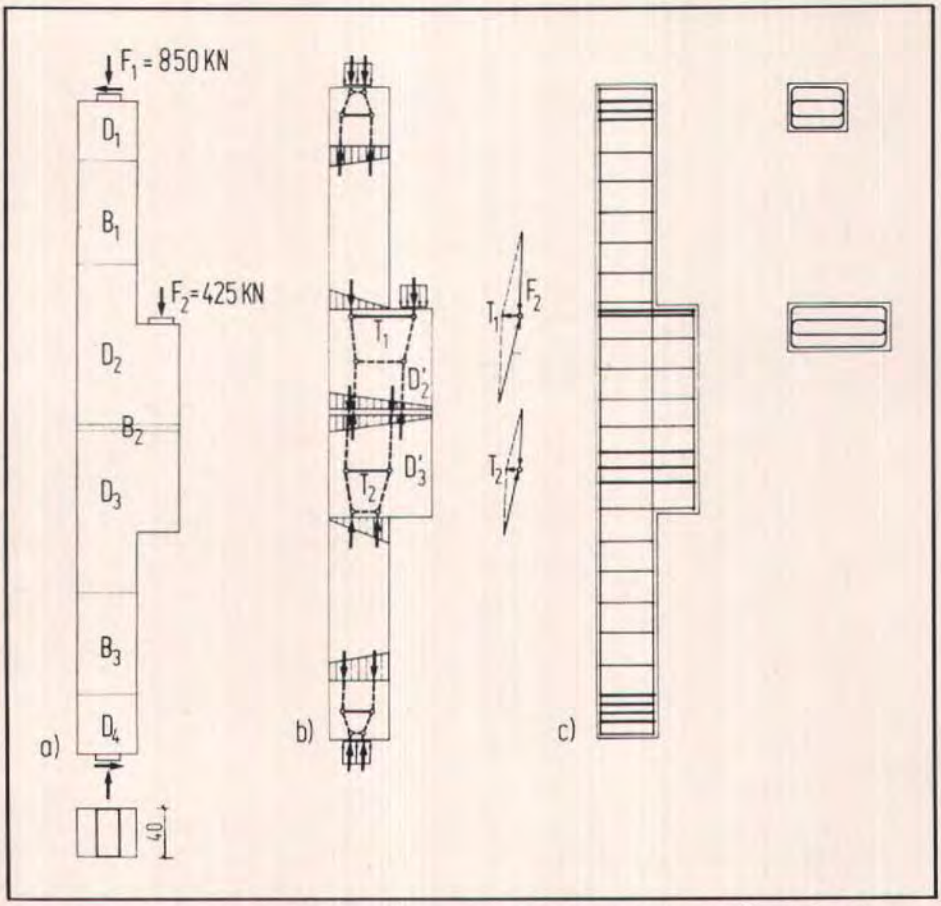

Fig. 41. Deep corbel projecting from a column: (a) B- and D-regions; (b) boundary forces of the D-regions and their models; (c) reinforcement layout.

The B_3-region is designed for a constant tensile force:

$$T_2 = \frac{M_2}{z} = \frac{6.15F_d}{1.15} = 5.35F_d$$

The lever arm $z = 1.15$ m is determined from the assumption of plane strain in the cross section in the middle of the opening by standard methods. Therefore, B_2 has to carry the axial compressive force $C = T_2$ (eccentrically with respect to the axis of the B_2-region) plus the differential moments $\Delta M = M - M_2$ plus the total shear force V.

Under the combined action of these forces, the B_2-region shows the transition from the column type B-region on its left end (resultant C_3) to the truss type B-region at the other end (C_4, C_5, T_3) (see Fig. 36). For simplicity, the model of the B_2-region is extended somewhat into the D_2- and D_3-regions, leaving over for modelling only the D_2' and D_3' regions in Fig. 44b.

With known boundary conditions from B_1, B_2 and B_3, the model for the D_2'-region can be developed (Fig. 44c): Looking for the counterparts of C_1, C_2 and T_1 at the opposite side of the D_2'-region it helps to split up C_3 into three forces C_3', C_3'' and C_3''' in order to establish the load paths, which balance their horizontal components: ($C_{3h}' = C_1$; $C_{3h}'' = C_{2h}$; $C_{3h}''' = T_2 - T_1$).

Vertical equilibrium in the D_2'-region is established by a vertical tension tie T_5 and by a vertical compressive strut C_8. Their forces depend on the choice of their position. Knowing that they represent transverse stresses which are inside the D_2-region and that these stresses tend to fill the available space, the resultant tension T_5 is chosen in the middle of the D_2'-region and the resultant compression C_8 at the right end of D_2', (which is inside D_2). Then:

$$\begin{aligned} T_5 &= (T_2 - T_1)\tan\theta_1 \\ &= (5.35F_d - 3.92F_d)\tan 46^\circ \\ &= 1.48F_d \end{aligned}$$

The tie force T_5 may be interpreted as the transverse tension necessary to anchor the differential force $T_2 - T_1$ of the beam's tension chord.

In a similar way, the D_3'-region at the other end of the opening may be treated. The transverse tension forces are:

$$T_7 = V = F_d \text{ and}$$

$$\begin{aligned} T_6 &= (T_8 - T_2)\tan\theta_2 \\ &= (T_4 - T_2 - V\cot\theta)\tan\theta_2 \\ &= (8.79F_d - 5.35F_d - 1.66F_d)\tan 50^\circ \\ &= 2.12F_d \end{aligned}$$

A striking result of this example are the stirrup forces which in some places considerably exceed the "normal shear" reinforcement for a beam without openings (Fig. 44d).

This example also shows, however, that it sometimes takes some effort to develop a realistic strut-and-tie-model. But if it is considered how many tests have been carried out and how many papers have been written on beams with openings without finishing the case, it was worth this effort.

5.2.6 Overlap of Prestressing Tendons

In Fig. 45a the flow of forces in the given cross section is investigated with its B- and D-regions. In a longitudinal section through the blister, the B-regions of the cross section may also appear as D-regions, because the curvature forces of the tendons are line loads.

(a) Prestress only

Loads acting on the D-regions are the anchor forces of the tendons P, the known concrete stresses along the boundaries between B- and D-regions and the curvature forces $P\alpha_1$ from the tendons (Fig. 45b). The horizontal components of all forces follow two load paths, whose position and direction is given at all D-region boundaries.

The relatively small shift of the load path in between must be accomplished by deviative forces within the D-regions. This is a rather strict condition, which limits the freedom of choice for the bends of the load paths. A further help in finding appropriate nodal points of the model is again the tendency of the deviative forces to fill the available

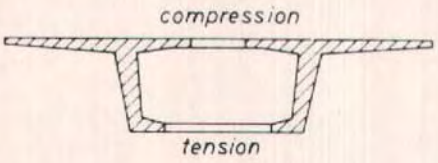
compression
tension

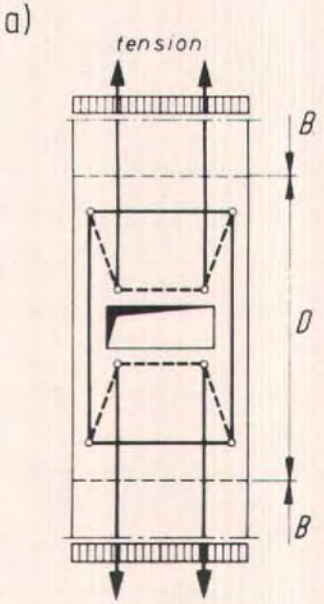
a)
tension
B
D
B

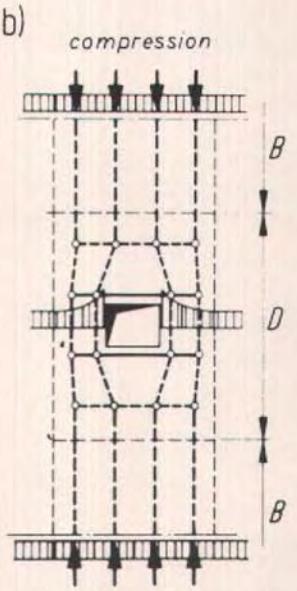
b)
compression
B
D
B

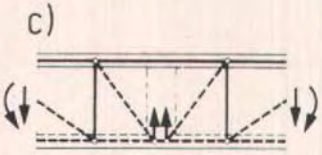
c)

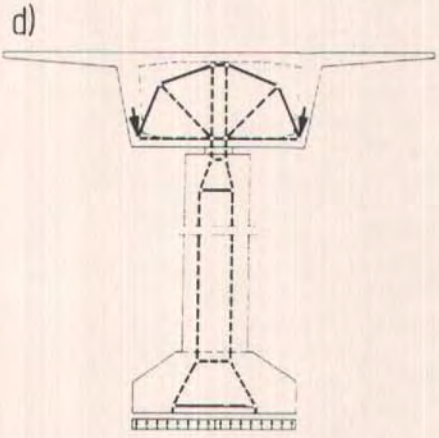
d)

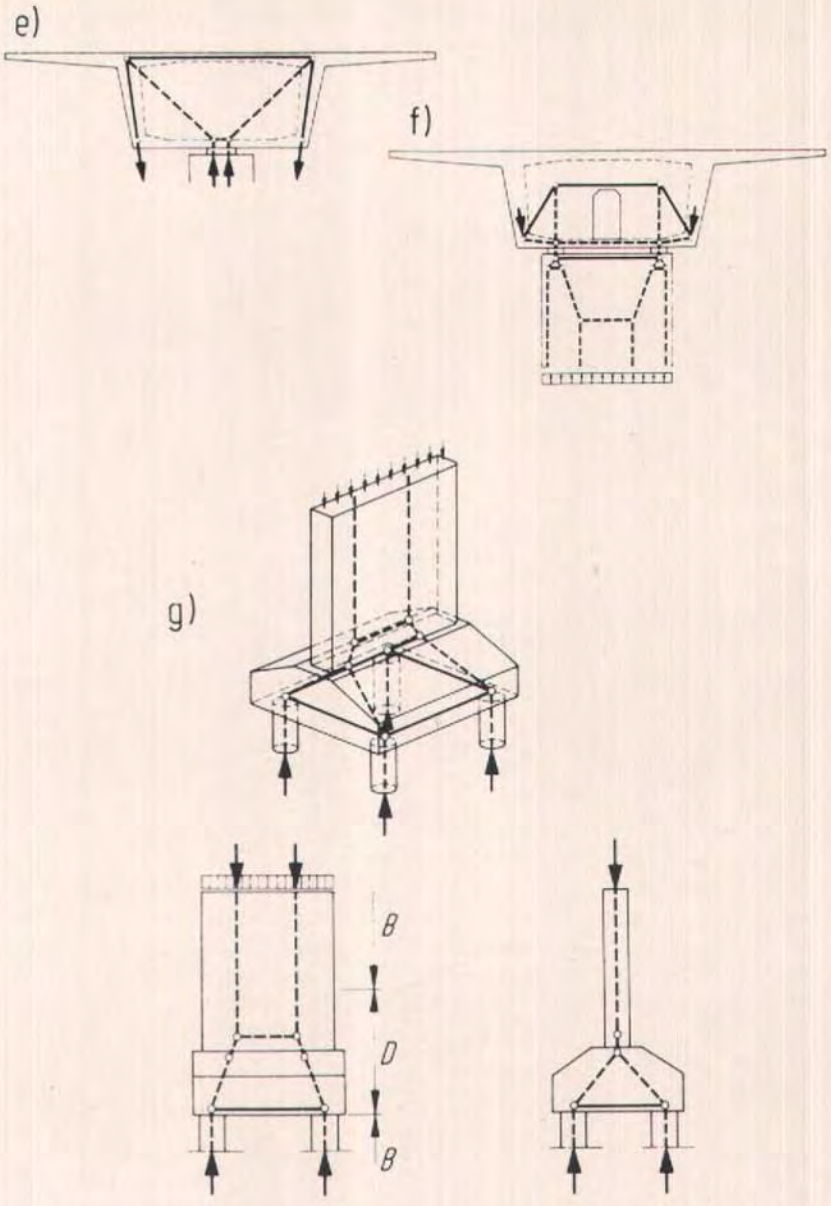

Fig. 42. Strut-and-tie-models of typical D-regions of a box girder bridge: (a) tensile flange with opening; (b) compression flange with opening; (c) web supported by diaphragm; (d) pier and diaphragm with single support; (e) other model for diaphragm; (f) pier and diaphragm with two supports; (g) pier on a pile cap.

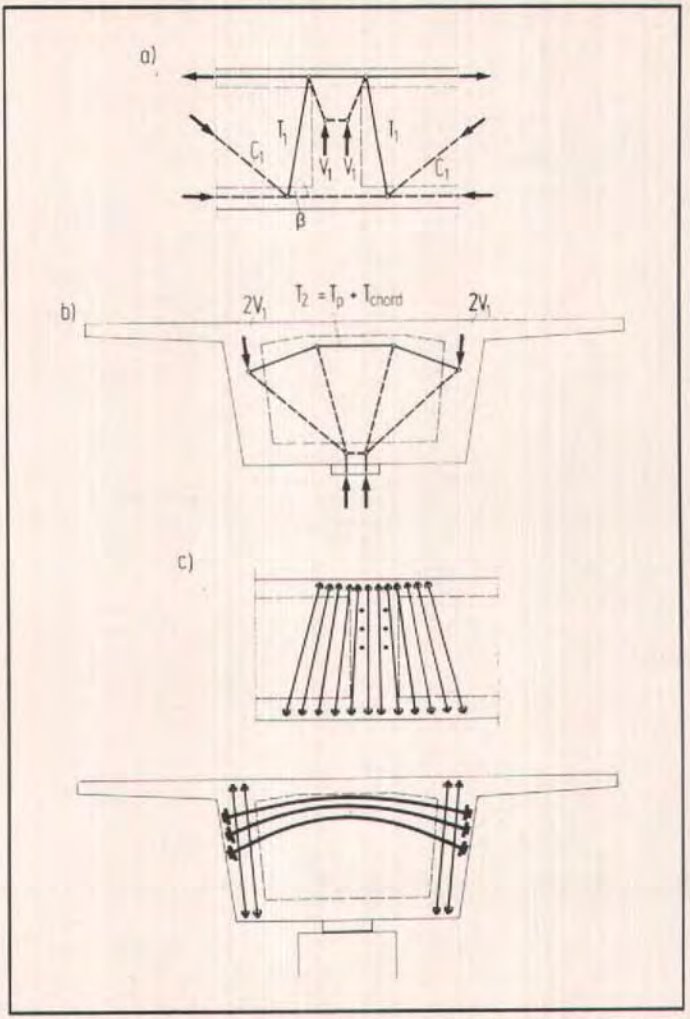

Fig. 43. Diaphragm of a box girder bridge: (a) D-regions and model of the web near the diaphragm; (b) diaphragm and model; (c) prestressing of the web and the diaphragm.

space of the D-region.

Then, $T_1 = P \tan \alpha_2 = 0.18\ P$ (see Fig. 45b).

The reinforcement for T_1 should be chosen with due consideration of acceptable crack widths in this serviceability state of stress, i.e., the tensile strength of the reinforcement should not be fully utilized and its slipfree anchorage should be accounted for.

(b) Prestress plus other loads

Tensile forces are assumed in the B_1-regions, which are considerably larger than the prestressing force, as is the case in an overloaded or partially prestressed structure. In case there is no additional reinforcement provided, and the tendon has to take all tension forces the excess force ($T_{p,chord}$ according to Section 5.3.6) was computed to be:

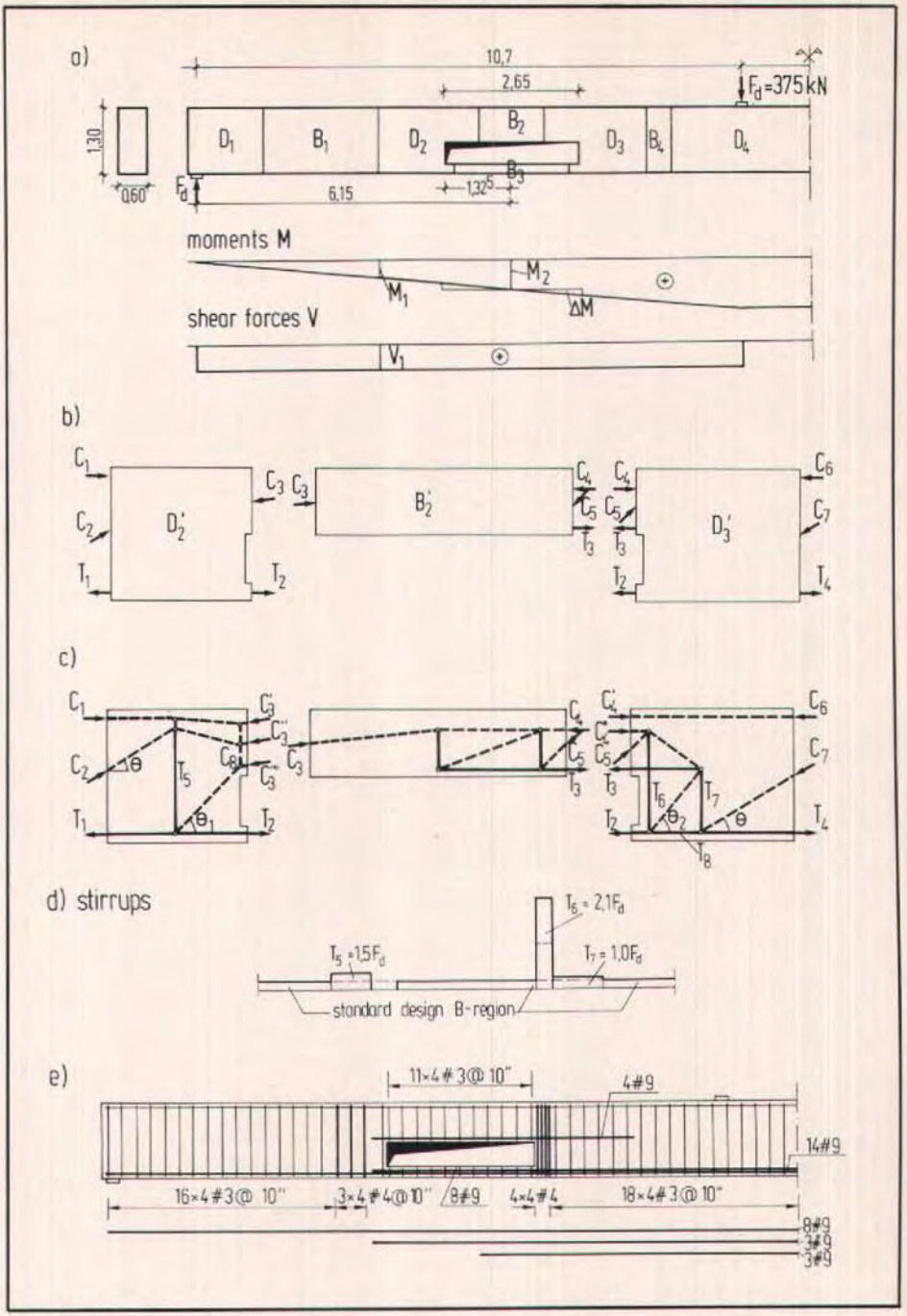

Fig. 44. Beam with opening: (a) B- and D-regions, sectional forces; (b) reduced D-regions at both ends of the opening with boundary loads from the B-regions; (c) strut-and-tie-models of the D_2-and D_3-regions; (d) distributed forces for the design of the stirrups; (e) reinforcement layout.

$T_2 = T\text{-}P = 0.33\,P$

The load path for T_2 and the resulting model (Fig. 45c) is now quite different from that for prestress alone, because the T_2 on both sides do not meet, but rather try to equilibrate on the shortest possible way with the nearby anchor loads of the other tendons. Thereby, transverse tension T_1 develops.

The position of T_1 may have to be shifted toward the center of the blister, if the bond of the tendon is very poor. It is the tension from these bond forces which now calls for transverse rein-

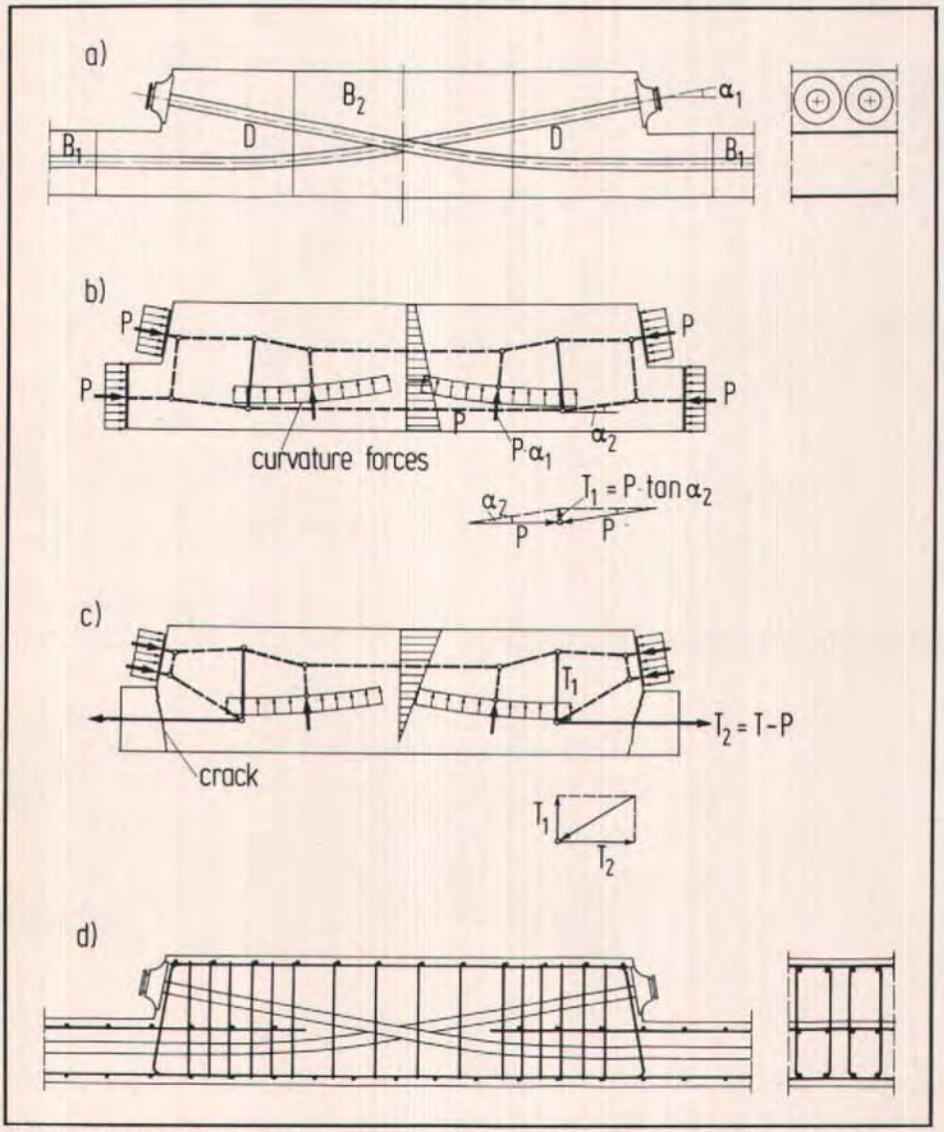

Fig. 45. Overlap of prestressing tendons: (a) layout, B- and D-regions; (b) model for prestress only; (c) model for prestress and additional load T_ϑ; (d) layout of the transverse reinforcement.

forcement $T_1 = 0.53\ T_2$, not the splitting action as for prestress alone.

The overlap of the prestressing tendons results in twice the prestressing force within the blister, which therefore remains basically uncracked and relatively stiff. The strains of the tendon in excess of the initial prestress will therefore accumulate within the bond length of the tendon in the blister and cause a crack at the jump of the wall thickness.

For large bond lengths this crack may open several millimeters wide, even if the B_1-region is reinforced for crack distribution in the usual way. Therefore, in this case not very large tendons with good bond properties have to be applied or additional parallel wall reinforcement must be provided, which takes over much of the tendon forces, *before* the tendons enter the blister.

5.2.7 Beam With Dapped End

It is common practice to suspend the reaction F of the beam in Fig. 46 besides

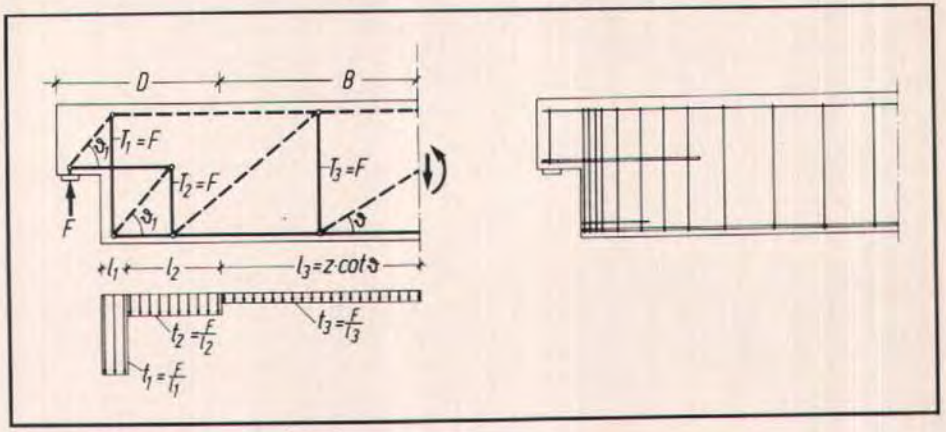

Fig. 46. Beam with dapped end.

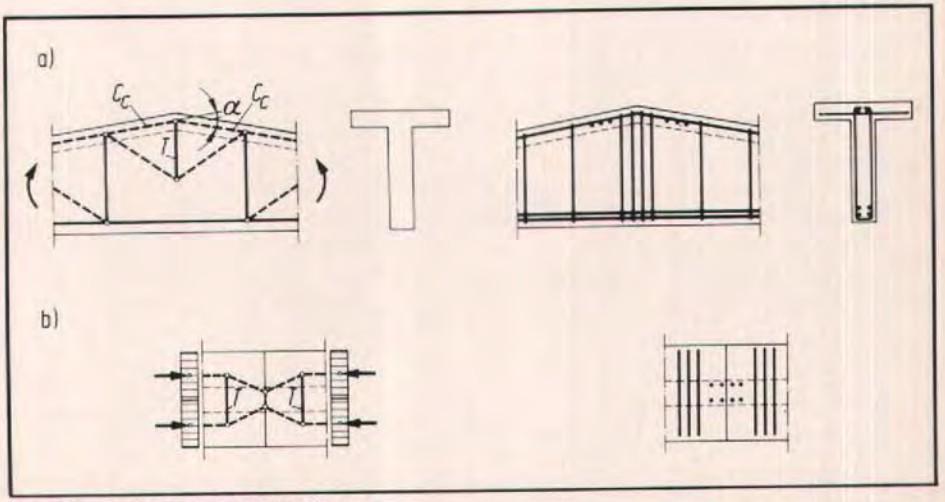

Fig. 47. Girder with bent top flange.

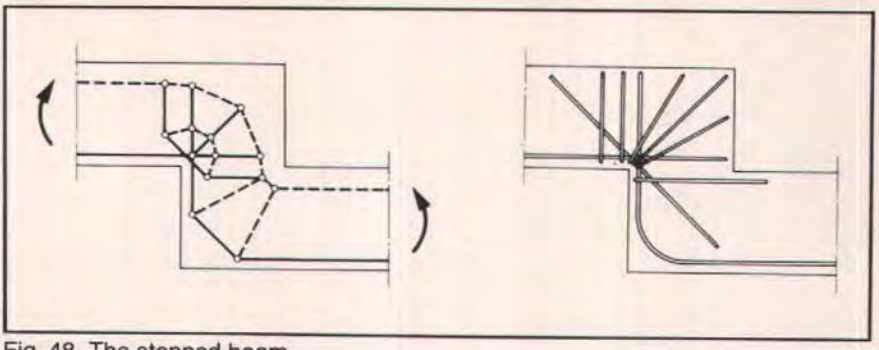

Fig. 48. The stepped beam.

the dapped end ($T_1 = F$). But the complete strut-and-tie-model clearly reveals that it is not sufficient to simply add T_1 to the regular "shear reinforcement" which amounts to the vertical tie forces $t_3 = F/l_3$. In fact, there are additional vertical tensile forces $T_2 = F$ because the horizontal tie force T at the recess needs to be anchored. The tie force T_2 is distributed over a length $l_2 < l_3$ and therefore t_2 is clearly considerably larger than t_3. If, as usual, an additional horizontal force H acts at the recess, the necessary amount of vertical stirrups further increases.

5.2.8 Tapered Beam With Bent Top Flange

The girder in Fig. 47a obviously produces a vertical tension force T at the bend of the compression chord. But where does it go? The straight horizontal tension chord cannot equilibrate it. The model shows that stirrups in the web are necessary throughout this web even in regions without shear forces.

Looking at Fig. 47b, it is apparent that the compression chord is narrowed by the stirrups, resulting in a concentration of compression stresses over the web. Furthermore, unfavorable tensile stresses in the transverse direction of the flange appear.

5.2.9 Stepped Beam

The stepped beam in Fig. 48 is frequently used and is usually detailed by overlapping the reinforcement coming from both sides with an elegant loop. The strut-and-tie-model supplies facts for a rational reinforcement layout.

5.2.10 Frame Corner

The frame corner with opening moment, more often discussed by researchers than actually occurring in practice, can be modelled quite differently (Fig. 49). Obviously, the design engineer has to choose between a relatively simple reinforcement combined with a reduced moment capacity (Fig. 49a,b) or a more sophisticated solution (Fig. 49c,d,e). The consequent application of strut-and-tie-models makes the designer aware of what is occurring while offering a rational choice.

5.3 Prestressed Concrete

As a last example, it will be shown that looking at prestressed concrete beams through strut-and-tie-models helps to understand their behavior which today gets hidden behind so many black box rules. There is a common denominator of all types of prestress: post-tensioning, pretensioning and unbonded prestress can be understood as reinforced concrete which is loaded by an artificial loading case, i.e., prestress.

As any other loading case, it simply has to be introduced into the analysis of the structure according to the actual history, e.g., for post-tensioning: con-

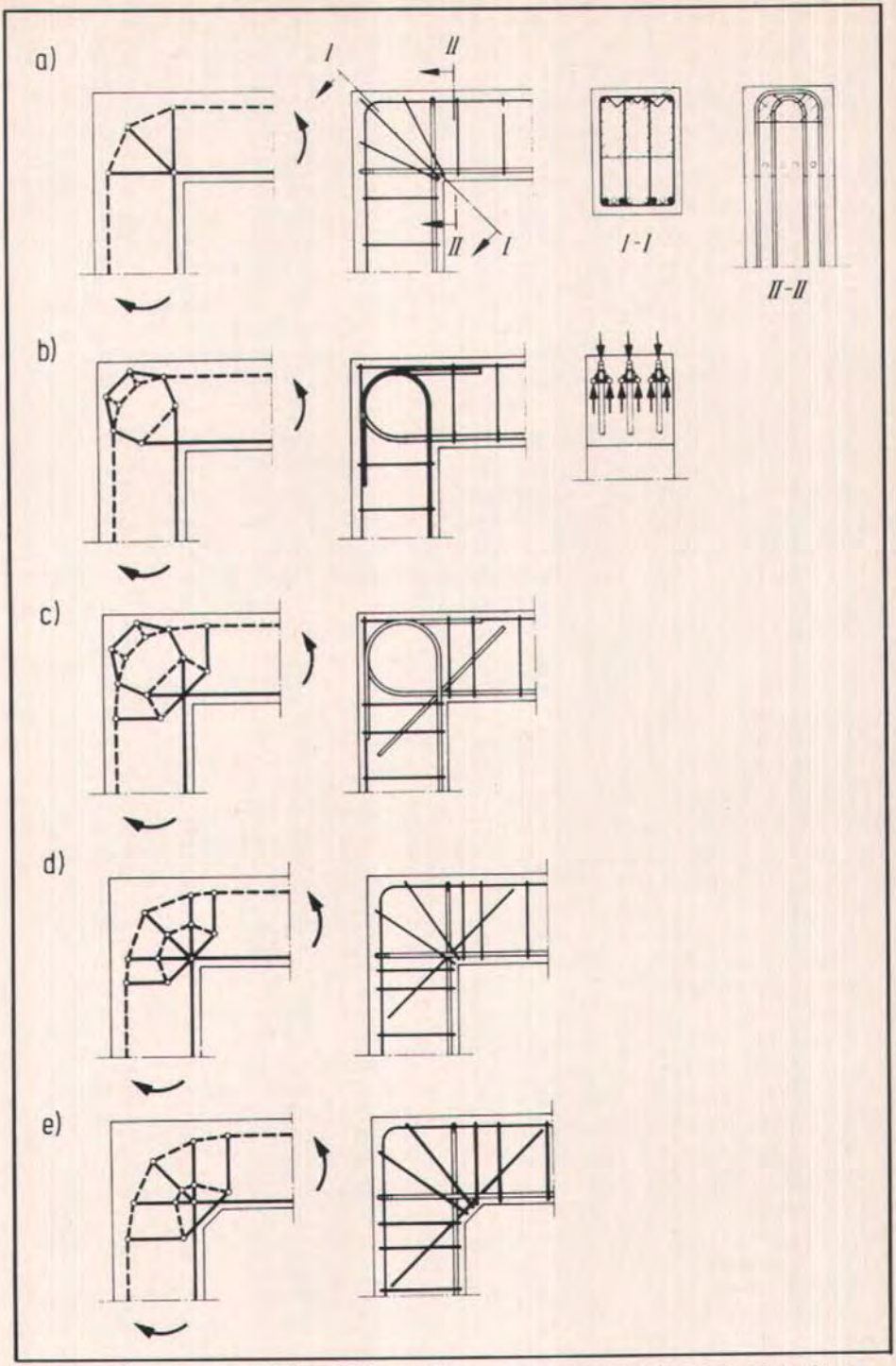

Fig. 49. Different strut-and-tie-models and the corresponding reinforcement for a frame corner with positive moment.

creting and hardening of the reinforced concrete, applying the prestress (thereby activating dead load), providing bond and imposing external loads. After bond is activated, the prestressing steel acts as reinforcement, like regular reinforcement does; only its preloading, its different surface with respect to the strength of bond and its sensitivity needs to be taken into account.

5.3.1 Prestress as a Load

By prestressing, forces are artificially created with the help of hydraulic jacks; on the one hand, these forces act as loads on the prestressing steel, on the other as loads on the reinforced concrete structure (Fig. 50). The loads acting on the prestressing steel and on the reinforced concrete are inversely equal. The design engineer chooses the tendon profile, the type and magnitude of the prestressing force in such a manner that these artificial loads influence the load paths and sectional effects or stresses due to the actual loads (dead and live loads and other loads) favorably and as efficiently as possible.

It is proposed to treat these prestressing loads like permanent loads which never change after the prestressing jack has been removed. All the changes of stress in the prestressing steel, which occur after removal of the jack, ought to be attributed to those load cases which cause them. In those load cases the prestressing steel adds to the resistance of the section or member like nonprestressed steel.

The view sometimes expressed that the prestressing itself increases under live loads because the stress in prestressing steel increases or decreases as a result of the bond with the concrete, is misleading. The stress also changes in normal reinforcing steel due to these effects and one would never regard this as a change of prestressing.

Accordingly, the changes of stress in the prestressing steel due to creep, shrinkage and steel relaxation (often referred to as prestress losses) are in reality simply stress redistributions as in any reinforced compressed member and can be treated accordingly.

If prestressing is introduced in this way into the design of reinforced concrete, all types of prestressed structures (linear members, plates, deep beams, shells) can be designed, analyzed and dimensioned like reinforced concrete structures: The sectional forces of a prestressed beam are determined and combined for the load cases prestress, dead load, live loads, etc., and the resistance of a cross section is derived as for reinforced concrete with prestressing steel as additional (passive) reinforcement.

Thereby, the same method of analysis and dimensioning can be applied to all load combinations in serviceability and ultimate limit states. Consequently, in the ultimate limit state the reinforced concrete sections (with reinforcement A_s and A_p) of a prestressed beam have to be dimensioned for the following (active) sectional effects:

$$\text{Normal forces: } N = -P + N_L$$
$$\text{Shear forces: } V = V_p + V_L$$
$$\text{Moments: } M = M_p + M_L$$

where

P = prestressing force immediately after prestressing

M_p, V_p = corresponding moment and shear force due to prestressing

N_L, V_L, M_L = sectional effects from other loads

The sectional effects given here are meant to include the (partial) safety factors according to the chosen safety concept.

The proposed treatment of prestressing leads to the same results as does the usual method with all stresses in the tendons regarded as being passive in the ultimate limit state. However, the method proposed here is more general.

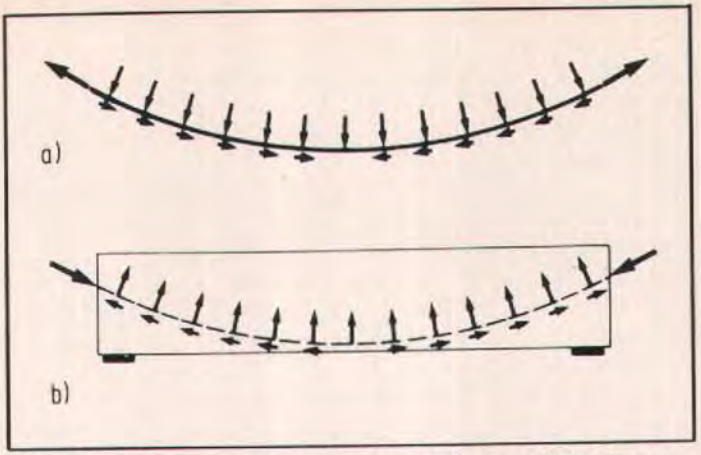

Fig. 50. Loads due to prestressing (anchor forces, friction forces, deviation forces due to the curvature of the tendon) acting (a) on the prestressing steel; (b) on the reinforced concrete member.

Also, the different degrees of prestressing (full prestressing, partial prestressing, no prestressing) and different applications like pretensioning, posttensioning and unbonded cables can all be treated alike with these principles: Forces due to prestressing as permanent active loads which never change and prestressing steel contributing to the resistance after the cable is anchored.

5.3.2 Prestressing of Statically Indeterminate Structures

In structures with statically indeterminate supports the properties of the materials and the geometry of the structure have to be considered when determining the sectional effects. Those from prestressing can be split up in:

$$V_p = P \sin \delta + V_{p2}$$
$$M_p = -V_e + M_{p2}$$

where δ denotes the inclination of the prestressing cable and e denotes the cable's eccentricity. V_{p2} and M_{p2}, the statical indeterminate portion of the prestressing effects resulting from support reactions due to prestressing, are of the same kind as the statically indeterminate moments which result from dead loads or live loads. M_{p2} is *not* the result of restraints such as those due to changes in temperature or settlements; these diminish or even disappear in the whole structure if the stiffness decreases due to cracking, those from prestressing are only redistributed.

If it can be assumed that the stiffnesses are not altered by loading, moments resulting from different loading cases may be superimposed. However, because part of the reinforced concrete girder passes from the uncracked to the cracked state and because plastic deformation of the concrete and the steel in the reinforced concrete girder is possible, the local stiffnesses change with variations of the load and, therefore, the distribution of moments also changes. When this occurs the individual moments can no longer be superimposed. Nevertheless, if the theory of linear elasticity is taken as a basis for calculating the forces, the resulting overall moments (including M_{p2}) can be adapted to the real loadbearing behavior by redistribution.

5.3.3 The Prestressed Concrete Beam With Rectangular Cross Section

In Fig. 52 the strut-and-tie or the truss model of a simple prestressed concrete beam with a straight eccentric tendon is

shown and in the preceding Fig. 51, for comparison drawn in the same manner, of a reinforced concrete beam. The design engineer selects the prestress P and combines it with the support force $A = F$ to a resultant, R, entering the beam at the support.

If the resultant meets the action line of the load F within the kern of the section, the condition is full prestress, if F is the working load F_w. Then the model has no tensile chord (Fig. 53). If the resultant meets the compression chord of the beam before it meets F_w such that vertical ties (stirrups) and, therefore, also a truss with a tension chord is necessary to transport F_w into the inclined resultant, the condition is partial prestress (Fig. 52).

It is apparent that the vertical tie and inclined strut forces of this truss are (almost, see below) the same as for the reinforced concrete beam, because the shear forces are the same. The span of the truss is only shorter and, therefore, the forces in the tensile chord are less, whereas the compression chord also includes the additional prestressing force.

If the load is increased from F_w to the ultimate F_u, of course, the inclination of the resultant R increases. The fully prestressed beam now becomes "partially" prestressed, the initially partially prestressed beam gradually approaches the reinforced concrete beams. (This, incidentally, shows that manipulating safety completely via a factored load is misleading in contrast to partial safety factors being put on the material *and* the load.)

Full prestressing transforms the girder under service loads into a "horizontal column" (Fig. 36); its eccentric normal force is generated artificially and the external load which actually has to be carried by it is relatively small. Whatever amount of prestress P is chosen, it shortens that part of the girder, where a truss must form to carry the load and replaces it by a direct and shorter load path. It is, thus, directly apparent that prestressing improves the load-bearing behavior as compared to the nonprestressed reinforced concrete girder.

Since prestress does not fully utilize the strength of the high tensile steel used for tendons, it can be used as $T_{p,chord}$ to cover a part of the tensile force of the chord T_{chord}. If the prestressing steel is not bonded with the concrete, it is unsuitable to serve as reinforcement for T_{chord}. It only affects the sectional forces in the reinforced concrete via additional anchor and deviation forces, and all tensile forces of the chord have to be taken by regular reinforcing steel to satisfy equilibrium.

The resultant entering the beam from the supported end, as discussed, has the tendency to spread in the web of the beam as in the bottle shaped compression field (Fig. 52b). Transverse tension forces develop as well as a "force whirl" in the corner (Fig. 53) which causes high tensile stresses near the anchor plate.[22] These tension forces have to be checked. If they cannot be covered by the tensile strength of the concrete (see Section 4.5), stirrups have to be provided (see Section 4.6).

Tensile edge forces, splitting tensile forces, tensile end forces, etc., in the zone of introduction of anchoring forces are thus simply part of the strut-and-tie-model. In fact, they require no special names suggesting that they are something special or specific to prestressed concrete. The "problem" of superposition of the reinforcement for the shear force and the splitting tensile force is resolved by the model.

5.3.4 The Prestressed Concrete I-Girder

If a beam is not plane (rectangular) but has a distinct profile like the T, I or box girders, with relatively large cross-sectional areas of the flanges, the resultant entering the beam as discussed above, will spread on a path different from that in the rectangular beam; though of course for the same applied

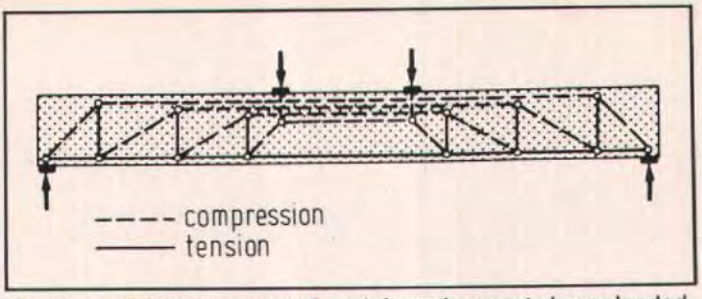

Fig. 51. Strut-and-tie-model of a reinforced concrete beam loaded with two single loads.

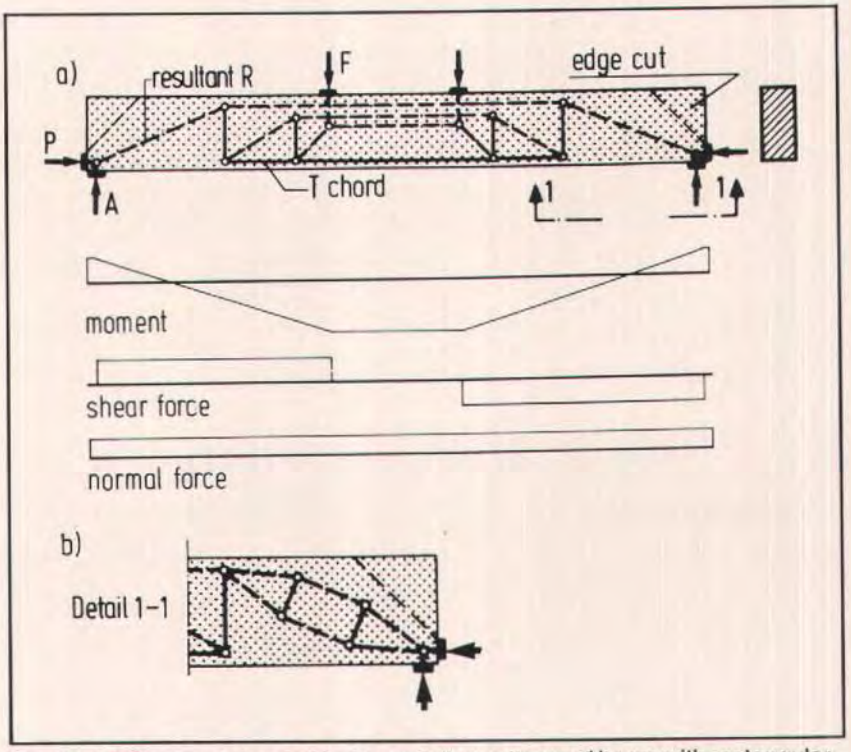

Fig. 52. (a) Strut-and-tie-model of a partially prestressed beam with rectangular cross section; (b) detailed strut-and-tie-model of the beam area, where the resultant is within the beam section.

forces P and A the simplified model is the same for any type of cross section (compare Fig. 54a with Fig. 53a).

The detailed strut-and-tie-model of the prestressed I-girder (Fig. 54) shows that a truss already develops in the area where the total resultant force remains within the kern zone of the girder section (Fig. 54b). This is because the longitudinal forces here are mainly concentrated in the flanges. Therefore, only a part of the prestressing force can join

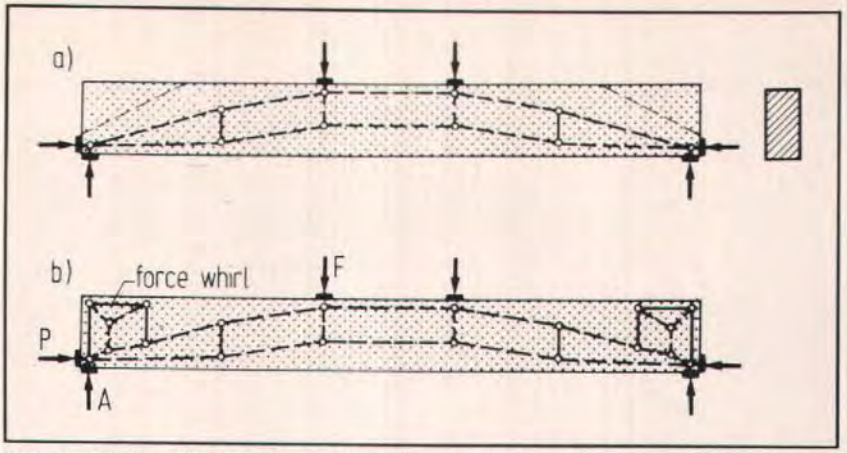

Fig. 53. (a) Simplified strut-model of a beam with its rectangular cross section "fully prestressed"; (b) detailed strut-and-tie-model.

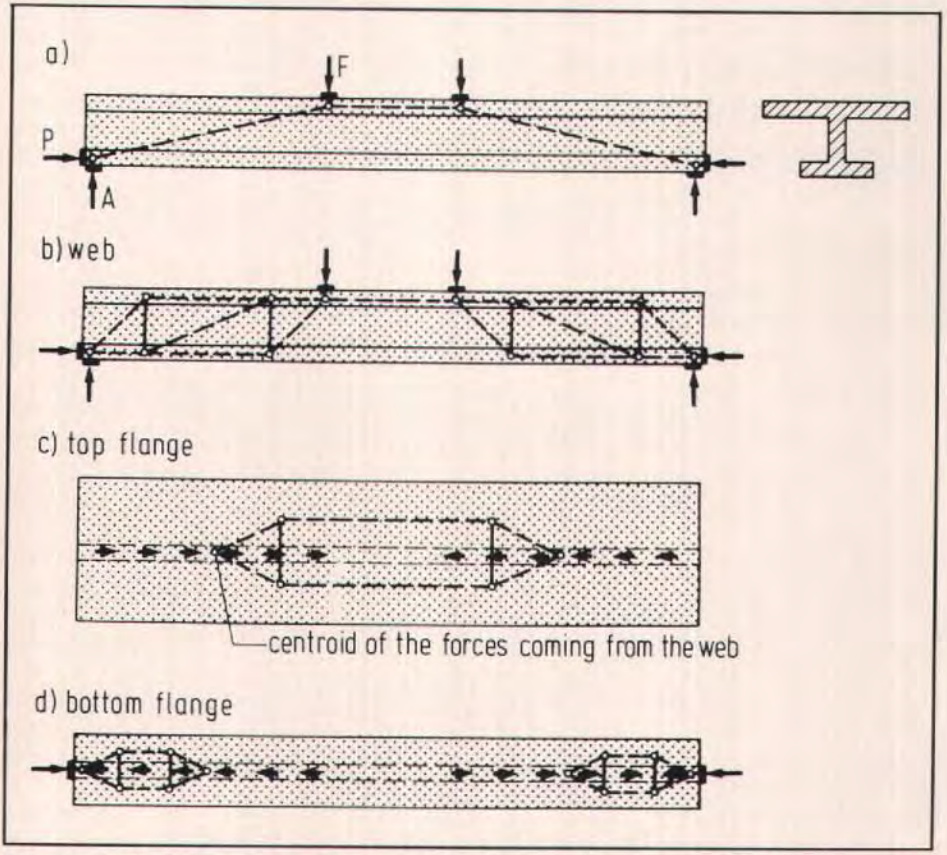

Fig. 54. Strut-and-tie-models of an I-girder with full prestress: (a) simplified model; (b) through (d) detailed models of the web, top flange and bottom flange, respectively.

with the support force to flow into the web. The effective resultant force in the web is, therefore, smaller and at a greater angle than in the prestressed girder with a rectangular cross section. It is, however, still at a smaller angle than in the nonprestressed reinforced concrete girder.

The chords in the two flanges are linked to one another via the web struts and ties. In this way, compression forces are introduced into the flanges (Fig. 54c, d). The strut-and-tie-model shows that the spreading of the forces from the width of the web to the width of the flange generates transverse forces in the flange. The transverse reinforcement must be distributed in accordance with the length and intensity of the introduction of forces.

5.3.5 The Loadbearing Behavior of the Web

The strut-and-tie-model of the prestressed girder with rectangular cross section shows, that the stirrup forces in the part of the girder where the total resultant force remains in the kern zone of the section result from the spreading of the compression forces (Fig. 52b, 53b). The "shear reinforcement" in that area is in reality a "tensile splitting reinforcement." As soon as the truss model develops in the web (which as shown happens for a rectangular beam further away from the support than for a beam with a profiled section), the dimensioning of its struts and ties follows as discussed for the B-regions of reinforced concrete.

Whether the web crack develops from the bending crack or begins in the web itself (as specified for example by the German Code DIN 4227 as "zones a and b") has no effect on the loadbearing behavior of the members in the cracked web. After the web has started to crack the prestressing normal force is only present in the compression chord, like any normal compression force. In the truss (or B-region) the web itself is influenced by the axial force due to prestressing only via the inclination α of the web crack, which is shallower than for a nonprestressed beam, corresponding to the shallower inclination of the principal tensile stresses in the concrete when cracking begins.

This effect of α can be considered in the web design as discussed in Section 5.1 (B-regions). From there it is shown that the greatest possible inclination of the diagonal strut is parallel to the crack in the web. The ultimate load capacity of the diagonal struts in a web of a prestressed concrete girder is therefore somewhat smaller than that of the web of a girder without prestressing, however, it requires less stirrup reinforcement for a similar beam and load.

5.3.6 Dimensioning the Prestressing Steel for the Different Types of Prestressing

As already mentioned above, the prestressing steel can and will serve as regular reinforcement, if it is bonded with the concrete, in other words it acts as the tensile chord of the truss, developed for the structure loaded with prestress and other loads. If the capacity of the prestressing steel still available after prestressing $T_{p,chord}$ cannot alone cover the force of the chord, reinforcement must be supplemented in such a way that the total chord force T_{chord} can be taken by the prestressing steel (p) and the reinforcing steel (s):

$$T_{chord} = T_{p,chord} + T_{s,chord}$$

In this equation T_{chord} represents the total chord force from the various loads (including prestress). The loads are to be multiplied by the partial safety factors γ which are, of course, different for various kinds of load. The right hand side of the equation stands for the resisting chord forces, divided by the appropriate partial safety factors.

The force $T_{p,chord}$ of the prestressing steel which is still available for the chord after prestressing is equal to its

permissible total force $T_{p,tot}$ minus the prestressing force $\gamma_p P$.

$$T_{p,chord} = T_{p,tot} - \gamma_p P$$

As a rule, under ultimate load the prestressing steel is strained beyond its yield point and, therefore, $T_{p,tot} = A_p f_{py}$. Then, the following simple equation applies:

$$T_{p,chord} = \frac{A_p f_{py}}{\gamma_s} - \gamma_p P$$

If this is not the case, f_{py} in the above equation has to be replaced by the stress σ_p of the prestressing steel corresponding to its total strain

$$\epsilon_{p,tot} = \epsilon_{p,p} + \epsilon_{p,chord}$$

where

$\epsilon_{p,p}$ = strain from prestressing (active strain)

$\epsilon_{p,chord}$ = strain of chord after bonding (passive strain)

$$= \frac{T_{p,chord}}{(A_p + A_s) E_s}$$

Some codes restrict the strain of the chord after decompression of the concrete to 0.005 (DIN 4227) or 0.010 (CEB Model Code). Considering the arbitrariness of these quantities, the small decompression strain including the strains from creep and shrinkage can be neglected, which means $\epsilon_{p,chord}$ is limited from 0.005 to 0.010, respectively.

If no bond is provided after prestressing, the prestressing steel cannot be considered as reinforcement in this way. Rather, it acts as a tie member. Its stress increment can only be determined from an internally statically indeterminate analysis. If the truss model contains a tension chord, supplementary bonded reinforcing steel must be provided.

If pretensioning is used and the tendon profile is straight, the prestressing force acts as an external normal force on the reinforced concrete girder. The prestressing steel is then part of the reinforcement.

5.3.7 Result

Considering prestressing forces as external loads is not only an advantage with regard to service load design, but also for checking ultimate load design and all other checks, because the load-bearing behavior of the entire prestressed concrete girder can then be simply explained in terms of a strut-and-tie-model.

Prestressing steel is used for two distinct purposes. On the other hand, its prestress applies favorable loads to the reinforced concrete girder, while on the other hand, it works as passive reinforcement when it is bonded with the concrete. In this latter respect it is not different from reinforcing steel. Otherwise, if it is not bonded it acts as a tie member.

As a result of this approach, the task of designing any type of prestressed concrete girder becomes the task of designing a reinforced concrete girder with regard to bending, shear forces, and normal forces, which among others include the additional loading case of prestress.

* * *

ACKNOWLEDGMENT

This paper is a progress report of the work in this field at the University of Stuttgart. The authors want to acknowledge the contributions of several former and present members of their Institute, mainly K. H. Reineck, D. Weischede, H. G. Reinke and P. Baumann.

The authors further received valuable contributions and encouraging support through many critical discussions with colleagues; thanks go mainly to B. Thürlimann (Zürich) and M. P. Collins (Toronto), who also promote the idea of a consistent design of concrete structures and to the members of the CEB Commissions concerned, in particular T. P. Tassios (Athens), G. Macchi (Pavia), P. Regan (London) and J. Perchat (Paris).

Finally, the authors wish to thank the reviewers of the PCI JOURNAL who offered us critical but constructive help. In particular, we wish to thank J. E. Breen (Austin) and J. G. MacGregor (Edmonton). It is by no means their fault if the paper is still a burden to the reader.

Lastly, the authors hope that this paper will generate fruitful discussions in the interest of producing quality concrete structures. To this end, we wish to thank the Editor of the PCI JOURNAL for offering us such a prominent forum.

* * *

NOTE: Discussion of this report is invited. Please submit your comments to PCI Headquarters by February 1, 1988.

REFERENCES

1. Schlaich, J., and Weischede, D., "Ein praktisches Verfahren zum methodischen Bemessen und Konstruieren im Stahlbetonbau" (A Practical Method for the Design and Detailing of Structural Concrete), Bulletin d'Information No. 150, Comité Euro-International du Béton, Paris, March 1982.
2. Schlaich, J., Schäfer, K., "Towards a Consistent Design of Reinforced Concrete Structures," 12th Congress of IABSE, Vancouver, British Columbia, September 1984.
3. Schlaich, J., and Schäfer, K., "Konstruieren im Stahlbetonbau" (Design and Detailing of Structural Concrete), Betonkalender 1984, Part II, W. Ernst & Sohn, Berlin-München, pp. 787-1005.
4. Ritter, W., "Die Bauweise Hennebique" (The Hennebique System), Schweizerische Bauzeitung, Bd. XXXIII, No. 7, January 1899.
5. Mörsch, E., "Der Eisenbetonbau, seine Theorie und Anwendung" (Reinforced Concrete, Theory and Application), Verlag Konrad Wittwer, Stuttgart, 1912.
6. Leonhardt, F., "Reducing the Shear Reinforcement in Reinforced Concrete Beams and Slabs," *Magazine of Concrete Research*, V. 17, No. 53, December 1965, p. 187.
7. Rüsch, H., "Über die Grenzen der Anwendbarkeit der Fachwerkanalogie bei der Berechnung der Schubfestigkeit von Stahlbetonbalken" (On the Limitations of Applicability of the Truss Analogy for the Shear Design of Reinforced Concrete Beams), Festschrift F. Campus "Amici et Alumni," Université de Liége, 1964.
8. Kupfer, H., "Erweiterung der Mörsch'schen Fachwerkanalogie mit Hilfe des Prinzips vom Minimum der Formänderungsarbeit" (Expansion of Mörsch's Truss Analogy by Application of the Principle of Minimum Strain Energy), CEB-Bulletin 40, Paris, 1964.
9. Thürlimann, B., Marti, P., Pralong, J., Ritz, P., and Zimmerli, B., "Vorlesung zum Fortbildungskurs für Bauingenieure" (Advanced Lecture for Civil Engineers), Institut für Baustatik und Konstruktion, ETH Zürich, 1983 (see further references here).
10. Marti, P., "Basic Tools of Reinforced Concrete Beam Design," *ACI Journal*, V. 82, No. 1, January-February 1985, pp. 46-56 (see also Ref. 25).
11. Collins, M. P., and Mitchell, D., "Shear and Torsion Design of Prestressed and Nonprestressed Concrete Beams," PCI JOURNAL, V. 25, No. 5, September-October 1980, pp. 32-100.
12. Weischede, D., "Untersuchungen zum methodischen Konstruieren im Stahlbetonbau" (Investigations on the Methodical Detailing of Structural Concrete), Thesis, Institut für Massivbau, Stuttgart, 1983.
13. Reinke, H. G., "Zum Ansatz der Betonzugfestigkeit bei der Stahlbetonbemessung" (On the Assessment of the Concrete Tensile Strength in the Design of Structural Concrete), Thesis, Institut für Massivbau, Stuttgart, 1986.
14. Kupfer, H., and Moosecker, W., "Beanspruchung und Verformung der Schubzone des schlanken profilierten Stahlbetonbalkens" (Stresses and Deformations of the Shear Zone of Slender Profiled Reinforced Concrete Beams), Forschungsbeiträge für die Baupraxis (Kordina-Festschrift), W. Ernst & Sohn, Berlin, 1979, pp. 225-236.
15. Jennewein, M. F., "Zum Verständnis der Lastabtragung und des Tragverhaltens von Stahlbetontragwerken mittels Stabwekmodellen" (Explanation of the Load Bearing Behavior of Structural Concrete by Strut-and-Tie-Models). Thesis being prepared, Institut für Massivbau, Stuttgart.
16. Reineck, K. H., "Model for Beams Without Shear Reinforcement," Work in preparation, Institut für Massivbau, Stuttgart.
17. Baumann, P., "Die Beton-Druckfelder bei der Stahlbetonbemessung mittels Stabwerkmodellen" (Concrete Compression Fields for the Design of Structural Concrete by Strut-and-Tie-Models). Thesis in preparation, Stuttgart.
18. Jahn, M., "Zum Ansatz der Betonzugfestigkeit bei den Nachweisen zur Trag- und Gebrauchsfähigkeit von unbewehrten and bewehrten Betonbauteilen" (On the Assessment of Concrete Tensile Strength for the Ultimate Capacity and the Serviceability of Concrete Members

With and Without Reinforcement), DAfStb.-Heft 341, Berlin, 1983.
19. König, G., "Control of Cracks in Reinforced Concrete and Prestressed Concrete," Proceedings 1 of the Tenth International Congress of the FIP, New Delhi, 1986, pp. 259-268.
20. Niyogi, S. K., "Concrete Bearing Strength — Support, Mix, Size Effect," *Journal of the Structural Division, ASCE*, V. 100, No. ST8, August 1974, pp. 1685-1702.
21. Schober, H., "Ein Modell zur Berechnung des Verbundes und der Risse im Stahl- und Spannbeton" (A Model for the Assessment of Bond and Cracks in Reinforced and Prestressed Concrete), Thesis, Stuttgart, 1984.
22. Stone, W. C., and Breen, J. E., "Design of Post-Tensioned Girder Anchorage Zones," PCI JOURNAL, V. 29, No. 1, January-February 1984, pp. 64-109; and V. 29, No. 2, March-April 1984, pp. 28-61.
23. Collins, M. P., and Vecchio, F., "The Response of Reinforced Concrete to In-plane Shear and Normal Stresses," Publication No. 82-03, University of Toronto, March 1982.
24. *Design of Concrete Structures for Buildings*, CAN3-A23.3-M84, Canadian Standards Association, Rexdale, Ontario, 1984.
25. Marti, P., "Truss Models in Detailing," *Concrete International*, V. 7, No. 12, December 1985, pp. 66-73.
26. *CEB-FIP Model Code for Concrete Structures*, Comité Euro-International du Béton (CEB), 1978.
27. Mueller, P., "Plastische Berechnung von Stahlbetonscheiben und Balken" (Plastic Analysis of Reinforced Concrete Deep Beams and Beams), Bericht No. 83, Institut für Baustatik und Konstruktion, ETH Zürich, July 1978.

* * *

APPENDIX — NOTATION

Geometry

a = width of anchor plate
b = width of compression field or plate
d = length of D-region
d_g = diameter of largest aggregate
e = eccentricity
h = depth of beam
l = span, length
t = thickness
v = vertical movement
w = crack width
x = depth of bending compression zone
z = lever arm of internal forces
Δ = sliding parallel to crack
α = crack inclination (see Fig. 30)
θ = diagonal compression strut angle
A_{ct} = area of concrete tensile zone
ΔA_c = area of assumed failure zone
$A_{c,ef}$ = effective concrete area for tension stiffening
A_s = cross section of reinforcing steel
a_s = cross section of reinforcing steel per unit length
$\omega = \frac{a_s f_{sy}}{t f_{cd}}$ = mechanical degree of reinforcement

Forces and Moments

C = compression force, compression strut
F = load
M = bending moment
M_T = torque
M_{p2} = statical indeterminate portion of moment from support reactions due to prestressing
P = prestressing force
p = load per unit length
p_a = pressure under an anchor plate
R = resultant force
T = tensile force, tensile tie
V = shear force

Strength

f'_c = specified compressive strength of concrete
f_{cd} = concrete compressive strength for design of undisturbed uniaxial stress fields
f_{cm} = average concrete cylinder strength
f_{ct} = specified tensile strength of concrete
f_{sy} = specified yield strength of reinforcing steel
f_{py} = specified yield strength of prestressing steel
γ = partial safety factor

Subscripts

c = concrete or compressive
d = design
p = prestressing, prestressing steel
s = steel
t = tensile, tension
u = ultimate
w = working, web

* * *